Vegetation mapping and variability assessment of Photosynthetically Active Radiation (PAR) in Urban Forest Division of Srinagar

Jamsheed Bin Jabar

(MSF-2020-121)

Division of Natural Resources Management

Faculty of Forestry

Sher-e-Kashmir
University of Agricultural Sciences & Technology of Kashmir
in partial fulfilment of requirement for the award of degree of

2023

Vegetation mapping and variability assessment of Photosynthetically Active Radiation (PAR) in Urban Forest Division of Srinagar

Jamsheed Bin Jabar

(MSF-2020-121)

Thesis

Submitted to

Division of Natural Resources Management

Faculty of Forestry

Sher-e-Kashmir
University of Agricultural Sciences & Technology of Kashmir
in partial fulfilment of requirement for the award of degree of

Master of Science in Forestry (NRM)

2023

Sher-e-Kashmir
University of Agricultural Sciences & Technology of Kashmir
Faculty of Forestry, Benhama, Ganderbal

Certificate-I

This is to certify that the thesis entitled, **"Vegetation mapping and variability assessment of Photosynthetically Active Radiation (PAR) in Urban Forest Division of Srinagar"** submitted in partial fulfilment of the requirements for the award of degree of **Master of Science in Forestry (NRM),** to the **Division of Natural Resources Management, Faculty of Forestry, Sher-e-Kashmir University of Agricultural Sciences & Technology of Kashmir** is a record of bonafide research work carried out by **Jamsheed Bin Jabar (Regd. No. MSF-2020-121)** under my supervision and guidance. No part of the thesis has been submitted for any other degree or diploma.

It is further certified that information received during the course of investigation has duly been acknowledged.

Prof. Akhlaq Amin Wani
Chairman
Advisory Committee

Endorsed

Dean,
Faculty of Forestry

Sher-e-Kashmir
University of Agricultural Sciences & Technology of Kashmir
Faculty of Forestry, Benhama, Ganderbal

Certificate-II

We, the members of the Advisory Committee of **Mr. Jamsheed Bin Jabar (Regd. No. MSF-2020_121)** a for the degree of **Master of Science in Forestry (NRM)** have gone through the manuscript of the thesis entitled, **"Vegetation mapping and variability assessment of Photosynthetically Active Radiation (PAR) in Urban Forest Division of Srinagar"** and recommend that it may be submitted by the student in partial fulfilment of the requirements for the award of the degree.

Advisory Committee

Major Advisor

Dr. Akhlaq Amin Wani,
Professor and Head, Division of Natural Resources Management,
Faculty of Forestry, SKUAST-K

Members

Dr. M. A. Islam
Professor, Division of Natural Resources Management,
Faculty of Forestry, SKUAST-K

Dr. Asif Ali Gatoo
Assistant Professor, Division of Natural Resources Management,
Faculty of Forestry, SKUAST-K

Dr. Shah Murtaza
Assistant Professor, Division of Natural Resources Management,
Faculty of Forestry, SKUAST-K

Dr. Fahim Jeelani
Assistant Professor, Division of Agricultural Statistics,
Faculty of Agriculture SKUAST-K

Dean's Nominee

Dr. Vaishnu Dutt
Associate Professor, Division of Silviculture and Agroforestry
Faculty of Forestry, SKUAST-K

Sher-e-Kashmir
University of Agricultural Sciences & Technology of Kashmir
Faculty of Forestry, Benhama, Ganderbal

Certificate-III

This is to certify that the thesis entitled, **"Vegetation mapping and variability assessment of Photosynthetically Active Radiation (PAR) in Urban Forest Division of Srinagar"** submitted by **Mr. Jamsheed Bin Jabar (Regd. No. MSF-2020-121)** to the **Faculty of Forestry, Sher-e-Kashmir University of Agricultural Sciences and Technology of Kashmir** in partial fulfilment of the requirements for the award of the degree of **Master of Science in Forestry (NRM)** was examined and approved by the Advisory Committee and External Examiner on ……..

Chairman **External Examiner**

Advisory Committee

Dean

Faculty of Forestry

Sher-e-Kashmir
University of Agricultural Sciences & Technology of Kashmir
Division of Natural Resources Management
Faculty of Forestry, Benhama, Ganderbal

Name of the student	:	**Jamsheed Bin Jabar**
Registration No.	:	MSF-2020-121
Major Subject	:	**Forestry**
Minor Subject	:	Natural Resources Management
Major Advisor	:	**Prof. Akhlaq Amin Wani** Head, Division of NRM Faculty of Forestry, SKUAST-K, Benhama, Ganderbal-191201 (J&K)
Title of the Thesis	:	**"Vegetation mapping and variability assessment of Photosynthetically Active Radiation (PAR) in Urban Forest Division of Srinagar"**

ABSTRACT

It is notable that plants vary in the sensitivity of the photosynthetic apparatus to radiation of various frequencies. For the organic and biological cycles of terrestrial ecosystems, the spectral range of PAR (photosynthetically active radiation) is crucial. which control the rate of vegetation's photosynthetic activity, altering the productivity of both agricultural and natural environments. The spectral region of light between 400 and 700 nm is known as photosynthetically active radiation, or PAR. At this spectral range, solar radiation is selectively absorbed by plant tissues to perform photosynthesis. Higher PAR promotes plant growth, and monitoring PAR is critical to guarantee plants are getting satisfactory light for this

process. Improved vegetation cover and species selection for varied environmental conditions can be made possible by a better understanding of the variable trait of photosynthetically active radiation under diverse biophysical settings.

The present study entitled, "Vegetation mapping and variability assessment of Photosynthetically Active Radiation (PAR) in Urban Forest Division of Srinagar" was carried out during year 2021-2022. The study area was delineated via visual image interpretation technique using Sentinel-2A data of 2021 into 13 Landuse/Landcover (LULC) classes out of which 12 classes were generated viz, Agriculture, Closed Forest, Forest Scrub, Grassland, Horticulture, Habitation, Open Forest, trees outside forest (TOF), Urban green Utilities, Wasteland, Waterbody and Wetland. LULC map (2021) revealed that among all the LULC classes, Habitation occupied the maximum area of the map i.e., 37.22 % while as the horticulture with an area of 1.10 % occupied minimum portion of the map. The LULC map was also validated using ground truth points. The overall classification accuracy of LULC map came out to be 91%. With Kappa coefficient of 0.909. For generation of Forest Cover Density (FCD) map (2021), mapping of satellite data was carried out at 1:20000 mapping scale. The satellite data was delineated into different forest density classes on the basis of tone and texture of Forest class in LULC map. FCD map of Study area was classified into closed forest, open forest, forest scrub and non forest area as per the scheme of classification of forests in terms of crown density followed in india (FSI, 2001). Density wise forest cover (2021) of study area reveals that closed forest occupied maximum portion (8.77%) of the total area (16596.12 ha) while as forest scrub occupied minimum portion (1.83%) of the total area of division.

Statistical analysis (Randomized Complete Block Design) of data collected for PAR with respect to different biophysical variables viz, canopy density, tree density, Tree age, elevation, species strata, ground slope, aspect and soil temperature from 96 sampling units of study area has been carried out. The analysis of data showed that the value of PAR varies with respect to different biophysical factors.

The results demonstrated that with increase in canopy density, total PAR transmitted showed a decreasing trend with open forest showing highest amount of PAR of 135.448 $\mu molm^{-2}s^{-1}$ and the lowest in closed forest with average PAR transmitted as 76.4207 $\mu molm^{-2}s^{-1}$. Tree density showed a similar trend with highest average PAR recorded at 200 trees/ ha and the lowest at tree density of 400 trees/ha and above. Young aged trees with high tree density showed the lower transmission of total PAR towards ground and highest values of PAR were recorded in old aged tree stands with reduced number of stems. Highest amount of PAR was seen in South-East aspect and lowest levels were recorded at North-East aspects. Other factors like elevation and ground slope showed an inverse relation with the total PAR as the values of these variables increased, PAR showed a decreasing trend and vice-versa. Conifer tree strata recorded the highest level of average PAR transmission towards ground in comparison to other deciduous tree layers and the change in the soil surface temperature was seen directly proportional to the amount of PAR received in both open and closed conditions.

We generated multiple regression model for deriving of total PAR using the above biophysical response variables. We found R^2 =0.41 for elevation, Aspect and slope when correlated with canopy density. R^2 =0.064 for aspect and slope when correlated with PAR in open conditions and R^2 =0.35 for canopy density and tree density when correlated with PAR under canopy.

Key words: PAR, LULC, FCD, TOF, Urban Forest, Sentinel-2A, Canopy density, Aspect and Strata.

Signature of Student Signature of Major Advisor

Dated_____ Dated_____

ACKNOWLEDGEMENT

No scientific accomplishment is the outcome of a single person's efforts. Now is the appropriate time to reflect on the route taken during this endeavor and to gratefully recall the names and spirits of those involved.

To begin by expressing my sincere gratitude to everyone who helped make this manuscript a reality, I would like to start by thanking the chairman of my advisory committee, Dr. Akhlaq Amin Wani, Professor, Head of Division of Natural Resources Management, Faculty of Forestry, for his invaluable and direct guidance, prompt suggestion, close counsel, critical evaluation, everlasting patience, and constant encouragement at every stage of research. Working under his guidance was a great opportunity for me.

I would like to place on record of my gratefulness to my advisory committee members viz, Prof. M. A. Islam, Professor, Division of Natural Resources Management, Dr. Asif Ali Gatoo, Assistant Professor, Division of Natural Resources Management, Faculty of Forestry, Dr. Shah Murtaza, Assistant Professor, Division of Natural Resources Management, Faculty of Forestry, Dr. Faheem Jeelani, Assistant Professor, Division of Agri-Statistics, Faculty of Agriculture and Dr. Vaishnu Dutt, Division of Silviculture and Agroforestry, Faculty of Forestry for their keen interest, guidance, useful suggestion, constructive comments and valuable help during the course of this investigation.

I am also thankful to Prof. G. M. Bhat, Head of Division of Silviculture and Agroforestry, Faculty of Forestry for their kind help, co-operation and valuable suggestions.

My sincere thanks are due to Prof. S. A. Gangoo, Dean, Faculty of Forestry, SKUAST-Kashmir, for his kind patronage.

I extend my sincere word of thanks to Mr. Sofi Jeelani, Library Assistant, Faculty of Forestry for his timely and sincere help during the course of experimentation.

I extend my special thanks to non-teaching staff of Faculty of Forestry especially to Mr. Mohammad Shafi, and Mr. Shafqat Azeem for their help when approached.

I am grateful to my parents, Mr. Ab Jabar Bhat and Ms. Shahida Begum, for their endless support. They have always stood behind me, and this was no exception. Their sacrifices, struggles and moral support have been a great source of motivation and morale-booster through thick and thin.

My deep and sincere gratitude goes to my brothers Mr. Jameel Mohammad Jabar and Mr. Junaid Jabar Bhat for their endless support and selfless service. I would Like to thank my sisters Ms. Jasra Jabar and Ms. Mariya Jabar for their prayers and all kinds of encouragement given to me during this crucial period.

I am grateful to many people who have assisted me in the course of this work. My sincere thanks to Mr. Talib Nazir Wani, Mr. Anayet Gul, Mr. Nisar Ah Mir, Mr. Waseem Abdullah, Mr. Talib Bashir, Mr. Ubaid Wani, Mr. Ishfaq Ahmad Mallah, Mr. Tajamul Hussain, Mr. Iqbal Beigh, Mr. Tanveer Ahmad Rather, Mr. Mohd Kaif, Mr. Ufaid Mehraj, Mr. Jauhar Ahmad Parray, Mr. Mir Adil, Mr. Zahid Ahmad Wani, Mr. Umar Nadeem, Mr. Umar Bilal, Mr. Muzamil Ahmad Parray, Mr. Jalib Hussain, Mr. Malik Masroor, Mr. Zahid Ahmad, Mr. Mir Mubashir and Mr. Syed Faizan,

Last but not the least I extend my heartfelt thanking to Central Library and ARIS for their contribution in providing books, Journals and other study materials.

Though acknowledging is an endless task. I would finally like to express my sincere gratitude and thanks to all those who I may have inadvertently failed to mention here.

Needless to say, errors and omissions are mine.

Place: Benhama Ganderbal **Jamsheed Bin Jabar**

Dated: _____

CONTENTS

chapter	Particular		Page No.
1.	INTRODUCTION		1-8
2.	REVIEW OF LITERATURE		9-23
	2.1	LULC and Urban Vegetation Mapping	9
	2.2	Variability of photosynthetically active radiation	17
3.	MATERIALS AND METHODS		24-34
	3.1	Study area	24
	3.2	Materials	26
	3.3	Sampling unit sites	27
	3.4	Methodology	27
4.	EXPERIMENTAL FINDINGS		36-80
	4.1	Lulc of Urban Forest Division of Srinagar	36
	4.2	Forest Cover Density Map	40
	4.3	Urban Green Space	45
	4.4	Accuracy assessment	45
	4.5	Variability assessment of PAR	49
	4.6	Individual relations of different biophysical variables with photosynthetically active radiation (PAR)	74
5.	DISCUSSION		81-86
	5.1	Landuse/Landcover (LULC) of Urban Forest Division of Srinagar	81
	5.2	Forest cover density map	82

	5.3	Variability of Photosynthetically Active Radiation (PAR)	83
	5.4	Variability of canopy density	86
6.	SUMMARY AND CONCLUSION		87-89
	LITERATURE CITED		i-xii
	APPENDIX		xiii-xv

LIST OF TABLES

Table No.	Particulars	Page No.
1.	Specifications of Sentinel-2A satellite	26
2.	Land use/Land cover of Urban Forest Division Srinagar	39
3.	Forest cover density of Urban Forest Div. Srinagar (2021)	43
4.	Urban Green Space cover of Urban Forest Div. Srinagar (2021)	43
5.	Confusion matrix for LULC and FCD mapping (2021) of Urban Forest Division Srinagar	46
6.	Accuracy assessment for validation of LULC map (2021) of Urban Forest Division Srinagar	47
7.	Model Summary for Variability of Canopy Density	50
8.	ANOVA for Variability of Canopy Density	50
9.	Parameter Estimates for Variability of Canopy Density	51
10.	Stepwise Selection Summary for Variability of Canopy Density	51
11.	Model Summary for Variability of PAR in open conditions	56
12.	ANOVA for Variability of PAR in open condition	56
13.	Parameter Estimates for Variability of PAR in open conditions	57
14.	Stepwise Selection Summary for Variability of PAR in open conditions	57
15.	Model Summary for Variability of PAR Under Canopy	62
16.	ANOVA for Variability of PAR Under Canopy	62
17.	Parameter Estimates for Variability of PAR Under Canopy	63
18.	stepwise selection summary of variability of PAR under canopy	63
19.	Model Summary for Variability of Surface temperature	69

20.	ANOVA for Variability of Surface temperature	69
21.	Parameter Estimates for Variability of Surface temperature	70
22.	Stepwise Selection Summary for Variability of Surface temperature	70
23.	Average PAR against Forest Density, Tree Density and Tree Age	77
24.	Average PAR in relation to Aspect	78
25.	Average PAR in relation to Elevation and Slope	78
26.	Average soil surface Temperature in relation to PAR	79
27.	Average PAR under plant canopy of different species strata	80
28.	sampling unit sites	xiii-xv

LIST OF FIGURES

Fig No.	Particulars	Page No.
1.	Study area map	25
2.	Distribution of sampling units over the study area	31
3.	Schematic representation of work to be done	35
4.	Percentage of LULC in Urban Forest Division of Srinagar	37
5.	LULC Map of Urban Forest Division Srinagar in 2021	38
6.	Forest Cover Density status in Urban Forest Division Srinagar in 2021	40
7.	Forest cover density map (2021) of Urban Forest Div. of Srinagar	41
8.	Urban Green Space Map (2021) of Urban Forest Div. of Srinagar	42
9.	Urban Green Space Percentage in the study area	44
10.	Ground truthing map for LULC mapping of Urban Forest Division Srinagar	48
11.	Pearson's correlation map for variability of canopy	52
12.	Grouped scatter plot between Canopy Density and Elevation	53
13.	Grouped scatter plot between Canopy Density and Ground Slope	53
14.	Grouped scatter plot between Canopy Density and Aspect	54
15.	Grouped scatter plot between Canopy Density and Tree Density	54
16.	Pearson's correlation map for variability of PAR in open conditions	58
17.	Grouped scatter plot between PAR in Open and Aspect	59

18.	Grouped scatter plot between PAR in Open and Elevation	59
19.	Grouped scatter plot between PAR in Open and Ground Slope	60
20.	Pearson's correlation map for variability of PAR under canopy	64
21.	Grouped scatter plot between PAR under canopy and Tree Density	65
22.	Grouped scatter plot between PAR under canopy and Aspect	65
23.	Grouped scatter plot between PAR under canopy and Elevation	66
24.	Grouped scatter plot between PAR under canopy and Ground Slope	66
25.	Grouped scatter plot between PAR under canopy and species strata	67
26.	Grouped scatter plot between PAR under canopy and Canopy Density	67
27.	Grouped scatter plot between Soil Temperature and Elevation	71
28.	Grouped scatter plot between Soil Temperature and Canopy Density	71
29.	Grouped scatter plot between Soil Temperature and Tree Density	72
30.	Grouped scatter plot between Soil Temperature and Aspect	72
31.	Grouped scatter plot between Soil Temperature and Ground Slope	73

LIST OF PLATES

Plate No.	particulars	After page No.
1.	LULC mapping and measurement of Photosynthetically Active Radiations	35
2.	Laying out of Quadrants, surface temperature recordings and measurement of canopy density	35
3.	Measurement of tree diameter at breast height and ground slope	35

Chapter 1

INTRODUCTION

LULC and Urban vegetation mapping

Ever since humans began to advance, forests have provided us with food, resources, and energy. Forests have seen misfortune and change throughout human history, yet despite the fact that our societies are becoming more urbanised, we continue to be remarkably dependent on them and they have a remarkable hold on our environmental values. They assist with keeping our environment steady, engrossing carbon dioxide and delivering oxygen, and they control our water supply and works on its quality. According to the FAO of the United Nations, a forest is any land that is more than 0.50 hectares in size and contains more than 10% tree cover (FAO 2000, 2001, 2010). The earth's surface is covered with forests in close to 4 billion hectares, or around 30% of its total land area. In India, forests cover an area of 7,13,789 sq. km, or 21.71% of the country's total land area. (FSI, 2021).

Urban vegetation depicts the absolute array of plants (including urban forests) inside and on the border of urban communities and towns. This includes a variety of plants for a wide scope of natural surroundings. They are set up and overseen for a variety of reasons, and show economic, social, aesthetic and ecological value. The environmental worth of urban vegetation is found in its commitment to the accomplishment of this objective at the most essential level. Trees can reduce greenhouse gas emissions by storing carbon, reduce stormwater runoff by intercepting and soaking up rainwater, and minimize the urban heat island effect by lowering localized surface and air temperatures (Wolf *et al.,* 2020).

The periodic assessment of forest cover of india is done by Forest Survey of India (FSI) using remote sensing technique. Remote Sensing (RS) as defined by Lillesand (1979) is “the science and art of obtaining information about an

object, area or phenomenon through the analysis of data acquired by a device that is not in direct contact with the object, area or phenomenon under investigation". The use of remote sensing in the forestry sector encompasses a wide range of techniques and procedures for extracting forest, some of which have been in use for decades while others have only recently emerged and are undergoing rapid growth (Koch *et al.,* 2008).

For the purpose of examining deforestation, remote sensing provides a quick and affordable method of mapping the forest cover (Francis *et al.,* 2017). Satellite data has transformed into an important application in forest change acknowledgment because of its noteworthy degree. Today's forest cover is mostly changed by facilitating human usage, and any beginning of overall change should include the specific impact of human activities (Sajjad *et al.,* 2015). An improvement in the Landsat satellite series has been exceptionally helpful for an assortment of forest mapping applications (Pimple *et al.,* 2017).

Historically, aerial image demarcation, visual image interpretation, and field trips have all been combined to create woodland mapping systems. Subsequently, their advancement is tedious, and limited to generally little regions. Likewise, shadow impacts limit the specific recognition of woodland boundaries or small gaps. By and large, the primary pictures taken from planes date from the start of the 20th century, trailed by the underlying improvement of photogrammetry and utilizations of aerial photography in the 1920s. When aerial photography first became popular in the 1950s, tree mapping was mostly done at the regional and national levels using simple demarcation or interpretation techniques based on aerial stereo images (Spurr 1960; Gillis and Leckie 1996).

New improvements in sensor innovation for airborne (digital aerial cameras, hyperspectral sensors, airborne laser scanning) and spaceborne (multispectral sensors, radar, airborne laser scanning) systems, for example greatly increased geometric, radiometric, and spectral resolution, has prompted

new points of view for mapping woodland. Significant progress has been achieved in 3D remote sensing over the past ten years, including using synthetic aperture radar (SAR) interferometry, digital aerial stereo-imagery, and light detecting and ranging (LiDAR) (Waser *et al.,* 2017).

The advancement of satellite remote sensing technology has fundamentally changed how we monitor the natural and inhabited resources on the surface of the Earth and allows us to monitor vast areas. The scientific community has witnessed a number of satellites with both commercial (such as IKONOS, SPOT (Satellite Pour observation de la Terre)) and non-commercial (such as Landsat, Sentinel) business models since the launch of the first satellite, which was dedicated to monitoring the surface of the Earth (Landsat 1), on July 23, 1972. These satellites produce various remotely sensed data for many applications, including monitoring of forests, cities, natural hazards, and agriculture (Phiri *et al.,* 2020).

Services reliant on multi-spectral high-resolution optical observations across all terrestrial surfaces worldwide are given continuation with the launch of the Sentinel-2A mission. Sentinel-2A's main goals are to: (1) provide systematic global acquisitions of high-resolution multi-spectral imagery with a high revisit frequency; (2) provide enhanced continuity of multi-spectral imagery provided by the SPOT series of satellites; and (3) provide observations for the next generation of operational products, such as land-cover maps, maps that show when a land change has occurred, and maps of geophysical variables. As a result, Sentinel-2A immediately enhances the services of land monitoring, emergency response, and Security. It is an Earth observation system with the Multi Spectral Instrument (MSI), which has 13 spectral bands ranging from the visible to the short-wave infrared. With a 290 km field of vision, the spatial resolution ranges from 10 m to 60 m depending on the spectral band (Drusch *et al*., 2012).

Forests can be stratified into homogenous parts using remote sensing data, making field inventory quite representative, effective, and affordable. It is also feasible to identify solitary areas of trees and other tree resources outside the forest using very high-resolution satellite data. Using visual, digital, and hybrid techniques, remote sensing is crucial for mapping and monitoring forest cover. Numerous research on the use of remote sensing technology have been conducted (Mohan *et al.,* 1990; Navalgund *et al.,* 2007; Moskal *et al.,* 2011).

Land Use and Land Cover (LULC) data are crucial inputs for countries to track how their land use and soil are changing over time. Using LULC data, it is also possible to determine the effects of growing urban environments on various ecosystems, monitoring protected areas, and the growth of deforested areas in tropical forests. It is possible to extrapolate ecosystem services (ES) estimates and values for larger areas and biomes around the world thanks to the land classes provided by the LULC technique, which enable estimating ES by unit area (Tavares *et al*., 2019).

The forest cover is displayed according to three different canopy densities: very dense forests (VDF) with a canopy density of more than 70%, moderately dense forests (MDF) with a canopy density of 40% to 70%, and open forests (OF) with a canopy density of 10% to 40%. According to the 2021 FSI assessment, VDF accounts for 99,779 square kilometres (3.04%) of the total forest cover in our nation, MDF for 3,06,890 square kilometres (9.33%), and OF for 3,07,120 square kilometres (9.34%) (FSI, 2021).

A region's LULC pattern results from how humans have used social and economic elements throughout the course of time and place. Because of intense agricultural and demographic demand, land is becoming a scarce resource. To choose, plan, and implement land use plans that will satisfy the rising demand for fundamental human requirements and welfare, it is therefore crucial to have knowledge on LULC and options for their best usage. This data also aids in

tracking the dynamics of land usage owing to shifting needs brought on by population growth (Kiran, 2013).

In comparison to traditional Land use/Land cover class methodologies, recent advancements in high resolution remote sensing and methods are sufficient for supplying more exact insights on the urban tree canopy, individual tree metrics, species, and age structures. For more accurate future predictions, life cycle inventories can be updated with these regionally consistent details (Tigges *et al.,* 2017).

Variability of Photosynthetically Active Radiation (PAR)

It is noteworthy that plants differ in their photosynthetic apparatus sensitivity to light at different frequencies (Rabinowitch 1951). For the organic and biological cycles of terrestrial ecosystems, the spectral range of photosynthetically active radiation, or PAR, is crucial (Mayer *et al.,* 2002; Sudharsan *et al.,* 2013), which decide the photosynthetic paces of vegetation, affecting productivity of natural and agricultural ecosystems (Akitsu *et al.,* 2015), with comparing consequences for CO_2 up- take from the air (Proutsos *et al.,* 2017). Plant tissues selectively absorb solar energy in this spectral region to carry out photosynthesis (McCree 1972; Liakatas *et al.,* 2002).

The spectral range of light from 400 nm to 700 nm is known as photosynthetically active radiation, or PAR (Leuchner *et al.,* 2007). Plants can access these wavelengths for photosynthesis because they closely correspond to the range of light that we sense as our visible light. Chlorophyll, a fundamental pigment in plant photosynthesis, efficiently absorbs blue (450 nm –495 nm) and red (620 nm –700 nm) wavelengths and reflects green (495 nm –570 nm) wavelengths (Figure 2). To facilitate photosynthesis, all chlorophyllic plants require light with a wavelength range of 400 nm –700 nm (Taiz & Zeiger, 2010).

The basic energy source for biomass is PAR, which is absorbed through the processes of chlorophyll production and photosynthesis and then converted into chemical energy for living organs by regulating the photosynthetic rate of organisms on land. The amount of PAR that reaches the surface has a significant impact on the Earth's climate system, energy budget, biomass production, natural illumination, and plant physiology (Wang *et al.,* 2015).

In order to ensure that plants are receiving enough light for this process, monitoring PAR is essential. Higher PAR encourages plant development. The range of PAR readings per square metre is 0 to 3,000 millimoles. PAR is 0 at night. In the summer, PAR usually exceeds 2,000 to 3,000 millimoles per square metre during the midday hours. A silicon photovoltaic detector measures photosynthetically active radiation (PAR). This detector measures light between 400 and 700 nanometres in wavelength. PAR is measured using PPFD (photosynthetic photon flux density) and some PAR sensors calculate PPFD of the radiations that is photosynthetically active. Among botanists, horticulturists, biologists, and other natural researchers, this is the most well-known type of light sensor (Nowarji 2019).

A plant canopy is a complex structure made primarily of stems, branches, and leaves that are arranged in a specific volume. Despite the fact that sun-oriented radiation's quantity and quality are constantly fluctuating, the majority of it is devoured by overhanging leaves and little of it is reflected (Campbell and Norman 1998). Consequently, a canopy's PAR absorption roughly equals the ratio of the incident PAR above the canopy (PARi) to the transmitted PAR below the canopy (PARt). The Lambert-Beer formula for exponential radiation extinction in plant canopies has been used to determine the leaf area index (LAI) of the canopy from ground measurements of PAR transmissivity (Monsi and Saeki 1953).

Within forest canopies, the PAR at the leaf surface varies greatly, and variations in the PAR at various leaves also alter over time as a result of changes in incident solar flux density and direction (Ma *et al.,* 2021).

The radiation incident on a plant canopy arrives as direct and diffuse fluxes. Photons that have travelled through the atmosphere unscattered constitute direct flux, whereas photons that have been scattered by air molecules, aerosols, or clouds make up the diffuse flux. Photons striking leaves and other plant components are intercepted, that is, removed from the incident fluxes, as the two fluxes pass through a vegetation canopy. The term "intercepted PAR flux" (IPAR) refers to the photon flux that hits plant components. Only the radiation that was intercepted, has the ability to provide energy for photosynthesis. However, only a portion of this potential is actually used because the intercepting element will always reflect or transmit some radiation. The photons that have been transmitted or reflected may eventually leave the vegetation canopy without contributing to photosynthesis (Mottus *et al.,* 2013).

A plant needs photosynthetically active radiation to survive, and it grows most quickly in higher PAR environments. During the late spring months when PAR is at its highest, plants sprout, grow, flower, and create natural products. However, when fall approaches and PAR levels start to fall, plants begin to slow down, dieback, and eventually go dormant. Oceanography, forestry, and agriculture all employ PAR measurements. Photosynthetic rate and related elements can be evaluated non-destructively using a photosynthesis system, and these instruments measure PAR and sometimes control PAR at set intensities. The euphotic depth in the ocean is also determined using PAR estimates.

In the study of plants, PAR measurements have been used to quantitatively describe radiation as the energy source for photosynthesis. The quantity of photons absorbed can forecast photosynthetic intensity more accurately than radiant energy received by a leaf (Mottus *et al.,* 2013).

Scope and significance

a) The study generated LULC and Forest cover density maps based on visual interpretation supplemented with extensive ground truthing.

b) The mapping of urban green spaces in city Srinagar is important for future environmental planning.

c) The study on Variability assessment of Photosynthetically Active Radiation with relation to biophysical variables is lacking and this is the first of its kind.

d) Photosynthetically Active Radiations is crucial for plant growth, and its variability with other biophysical factors needs to be studied. This study will help us draw some important inferences while studying the relationship between the two.

e) Data obtained from the study can be very helpful in the management techniques of urban vegetation.

Keeping in view the above facts, the present research topic entitled, "Vegetation mapping and variability assessment of photosynthetically active radiation (PAR) in urban forest division of Srinagar" was undertaken with following objectives:

- Vegetation classification of urban Forest Division Srinagar using Sentinel-2A data.
- Assessing photosynthetically active radiation (PAR) and its relation with biophysical factors under different vegetation classes in the study area.

Chapter 2

REVIEW OF LITERATURE

The review of past studies frames the base for additional scientific enquiry. Moreover, review of related studies helps us to conceptualize our research theme and to set research methodologies. Accordingly, the ensuing section gives a brief account of various studies conducted at National and International levels relating to the present theme. A lot of workers have made a significant contribution in the proposed field of study. Keeping in view the multiple perspectives of the study entitled, "**Vegetation mapping and variability assessment of photosynthetically active radiation (PAR) in urban forest division of Srinagar**" an account of literature was reviewed under different headings as given below.

2.1 LULC and Urban vegetation mapping

Mohammadpour *et al.* (2022) mapped the complex and mixed vegetation of the Lousa district in Portugal using Sentinel-2 (S2) data. Ten multispectral bands were employed, each with a spatial resolution of 10 m, and four vegetation indices were applied: the Normalized Difference Vegetation Index (NDVI), Green Normalized Difference Vegetation Index (GNDVI), Enhanced Vegetation Index (EVI), and Soil Adjusted Vegetation Index (SAVI). Four texture features were generated for the first three principal components of the 10 S2A bands using principal component analysis (PCA), including mean (ME), homogeneity (HO), correlation (CO), and entropy (EN). The Gray-Level Co-Occurrence Matrix was used to obtain the textures (GLCM). So, from S2, 26 independent variables were taken out. The Random Forest (RF) classifier was used after the land use classes were defined using an object-based strategy. Using the criteria of overall accuracy (OA), producer accuracy (PA), user accuracy (UA), and kappa coefficient, the confusion matrix was used to assess the map's correctness (Kappa). For mapping vegetation, the described classification algorithm demonstrated a high OA of

90.5% and kappa of 89%. However, classification utilising GLCM texture features and spectral bands achieved the highest OA (92%), suggesting the texture feature's capabilities in recognising the heterogeneity of forest species at stand level. Using GLCM texture features and vegetation indices boosted the accuracy by up to 2%.

Breidenbach *et al.* (2021) employed Sentinel-2 data along with National Forest Inventory (NFI) plot data for modelling and ensuing mapping of Spruce, Pine, and deciduous-dominated forest in Norway at a 16 m × 16 m resolution. The best model's accuracy ranged from 74% for Spruce to 87% for deciduous woodland. Using independent data from more than 42000 stands, a stand-level accuracy of 90% was determined overall. The accuracy of the model was reduced by 10% by errors that were primarily caused by a forest mask. Following the creation of the map, model-assisted (MA) and post-stratified (PS) estimations of the area of species-specific forests were produced.

Randazzo *et al.* (2021) studied for LULC mapping of the Pocket Beaches (PBs) in the province of Messina using the supervised classification algorithms. Maximum Likelihood (MaL), Minimum Distance (MiD), Mahalanobis Distance (MaD), and Spectral Angle Mapper (SAM) classification techniques were used to examine Sentinel-2B satellite pictures. The primary goal of the study was to identify the classification approach that would be suitable for small scale Sentinel-2 imaging processing and yield reliable findings for the LULC mapping of PBs. In addition, linear features within 500 m of the inland buffer zone of the PBs were extracted using an occurrence-based filter technique in conjunction with OpenStreetMap data and Google Earth imagery. The findings show that LULC mapping on Sentinel-2 data can provide data on the biophysical characteristics, specifically surface cover percentages, of the coastal area.

Gebreslasie *et al.* (2020) used a Landsat 8 image to map a natural forest in South Africa. The primary objective was to categorise the forest into distinct

thematic cover classes that indicate its condition, compare the performance of the two classification algorithms based on their default parameters, and identify the key factors that contributed to the mapping accuracy. The open canopy forest, grassland, and barren areas were found to be the secondary thematic classes, with the closed canopy forest emerging as the primary thematic class. According to the study, mapping techniques could be applied to other natural forest ecosystems to determine the spatial coverage of a certain theme cover for conservation efforts.

Nguyen *et al.* (2020) tested a parametric classification (logistic regression) and three non-parametric machine learning classifiers (improved k-nearest neighbours, regression trees, and the support vector machine) for classifying of multi-temporal Sentinel 2 satellite imagery into LULC categories in Dak Nong province, Vietnam. Pre-processing was done on a total of 446 photos, 235 from 2017 and 211 from 2018, to produce high-quality images for mapping LULC in the 6516 km^2 research area. Five of the eleven LULC classes that were differentiated were classes related to the forest. A confusion matrix was created for each pairing of a temporal image set and a classifier using independent reference data and pixel classifications, and the estimated area on the ground for each class was calculated. Overall accuracy for all time periods and classifiers varied between 63.9% and 80.3%, and the Kappa coefficient did too, between 0.611 and 0.813. Individual class area estimations ranged from 70 km^2 (1% of the research region) to 2200 km^2 (34% of the study area), with larger uncertainties for smaller classes.

Qiu *et al.* (2020) explored Sentinel-2 images for urban land cover classification studies that were essentially aimed at large-scale mapping with publicly data available. Additionally, it was discovered that Sentinel-2's five-day return time (near the equator) enables previously undetected pattern recognition and long-term surveillance of the global urban area. When a residual convolutional neural network (ResNet) architecture was utilised as the baseline network for urban land cover classification, they specifically looked at

multiseasonal Sentinel-2 photos and showed improved results over the single-seasonal input.

Phiri *et al.* (2020) found that Sentinel-2 has a positive impact on monitoring land cover and Land use, particularly in monitoring of crops, forests, urban areas, and water resources. Sentinel-2's high spatial resolution (10 m), high temporal resolution (5 days), and accessibility of the red-edge bands with several applications can be credited for the satellite's widespread modern adoption and use. The overall accuracy (OA) while using Sentinel-2 photos is improved by the capability to combine Sentinel-2 data with additional remotely sensed data as part of data analysis. The open access policy encourages the growing use of Sentinel-2 data, particularly in developing nations where there are few financial resources available for the collection of remotely sensed data.

Cavur *et al.* (2019) found that Sentinel-2 has a beneficial effect on monitoring land cover and Land use, particularly in monitoring of crops, forests, urban areas, and water resources. Sentinel-2's high spatial resolution (10 m), high temporal resolution (5 days), and accessibility of the red-edge bands with several applications can be credited for the satellite's widespread modern adoption and use. The overall accuracy (OA) while using Sentinel-2 photos is improved by the capability to combine Sentinel-2 data with additional remotely sensed data as part of data analysis. The open access policy encourages the growing use of Sentinel-2 data, particularly in developing nations where there are few financial resources available for the collecting of remotely sensed data.

Grabska *et al*. (2019) evaluated the functionality of the Sentinel-2 time series for mapping tree species in the complex, mixed forests of the Polish Carpathian Mountains. 18 photos from the Sentinel-2 time series from 2018 were used in the analysis. On the basis of temporal phonological pattern analysis, mean decrease accuracy (MDA), mean decrease Gini (MDG), and other metrics, various combinations of Sentinel-2 imagery were chosen. The Random Forest

classification technique was used to differentiate between different species of trees. The findings demonstrated that the mapping of forest tree species was much more accurate by about 5–10% when using the Sentinel-2 time series as opposed to single date images.

Grabska *et al*. (2019) noted that precise knowledge of the species composition of forest trees is helpful for a variety of uses, including forest management and scientific study. Sentinel-2's launch has opened up new possibilities for mapping tree species because of its high geographical, spectral, and temporal resolution. Due to the phenological phases' effects on reflectance, the short revisit cycle (five days) is essential for vegetation mapping.

Sanchez *et al.* (2019) compared the precision and dependability of the surface observed by both satellites using the Sentinel-2 and Landsat 8 data to create LULC maps in a Mediterranean wetland area using an object-based categorization approach. The findings demonstrate that an object-based classification method using only Sentinel-2 and Landsat 8 image information, without band indexes or ancillary data, provides remarkably similar results for the majority of LULC classes, with an overall accuracy of about 87-88% and comparatively better results when using Sentinel-2.

Hoscilo and Aneta (2019) analysed that the multi-temporal, openly accessible Sentinel-2 data collected during various phenological stages has the potential to map the forest cover, forest type, and delineate tree species on a wide regional scale. Using the multi-temporal Sentinel-2 data, it was possible to map the forest type and cover with success at a spatial resolution of 10 m. It must be emphasised that only using reference samples of the highest caliber, which might occasionally be challenging to obtain—can the classification of tree species be done successfully. With a reasonable high spatial resolution of 10 m over vast distant forest areas, free and open Sentinel-2 data is useful for enabling large-scale monitoring of forest resources.

Ahmed *et al*. (2018) used multispectral ASTER and Sentinel-2A MIS images collected in 2001 and 2015, respectively, to analyse the spatial and temporal dynamics of forest cover in the eastern part of Beni-Mellal Province (Morocco). For the purpose of measuring the extent and density change of different forest cover stands, including Holm Oak, Aleppo Pine, Thya, Zea Oak, Crops & others, and bare ground, the supervised classification algorithm and NDVI were coupled in a GIS (geographic information system) context. In photos from 2001 and 2015, the total categorization accuracy was 97.76% and 95.80%, respectively. The outcome showed an increase in wooded area and a general change in the forest cover. The expansion of every species was at the expense of the bare ground, crops, and other kinds. The growth of the dense forest class resulted in a net shift in density as seen on the density maps. These findings were the first application of a remote sensing-based product for mapping and monitoring forest cover change in the research region.

Dostalova *et al*. (2018) examined the application of Sentinel-1 seasonal backscatter signals for estimating forest area and classifying forest types. Three test locations with a variety of forest types, including broadleaf temperate, boreal, and montane forests, were used to introduce and test a categorization system based on time series similarity metrics. The outcomes were contrasted with two high-resolution Copernicus layers that span all of Europe, namely forest type and tree cover density (TCD). With overall classification accuracy for forest/non-forest classification between 86% and 91% and Pearson correlation coefficients for TCD between 0.68 and 0.74, the relationship between forest/non-forest maps and TCD was strong in all test locations. The accuracy of the classification of the forest types (non-forest, coniferous, and broadleaf forests) was best in temperate forests, where it is 85% overall; in boreal forests, it was only 65%. In general, the method allows for the classification of forest types in temperate forests and yields accurate findings for the estimation of forest area, even in mountainous places where methods based on static characteristics are sometimes troublesome.

Basavarajappa *et al*. (2017) conducted LULC mapping in the Chamarajanagara Taluk of Karnataka using Google Earth and LISS-III satellite images through ArcGIS software, and identified the level 1, level 2, and level 3 LULC classes using both Digital Image Processing (DIP) and Visual Image Interpretation Techniques (VIIT), with partial Ground Truth Checks (GTC). The research area was divided into six classes, including agricultural land, built-up land, forests, wastelands, water bodies, and others, for level 1 classification. Level 2 and level 3 classifications further divided these classes into subclass.

Doke (2017) used multitemporal Landsat TM data to carry out LULC mapping in the Konkan region of Maharashtra and found 8 LULC classes, including thick forest, open forest, scrub, farmland, fallow land, wetland, settlement, and water bodies. Additionally, he stated that farmland took up the largest area of 10814 km^2 (35.17%) and the lowest area of 678 km^2 (2.18%) of the total area.

Kara (2017) with the aid of GIS and remote sensing techniques, studied the LULC pattern of the Turkish province of Izmir. The major data used were 30 m spatial resolution Landsat images (OLI and TM) from 1986 and 2015. The study used object-based image classification to divide up the images into segments before classifying them, and it also produced a transition matrix for determining change. There was a stated accuracy of 93%. In addition, the study showed that the primary aspects of LULC change in the study area included an increase in the area of impervious surfaces and a decrease in natural areas like woods and meadows.

Rwanga and Ndambuki (2017) in their study of LULC of the province of Limpopo determined the key classes to be agriculture (4638 km^2), built up areas (1309 km^2), shrubs (499 km^2), mixed forest (372 km^2), water body (283 km^2), and barren/bare ground (37 km^2). According to reports, agriculture made up the majority of land uses (65.0% of the entire study area). Their Kappa coefficient (K)

was 0.722, and their overall classification accuracy was 81.7%. LULC maps were produced using 2015 Landsat 8 (OLI) photos.

Ankana (2016) in his study generated four LULC classes including built up, agricultural land, forests, and water bodies in the Chakia Tehsil using LULC analysis employing remote sensing and GIS. The thematic map of LULC (2013 and 2014) and the shifting pattern of land LULC over the past ten years were prepared using IRS P6, LISS III (2004, 2013, and 2014; Path 102, Row 54). The study found that while the southern section, which makes up nearly 76.6% of the territory, is defined by plateau and is covered in forest, the northern part, which offers for settlement and all agricultural techniques constitutes nearly 23.48% and is a dead flat plain.

Kayat *et al.* (2016) worked on landuse/Landcover change detection in Saranda Forest in Jharkhand between 1992, 2005 and 2014. They used ERDAS Imagine and Arc GIS software's for the purpose. The overall result suggested that the forest is getting converted into other landuse classes. Intersection method revealed that 0.58% of the dense forest area got converted into open forest during the study period. The present study revealed the overall classification accuracy of 88.54% in 1992, 89.23% in 2005 and 90.03% in 2014.

Crowther *et al.* (2015) created prescriptive regression models for the forests in each of The Nature Conservancy's 14 biomes. These models relate tree density to layers of climate, topography, vegetation, and anthropogenic land use via spatially explicit remote sensing and geographic information systems (GIS). The measurements at the plot level were the recorded which came from more than 50 different countries, the measured tree density values were inherently variable within and between biomes. However, the numerous assessments of tree density made it possible to have high confidence in mean (and overall) estimates.

Ahmadizadeh *et al*. (2014) employed GIS and remote sensing for landuse and change detection study in Brijand, Iran, between 1986 and 2010. The classification of Landsat images was done using an artificial neural network. These were five distinct categories of land use: pasture, irrigated agriculture, dry agriculture, barren land, and urban. Cross-tabulation was used as a post-classification approach to track land use change. To evaluate the accuracy of the classification results, experts in the study region used ground truth information gathered through fieldwork, and visual interpretation. The overall accuracy of the picture categorization in 2010 was 89.67 (Kappa coefficient: 0.8539), and in 1986 it was 88.78 (Kappa coefficient: 0.8424). For the designated study area, the results indicated considerable changes in land usage.

Sreenivasulu *et al*. (2014) worked on Landuse/Landcover and change detection in Rajampet Kapada district Andhra Pradesh, India. The mapping was done at a scale of 1:50000 and the softwares used were Erdas Imagine and Arc GIS. The research concluded that there is a rapid expansion of built-up area. Agricultural land makes up a large portion of the study area. Information on land use and land cover will aid in the most effective macro- and micro-scale land use planning when combined with data on other natural resources, such as water, soil, hydro-geomorphology, etc.

2.2 Variability of Photosynthetically (PAR) active radiation

Proutsos *et al.* (2022) In their research, they evaluated the radiation data for a forest site in Greece from 2009 to 2014 to determine the impact of meteorological factors on the development of the photosynthetically active to global solar radiation ratio. The temporal changes of the ratio are also discussed. As a result, the ratio values are greater in the summer (0.462) and lower in the autumn (0.432), giving rise to an annual average of 0.446. Additionally, it was discovered that the atmospheric water content and clarity were the main determinants of the composition of the global solar radiation in the PAR

qqwavelengths for the analysed site, which was distinguished by a relatively high-water content in the atmosphere. On the other hand, it was discovered that the influence of temperature and associated climatic factors (such as relative humidity, vapour pressure deficit, and saturation vapour pressure) was minimal.

Adrian *et al*. (2021) focused on the fact that, despite estimating capacity at many locations, vegetation indices derived from solar and photosynthetically active radiation (PAR) sensors (i.e., radiation derived) have been under-utilized in determining biological system function. This underutilization may be attributed to specific discrepancies between the irregularity of radiation- and satellite-inferred vegetation records and canopy photosynthesis, also known as measurement biases. Using a decadal record of data from satellite and ground-based spectroradiometers, ecosystem phenology and CO_2 fluxes, and radiation-derived vegetation indices (i.e., the Normalized Difference Vegetation Index [NDVI], the two band Enhanced Vegetation Index [EVI2]) from a high latitude tundra site, biases in radiation-derived reflectance and vegetation indices were assessed in this study (i.e., Imnaviat). Poor correspondence between the three types of reflectance and vegetation files was found at Imnaviat, especially during the latter part of the growing season. Inaccurate estimates of phenological timing by as much as a month were made using radiation-inferred vegetation records, and the connections with shade photosynthesis (i.e., Gross Ecosystem Exchange (GEE)) were unsatisfactory.

Rosati *et al*. (2021) measured the PAR transmitted under the canopy along transects at various distances from the tree rows to quantify the photosynthetically active radiation (PAR) interception in a high-density (HD) and super high-density (SHD) or hedgerow olive system. Minutely measurements of the transmitted PAR were taken, and the totals for the day and season were added. Calculations were made to determine the daily frequency of the various PAR values. SHD intercepted significantly but slightly less cumulative PAR than HD (0.57 mol m^{-2}

± 0.002 mol m^{-2} vs. 0.62 ± 0.03(mol m^{-2}) of the PAR incidents above the canopy) and had a much higher spatial variability of transmitted PAR (0.21 mol m^{-2} under the tree row, up to 0.59 mol m^{-2} in the alley centre), contrasted to HD (range: 0.34 mol m^{-2} – 0.43 mol m^{-2}). The more shaded positions saw higher frequencies of low PAR values, which led to more variability in the daily PAR frequency distribution.

Tian *et al.* (2021) conducted studies and created a method based on light detection and ranging (lidar) to monitor the spatiotemporal patterns of photosynthetically active radiation (PAR) and sunlit and shaded leaves inside forest canopies. They examined the effects of various scanning geometries and related point densities on the distinction between leaves that are in the sun and those that are in the shadow using both terrestrial laser scanning (TLS) and an unmanned aerial vehicle-based lidar system (UAV-LS). They also separated the foliage from the woody elements and estimated the penumbras of the sunlit leaves in order to study the influence of these factors on distinguishing between sunlit and shaded leaves. The study revealed that the proposed lidar-based PAR model could well capture the variations of field-based pyranometer measurements using fused point data by combining UAV-LS and TLS data (mean R-square = 0.88, mean root mean square error (RMSE) = 155.5 $\mu mol \cdot m^{-2} \cdot s^{-1}$, $p < 0.01$). The separate UAV-LS and TLS-based fractions of sunlit leaves were averagely overestimated by 34.3% and 21.6% when compared to the fused point data due to their different coverages and comprehensiveness.

Ningyi *et al*. (2020) explored that the individual trait interactions to canopy shading can have both positive and negative effects on plant photosynthesis. Trait responses to reduced R:FR (red to far red ratio) on photosynthesis were often unfavourable and of a bigger magnitude than effects of reactions to reduced PAR under mild canopy shadowing. On the other hand, under dense canopy shadowing, phenotypic responses to lower PAR became dominant. According to interactions between individual trait responses, the combined effects

of low-R:FR responses and low-PAR responses on plant photosynthesis were not equivalent to the total of the independent effects.

Proutsos *et al.* (2019) monitored hourly PAR and Rs (shortwave radiation) flux densities over a deciduous oak forest in Greece from 1999 to 2005, and their relationship was examined under various circumstances. The results suggest that the yearly mean hourly PAR/Rs is 0.454, with spring and autumn having intermediate values of 0.443 and 0.478, respectively (0.459). While the ratio falls as the sun elevation angle or Rs rises, it rises with dew point temperature. The main determinants of the ratio are the real water vapour pressure (ea) and the atmospheric clearness index (Kt), but relative humidity (RH) also appears to have an indirect impact by changing the values of ea and Kt.

Baird *et al*. (2017) in their study assessed leaf mass per area (LMA), leaf morphological features, and leaf gas exchange in young *Populus tremuloides* Michx. trees in order to discover coordinated leaf responses to low-water (LW) versus low-light (LL) availability. It was found that decrease in PAR lead to plastic responses that alter leaf morphology, increase photosynthetic nitrogen, increase specific leaf area, and increase the proportion of assimilates partitioned to the leaf, among other things.

Choosri *et al.* (2017) used satellite data to calculate the monthly average hourly diffuse photosynthetically active radiation (PAR). At four locations in Thailand, diffuse PAR was analysed. The diffuse PAR under cloudless skies was calculated using a radiative transfer model. The differences between the diffuse PAR obtained from the ground-based observations and those from the model under all sky conditions were typical of cloud effects. Two models were created: one that solely considered diffuse PAR as a function of solar zenith angle, and the other that combined satellite reflectivity, solar zenith angle, and aerosol optical depth into a multiple linear regression. With a higher coefficient of variance R^2 (0.78 vs. 0.70), lower root mean square difference (RMSD) (12.92% vs. 13.05%),

and the same mean bias difference (MBD) of 2.20% when tested with an independent data set, the multiple regression model performed better.

Dong *et al.* (2016) conducted a study for a thorough sensitivity analysis on the contributing factors of fraction of absorbed photosynthetically active radiation (FPAR) variation, to show the effects of the interference factors on FPAR estimation using remote sensing and to enhance the model's accuracy. A coupled leaf-canopy-atmosphere radiative transfer model and a global sensitivity analysis algorithm were used to conduct the analysis. They also examined the diffuse FPAR's determining factors because of how diffuse FPAR affects the variation of FPAR. The findings demonstrated the significance of the leaf area index (LAI) and average leaf inclination angle (ALA) in affecting FPAR variability, particularly prior to canopy closure. With canopy development, it was discovered that these two variables had differing effects on FPAR.

Wang *et al.* (2014) studied for the first time, the temporal variability of the PAR fraction [PAR/G (here G refers for global solar radiation)] and its dependency on various sky conditions during a three-year study of photosynthetically active radiation (PAR) and other solar components in Wuhan, China. The seasonal patterns of PAR, G, and PAR/G were comparable, with summertime peaks and wintertime lows. With a mean value of 1.89 E MJ^{1} each year, the seasonal PAR/G had a range from 1.70 E MJ^{1} in the winter to 2.01 E MJ^{1} in the summer. The average shift in hourly PAR/G values from clear to cloudy skies was from 1.78 to 2.11 E MJ^{1}. Monthly mean hourly PAR/G revealed a diurnal variation, with highest values observed around sunrise and sunset, slightly higher PAR fractions were also found around noon for most months. The effect of daylength on PAR/G was also studied and no significant impact was found.

Kume *et al.* (2011) conducted a study in which the daily total photosynthetically active radiation (PAR; wavelengths 400–700 nm) and near-

infrared radiation (NIR; wavelengths 700–1000 nm) were assessed in the understory beneath the canopy (PARt and NIRt) and above the canopy (PARi and NIRi) of a Japanese cool–temperate deciduous broad-leaved forest during the snow-free period (May to November). The optical spectrum difference as well as the heterogeneity of the canopy structure, the sky condition, and the solar elevation were minimised by the daily integrations of instantaneous NIR and PAR as well as the spectral radiation for NIR and PAR. (R^2 = 0.96) NIRt/PARt and PARi/PARt were linearly associated. Cloudiness had little impact since, compared to the range of NIRt/PARt in the forest, the variation of NIRi/PARi was fairly minor year-round and in all-weather situations. With a wide range from 0 to 5.25 mol m^{-2} (R^2 = 0.97), the ratio of NIRt/PARt beneath the canopy was log-linearly related to the in-situ leaf area index (LAI). They came to the conclusion that transmitted NIRt and PARt beneath a canopy can be used to accurately estimate seasonal variations in fAPAR (= 1 PARt/PARi) and LAI.

Leuchner *et al*. (2011) studied the vertical and horizontal solar radiation variations in a mature mixed stand of Norway spruce (*Picea abies*) and European beech (*Fagus sylvatica* L.) in southern Germany. An extensive dataset with more than one million spectral measurements of photon flux rates at six vertical levels inside the stand was examined with regard to tree species, meteorological sky conditions, and the impact of solar elevation angle on canopy penetration. The three-dimensional radiation field was described by irradiance probability density functions of the photosynthetically active waveband. In-canopy percentages of photon fluence rates in the photosynthetically active waveband were examined in order to quantify umbra, penumbra, and sun fleck frequencies. Comparing the effects of different beech phenological stages on the in-canopy light climate. As a result of their predominantly diffuse nature, overcast conditions (OVC) have larger proportions of photosynthetically active radiation (PAR) at all canopy levels than clear sky conditions (CS). The shade crown of beech trees and the ground level exhibit the lowest median PAR level, which is less than 1% of

above-canopy PAR. More PAR can penetrate the canopy at a higher solar elevation under CS conditions. This effect is more pronounced for spruce than for beech due to the conical crown shape of the conifers that allows photons from higher angles to enter the gaps in between trees in contrast to the more homogeneously closed beech canopy.

Timo *et al*. (2008) predicted the geographical distribution of direct and diffuse photosynthetically active radiation beneath a heterogeneous canopy of a *Pinus sylvestris* stand in eastern Finland using a simulation model. Growth of the seedlings was correlated with both measured and anticipated radiation. The overall pattern of radiation dispersion beneath the canopy was quite accurately predicted by the model. Height, current height increase, and mean height increment of *Pinus sylvestris* seedlings all showed positive correlations with the quantity of both measured and anticipated radiation. For expected diffuse radiation as opposed to total radiation, there was a stronger association between seedling development and irradiance. This was likely due to the fact that diffuse radiation correlates more strongly than direct radiation with other parameters affecting seedling growth due to its symmetrical distribution around plants.

Guangren *et al.* (2007) studied the mean annual daily value of PAR fraction ranging from 1.75 ± 0.12 to 2.3 ± 0.15 mol MJ^{-1} over China. Tropical locations provide the highest score due to increased relative humidity (RH). Instead of locations in China's driest northern desert region, the lowest value is discovered at the Luancheng site, which has low humidity and a surplus of fine particles. Aerosol particle scattering and water vapour absorption are the key factors that regulate the fluctuation of the PAR fraction. In China, there are two distinct diurnal trends in the proportion of PAR. The PAR proportion typically peaks at sunrise or sunset and declines after noon at most locations. However, due to the different diurnal variation of water vapour in this location, it presents a contrary tendency in the northern desert area.

Chapter 3

MATERIAL AND METHODS

Any study's research findings must be of significant worth, precision, and authenticity, which depends on how far suitable methods last. The method used and the resources used for the inquiry are explained in this section.

3.1 Study area

The present study entitled, "vegetation mapping and variability assessment of photosynthetically active radiation (PAR) in urban forest division of Srinagar" was carried out in urban forest division Srinagar of Jammu and Kashmir union territory (Fig. 1).

3.1.1 Location of study area

The total geographical area of union territory of Jammu and Kashmir is 54,624 sq. km. which constitutes about 1.66 per cent of the total area of the country (FSI, 2021). The forest cover in the union territory is 21,387 sq. km, which is 39.15 per cent of union territory's geographical area (FSI, 2021).

District Srinagar of J&K lies between 33°58'0"N and 34°13'0"N latitude and 74°40'0"E and 75°9'0"E longitude. The boundary confronts to the extent of urban forest division Srinagar. The district is located on the banks of the Jhelum River a tributary of the Indus, and Dal and Anchar lakes. Spreads between the plains of valley upto the mountainous region of famous Dachigam forest area extending further more covering areas possessing Tarsar and Marsar lakes. It represents one of the world's most populated, tectonically unstable, ecologically vulnerable, and economically developing mountain environments. The research area's general relief ranges from 1580 to 2500 m above mean sea level. The overall landscape is hilly with a moderate gradient.

3.1.2 CLIMATE

A humid subtropical climate prevails in Srinagar. The Himalayas encircle the valley on all sides. Winters are cold; the average daytime temperature is 2.5 °C (36.5 °F), while the overnight low is below freezing. In the winter, there is moderate to heavy snowfall. The average daytime temperature in July is 24.1 °C (75.4 °F), making summers warm. 720 millimetres of rain fall on average every year (28 in). The wettest and driest seasons are spring and fall respectively. The lowest recorded temperature is 20.0 °C (4.0 °F), and the highest is 39.5 °C (103.1 °F).

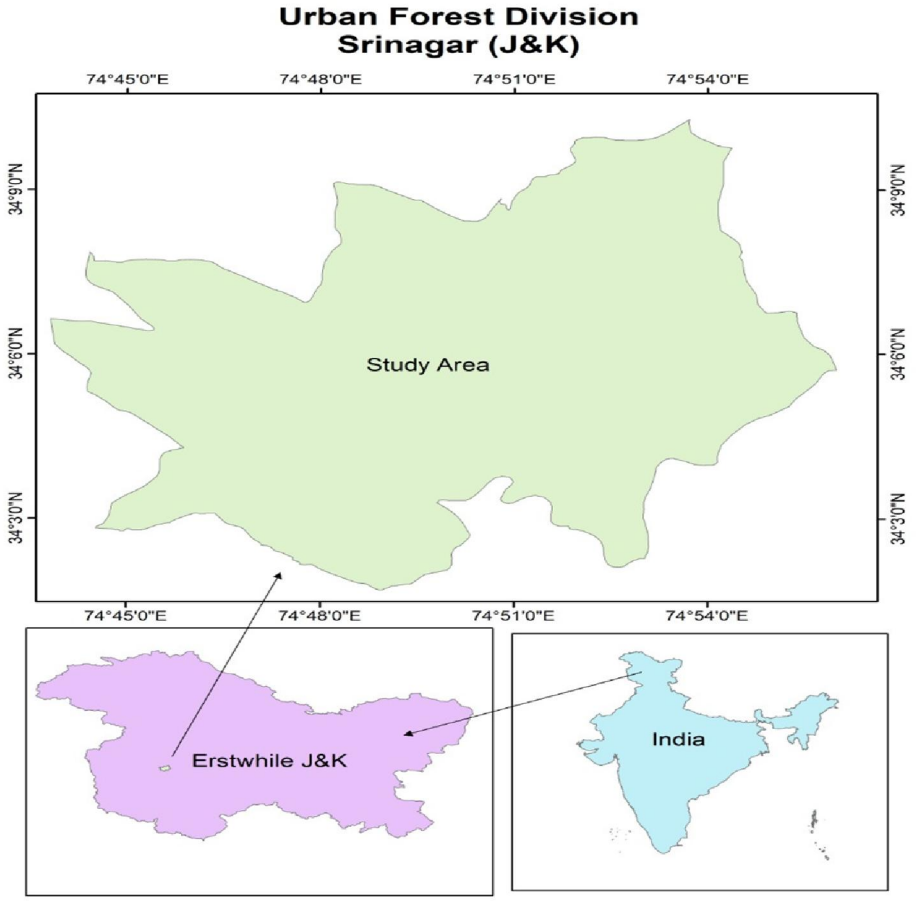

Fig. 1: Study area map

3.2 Materials

The materials used are described under following 3 headings:

3.2.1 Lab work

1) Satellite data
   - Sentinel-2 data was used. The satellite data specifications of Sentinel-2A are given below in Table 1.

Table 1: Specifications of Sentinel-2 satellite

Satellite name	Sentinel-2A
Sensor	MSI (multi-spectral instrument)
Spatial resolution	10m, 20m, 60m
Number of bands	13
Temporal resolution	10 days
Swath	290 km

2) Software
   - ERDAS-imagine (image processing software)
   - ArcGIS (mapping software)
   - Google earth
   - Microsoft Excel (Statistical software for data analysis)
3) Date of acquisition of satellite data: 2021
4) Season: October
5) Scale: 1:20000

3.2.2 Field work

1) GPS (Ground Truth Location, Latitude/Longitude/Altitude/Aspect)
2) Spherical crown densiometer
3) Diameter tape (for estimation of diameter at breast height (DBH) of trees)
4) PAR-meter (Model: LI-COR-LI-250A) (for recording of PAR values)
5) Surface temperature recorder (for recording of soil temperature)
6) Clinometer (for measuring the angle of slope)
7) Field book and pen (for recording the data)

3.3 Sampling unit sites

The sampling unit sites from where the data was recorded in the study area are presented in Table 28.

3.4 Methodology

3.4.1 Objective 1 was carried out using the detailed method as follows:

a) Procurement of satellite data

Satellite data was procured from freely available data of European Space Agency.

b) Pre-processing of satellite data

Using image processing software, the satellite data was prepared to create a False Colour Composite (FCC) with the appropriate band combination. In the Urban Forest Division of Srinagar, various image enhancement techniques were used to improve the interpretation of vegetation cover classification.

c) Preliminary survey of the study area

In order to get first-hand information about Land-use, Topography, Accessibility, etc., a preliminary survey was conducted in the study area of Urban Forest Division Srinagar. The information generated was very useful in determining the nature of mapping to be done.

d) Generation of LULC map (2021)

Mapping of satellite data was carried out using mapping software (ArcGIS) at 1:20000 mapping scale. The satellite data was delineated into 13 LULC classes as follows:

i. Agriculture
ii. Habitation
iii. Forest-closed
iv. Forest-open
v. Forest-scrub
vi. Grassland
vii. Horticulture
viii. Snow
ix. Trees Outside Forest (TOF)
x. Waterbody
xi. Wetland
xii. Wasteland
xiii. Urban Green Utilities

e) Generation of FCD map (2021)

For generation of FCD map (2021), The mapping of satellite data was done at a scale of 1:20000. Based on the tone and texture of the Forest classes in the LULC map, the satellite data was divided into several classes of forest density.

FCD map of urban forest division Srinagar was classified into closed forest, forest-open, forest- scrub and grassland as per scheme of classification of forests in terms of crown density followed in India (FSI, 2019). The whole scheme of classification was based on the preliminary survey of whole study area.

f) Forest Cover Density map

Forest cover density map was generated in accordance with the visual interpretation of different tone and texture from FCC and as per the scheme followed in India (FSI, 2001) which is as under:

1. Closed forest having forest crown density of more than 40%.
2. Open forest having 10% to 40% crown density.
3. Forest scrub having less than 10% crown density.
4. Grassland.

g) Accuracy Assessment of LULC and FCD map

The accuracy of LULC and FCD maps generated was assessed on the ground truth points for accuracy assessment:

i. Latitude
ii. Longitude
iii. Altitude
iv. Aspect
v. Slope°
vi. Dominant species
vii. Block

h) **Validation of LULC map**

KAPPA (KHAT coefficient) will be estimated based on the overall accuracy of the producer and the overall accuracy of the forest cover map, which will be constructed using error matrices. User accuracy is a measure of error of commission, whereas producer accuracy measures error of omission. KAPPA analysis is a discrete multivariate that is used to evaluate accuracy.

$$producer's\ accuracy = \frac{No.\ of\ correctly\ classified\ pixels\ in\ each\ category}{\text{Total No. of validation points used for that category (column total)}}$$

$$user's\ accuracy = \frac{No.\ of\ correctly\ classified\ pixels\ in\ each\ category}{\text{Total No. of validation points used for that category (row total)}}$$

$$Overall\ accuracy = \frac{No.\ of\ correctly\ classified\ pixels}{\text{Total No. of validation points}}$$

$$K = \frac{N\sum_{i=1}^{r} xii - \sum_{i=1}^{r} (x_{i+} x_{+i})}{N2 - \sum_{i=1}^{r} (x_{i+} x_{+i})}$$

$$Also, K = \frac{observed\ accuracy - chance\ agreement}{1 - \text{chance agreement}}$$

Were,

k = Kappa coefficient

r = number of rows in the error matrix

N = Number of observations

xii = the number of observations in row i and column i (on the major diagonal)

xi+ = total number of observations in row i (shown as marginal total to right of the matrix)

x+i = total number of observations in column i (shown as marginal total at bottom of the matrix)

3.4.2 Objective 2

Under the objective 2, the study was carried out using the detailed methods as follows:

3.4.2.1 Sampling design: stratified random sampling

3.4.2.2 Data collection

Data was collected from 96 sampling sites which were chosen randomly from the study area. Recordings for different biophysical parameters was taken for their further analysis. Data was collected for the following parameters:

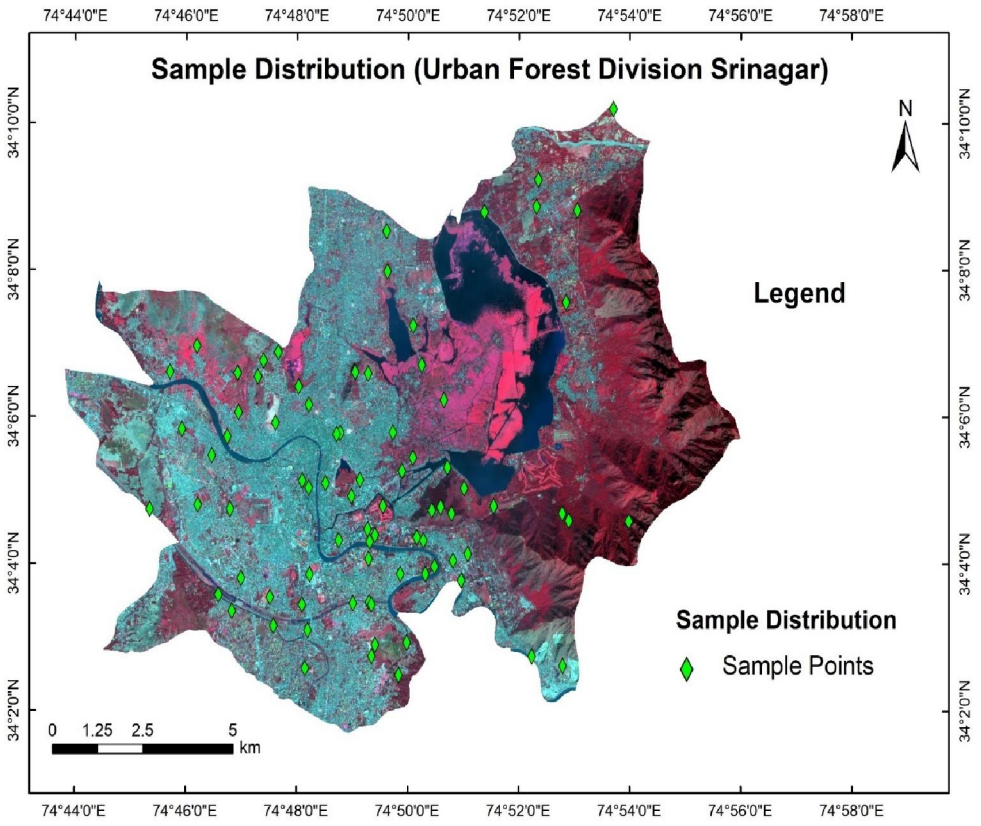

Fig 2: Distribution of sampling units over the study area

i. PAR in relation to canopy density.

With the help of a PAR meter, recordings of PAR values were made under various classes of forest density. The crown density measurements, which were taken with the help of a spherical crown densiometer, were used to categorise the canopy density classes. To examine the relationship between PAR and canopy density, the values of PAR were examined for each density class.

ii. PAR in relation to tree density

A quadrant measuring 20m x 20m (within forests) and 10m x 20m (by the side of the road) was established at each sampling unit to measure the recordings. The number of trees in each quadrant were counted, and the number of trees per hectare was therefore estimated in order to determine the sampling unit's tree density. Following the cumulative root frequency stratification method, several tree density strata were created from the previously gathered data after determining the tree density per hectare. To examine their interrelationship, various tree density values were compared to the PAR values at the respective sites.

iii. PAR in relation to age

Different classes of tree ages were considered while evaluating the variability of photosynthetically active radiations (PAR). Based on the mean diameter of the trees in each age class, three distinct age classes were created. There were three age groups: old, middle, and young. The average tree diameter was higher in the older age groups than in the middle, and lowest in the younger age groups. With the help of a diameter tape held at chest height, the diameter of each tree in the sampling plot was measured.

iv. PAR in relation to elevation

The PAR values at various elevations in the study area were recorded in order to quantify the variability of PAR with respect to elevation. Using a GPS, the elevation of each location was recorded. The two parameters were corelated with one another after gathering the data from each site to examine their interrelationship.

v. PAR in relation with species

Values of PAR were measured with the help of PAR-meter under different species strata. The recordings of PAR were analysed to estimate the variability of PAR under the canopies of different tree species.

vi. PAR in relation with slope

In order to study the relationship between the variability of PAR and the degree of slope, the slope of the ground was measured using a clinometer and classified into distinct slope classes using the cumulative root frequency stratification method.

vii. PAR in relation with aspect

Aspect of every sampling site was recorded with the help of GPS and the values of PAR were also recorded at every aspect to correlate the two parameters.

viii. PAR in relation with soil temperature

Using a digital pyrometer, the soil's surface temperature was monitored in an open environment. The measurements were made in degrees Celsius. The objective was to investigate how the amount of total PAR that reached the soil surface changed with the soil temperature. The ranges of surface temperatures at the various sites were then correlated with the obtained values of the various PAR values.

3.4.2.3 Calculations

a) Tabulation

Data collected from the study area for various parameters was summarised for additional calculations. In order to compare the variability of PAR with these classes, variables such as tree age, slope, canopy density, and tree density were categorised into distinct groups. The number of trees per hectare was calculated from the tree density of each sample site. A few conversions were also done between diameter measurements and canopy density to provide the tree age and canopy density % values, respectively.

b) Analysis

Design of experiment: Stratified random sampling

- Vegetation classes: 8
- Number of strata (4/ vegetation class): $8 \times 4 = 32$
- Replicates (3/ strata): $32 \times 3 = 96$
- Total no of sampling units = 96

c) ANOVA and stepwise regression modelling

Analysis of variance was done to compare variances across the means (or average) of different variables. The degree of freedom among replicates and the significance of the different variables was analysed by this statistical test. parameters were tested individually with their dependent variables to check their significance on its variability. To create a regression model that would offer a function that defines the relationship between one or more independent variables and a response, dependent, or target variable, stepwise regression analysis was used. Coefficient of determination (R^2) was also calculated for each model.

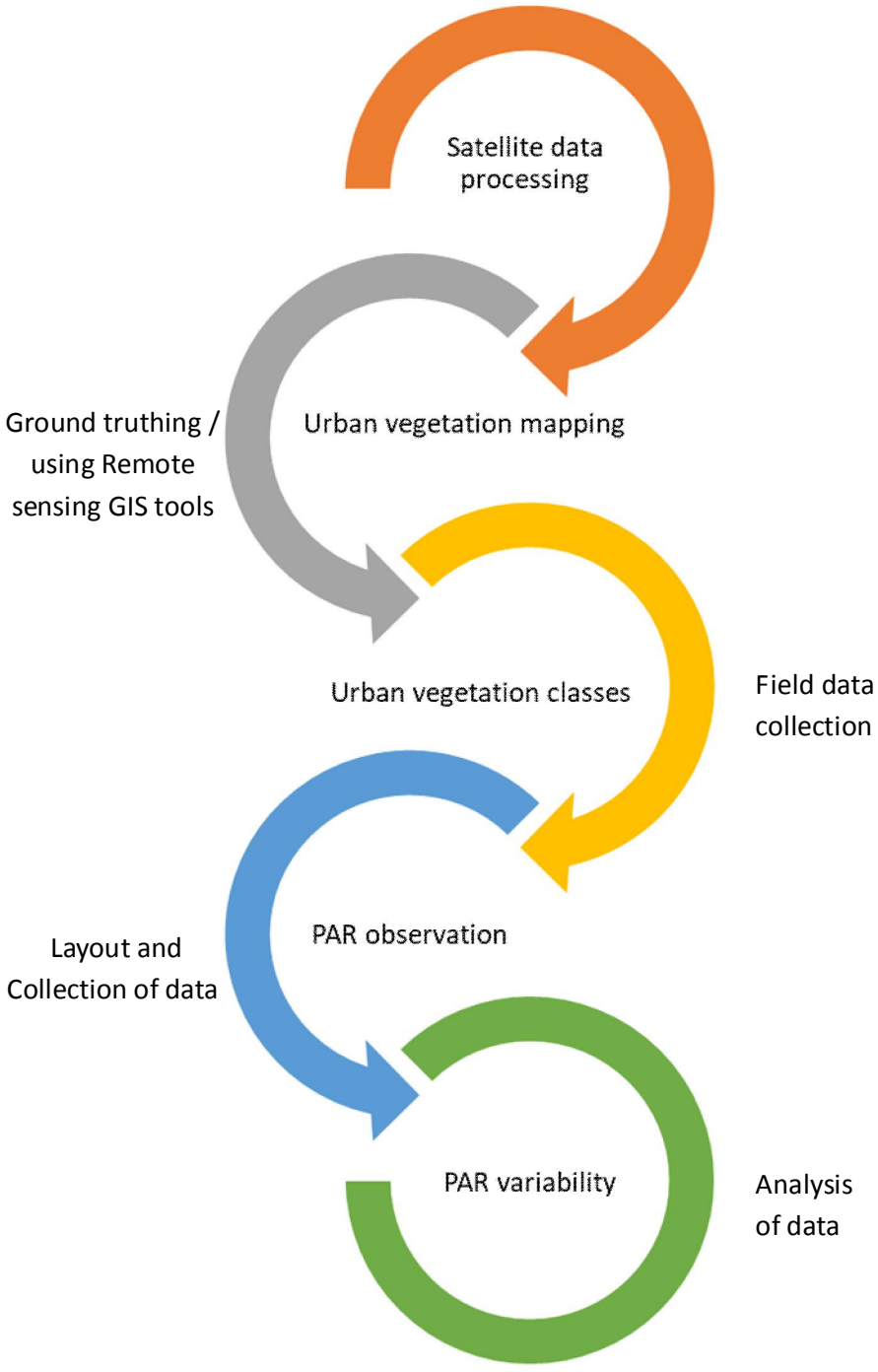

Fig 3: Schematic representation of work to be done

Plate 1: LULC mapping and measurement of Photosynthetically Active Radiations

Plate 2: Laying out of Quadrants, surface temperature recordings and measurement of canopy density

Plate 3: Measurement of tree diameter at breast height and ground slope

Chapter 4

Experimental findings

The results pertaining to the present investigation entitled, "Vegetation mapping and variability assessment of Photosynthetically Active Radiation (PAR) in urban forest division of Srinagar" are presented in this chapter under following headings:

4.1 Lulc of Urban Forest Division of Srinagar
4.2 Forest Cover Density Map
4.3 Urban Green Space
4.4 Accuracy assessment
4.5 Variability assessment of PAR
4.6 Individual relations of different biophysical variables with photosynthetically active radiation (PAR)

4.1 LULC of Urban Forest Division of Srinagar

The LULC of Srinagar's Urban Forest division for the year 2021 is displayed in Table 2. LULC map (2021) revealed that among all the LULC classes, Habitation occupied the maximum area of the map i.e., 37.22 per cent while as the horticulture with an area of 1.10 per cent occupied minimum portion of the map. In the Urban Forest division of Srinagar 2021 LULC map, distinct classes are represented by different colours. The area covered by the various LULC classes can be seen on the LULC map (2021), as illustrated in Fig. 4. Figure 5. shows the distribution of the various LULC classes in the Urban Forest division of Srinagar in 2021.

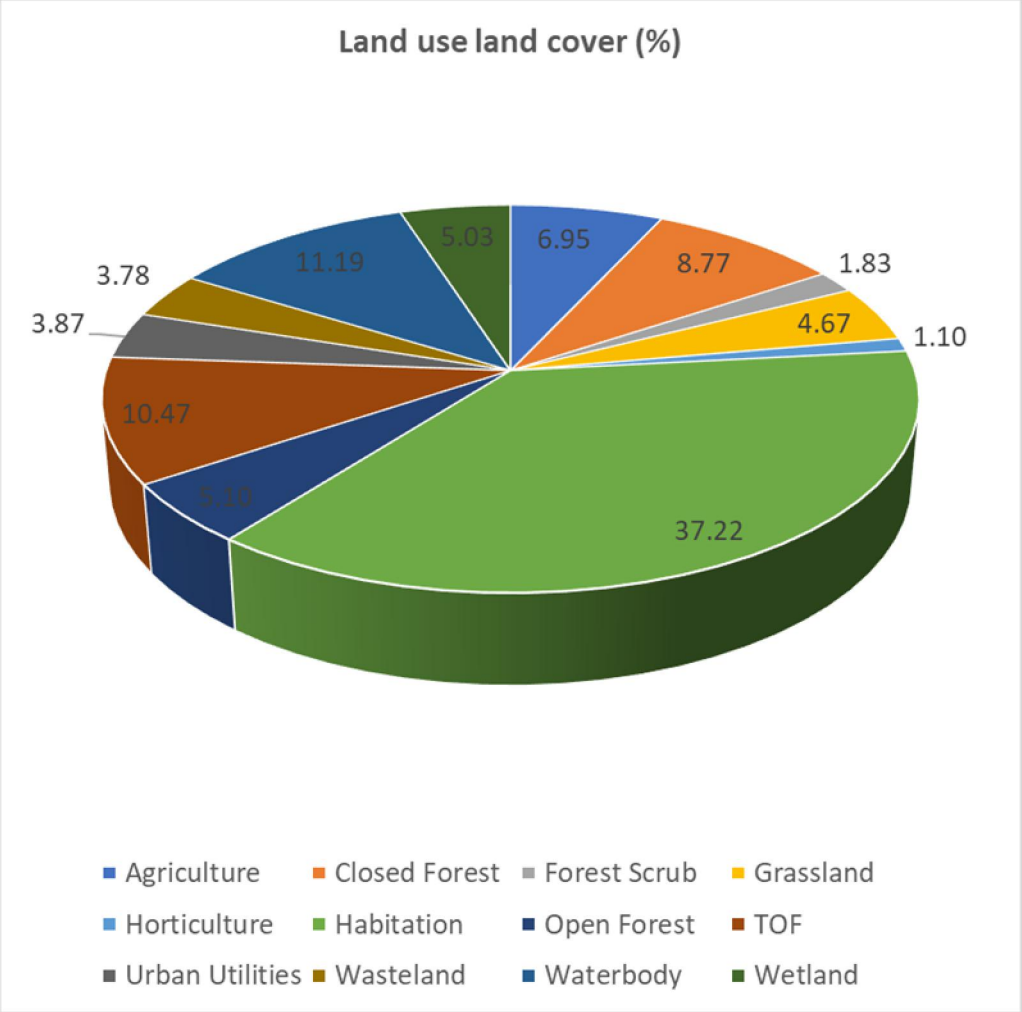

Fig 4: Percentage of LULC in Urban Forest Division of Srinagar

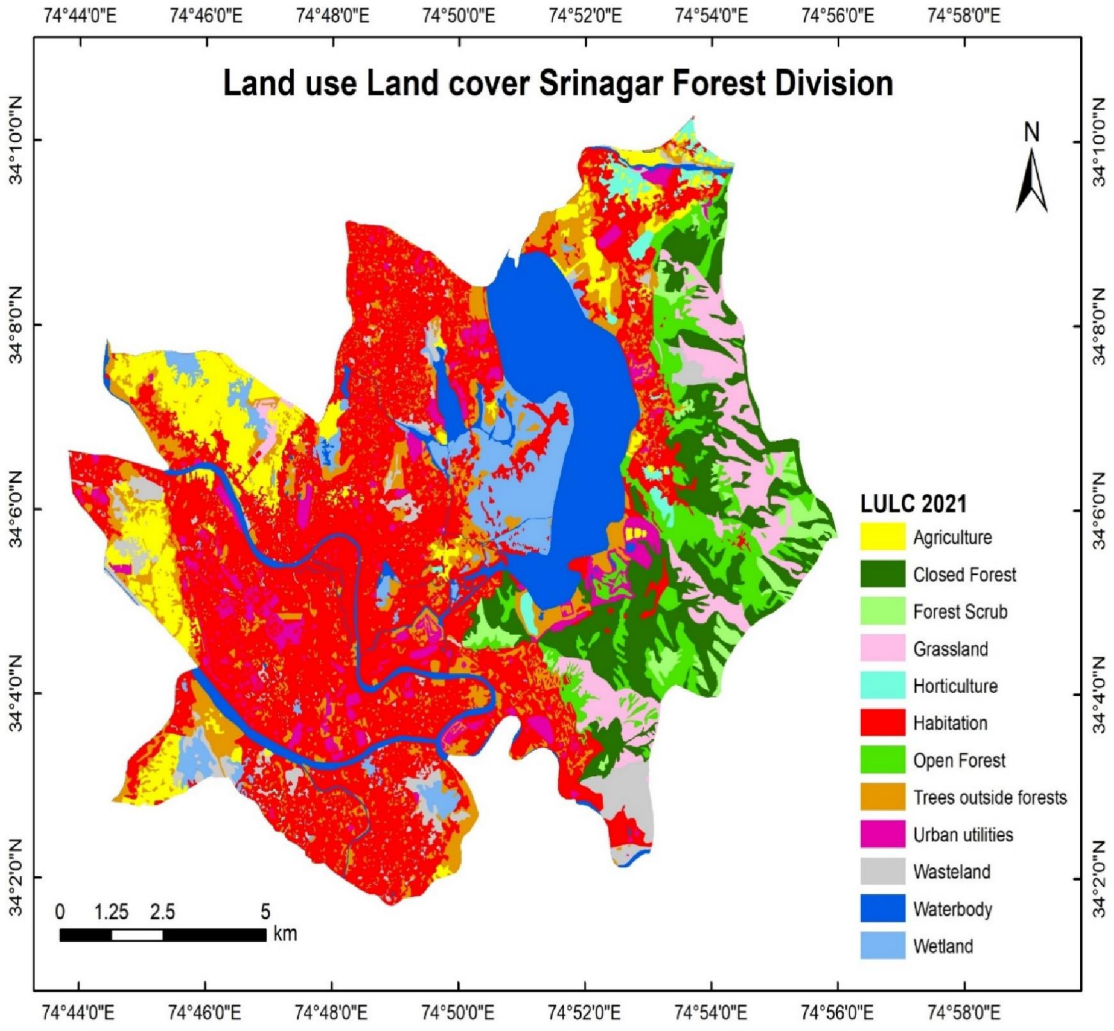

Fig 5: LULC Map of Urban Forest Division Srinagar in 2021

Table 2: Land use/Land cover of Urban Forest Division Srinagar

LULC	Area (ha)	Area (%)
Agriculture	1154.25	6.95
Closed Forest	1455.70	8.77
Forest Scrub	303.97	1.83
Grassland	775.23	4.67
Horticulture	183.34	1.10
Habitation	6177.78	37.22
Open Forest	846.91	5.10
TOF	1737.54	10.47
Urban Utilities	642.64	3.87
Wasteland	626.95	3.78
Waterbody	1857.66	11.19
Wetland	834.16	5.03
Total	**16596.12**	**100.00**

4.2 Forest Cover Density Map

Density wise forest cover of Urban Forest division of Srinagar is tabulated in Table 3. and depicted in percentage in Fig. 6. Density wise forest cover (2021) of Urban Forest division of Srinagar reveals that closed forest occupied maximum portion (8.77%) of the total area (16596.12 ha) while as forest scrub occupied minimum portion (1.83%) of total area of the division (Fig. 7).

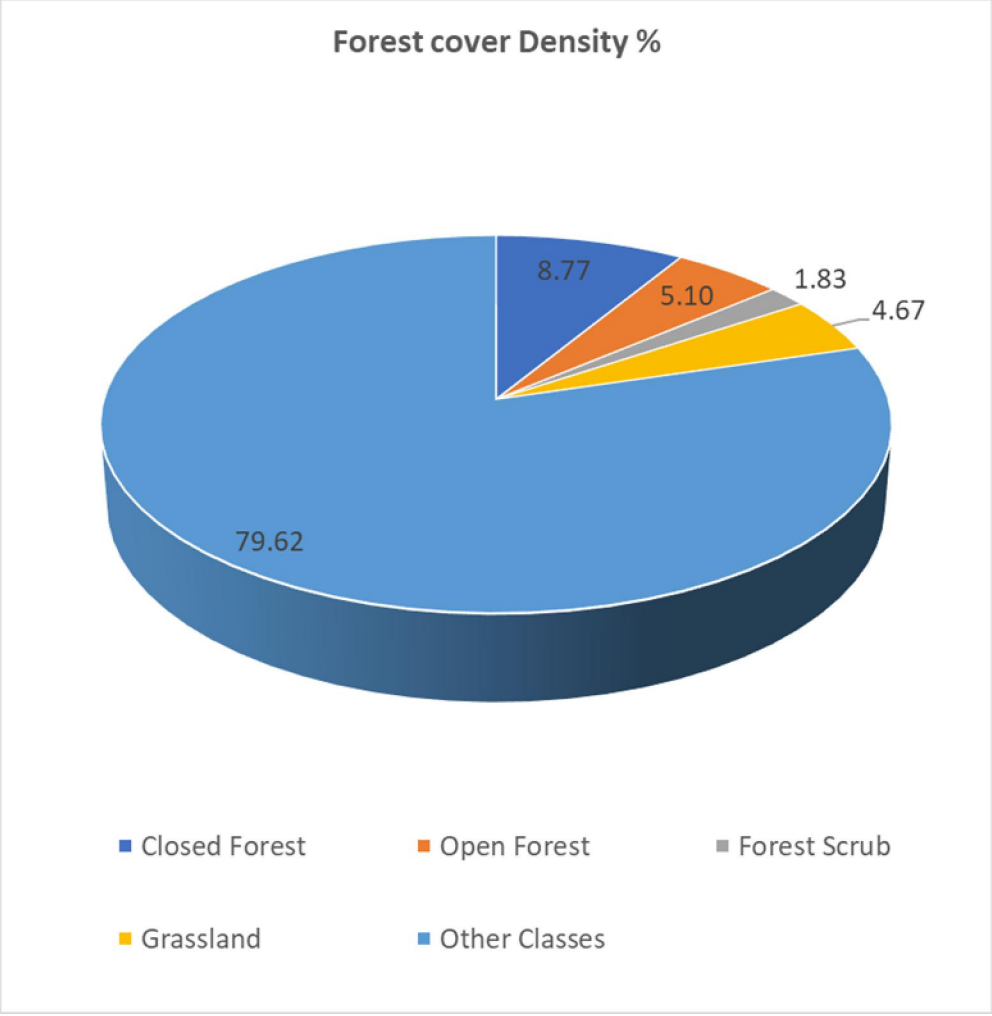

Fig 6: Forest Cover Density status in Urban Forest Division Srinagar in 2021

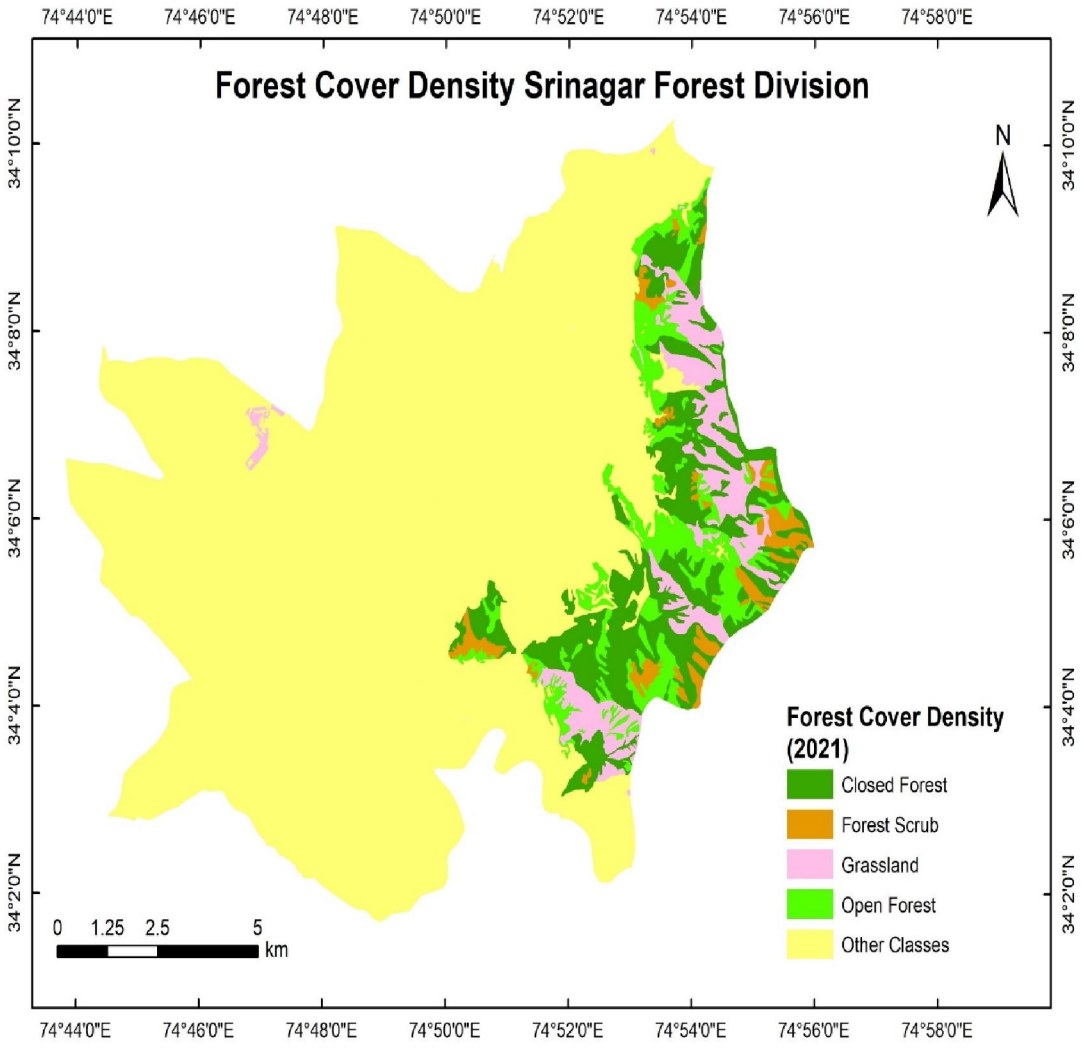

Fig 7: Forest cover density map (2021) of Urban Forest Div. of Srinagar

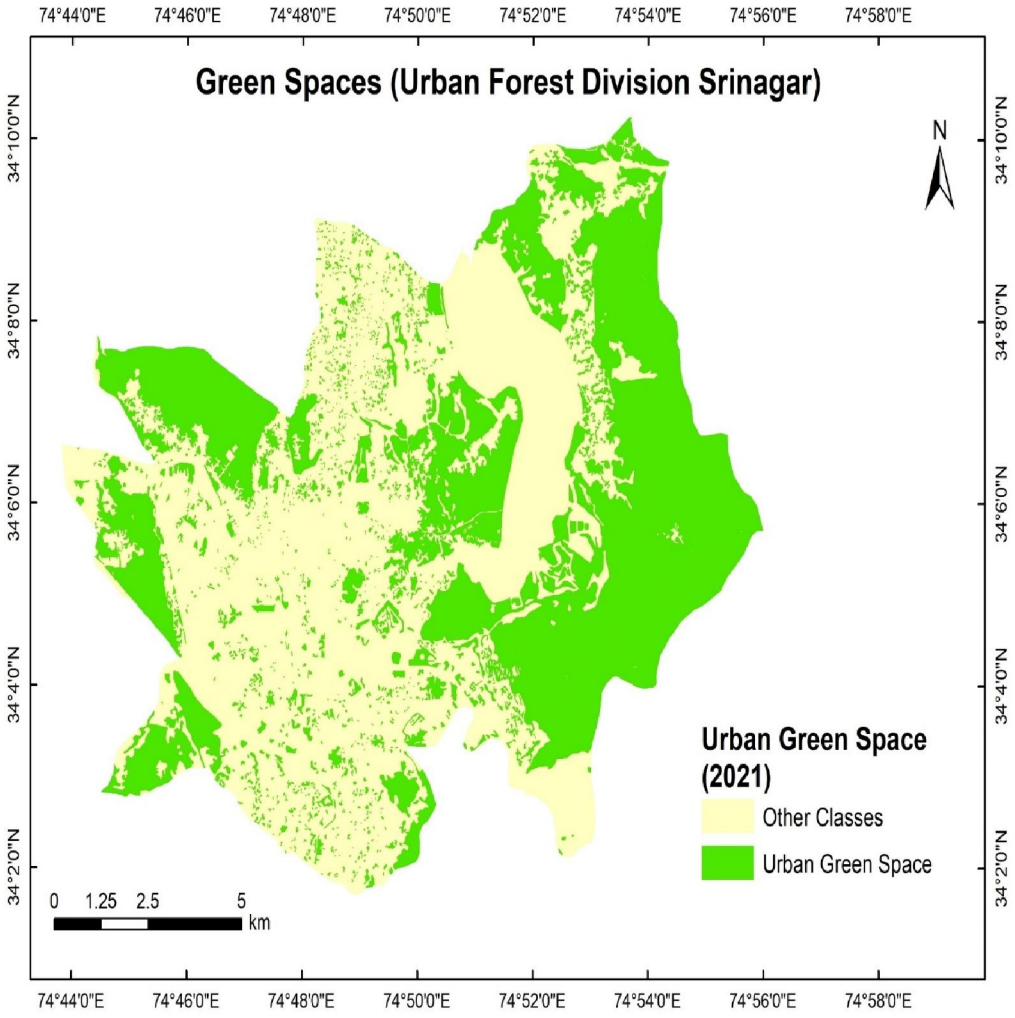

Fig 8: Urban Green Space Map (2021) of Urban Forest Div. of Srinagar

Table 3: Forest cover density of Urban Forest Div. Srinagar (2021)

Forest Density	Area (ha)	Area (%)
Closed Forest	1455.704	8.77
Open Forest	846.9071	5.10
Forest Scrub	303.9681	1.83
Grassland	775.23	4.67
Other Classes	13214.31	79.62
Total	16596.12	100

Table 4: Urban Green Space cover of Urban Forest Div. Srinagar (2021)

Green/Non-Green	**Area (ha)**	**Area (%)**
Urban Green Space	7291.10	43.93
Non-Green Areas	9305.02	56.07
Total	16596.12	100.00

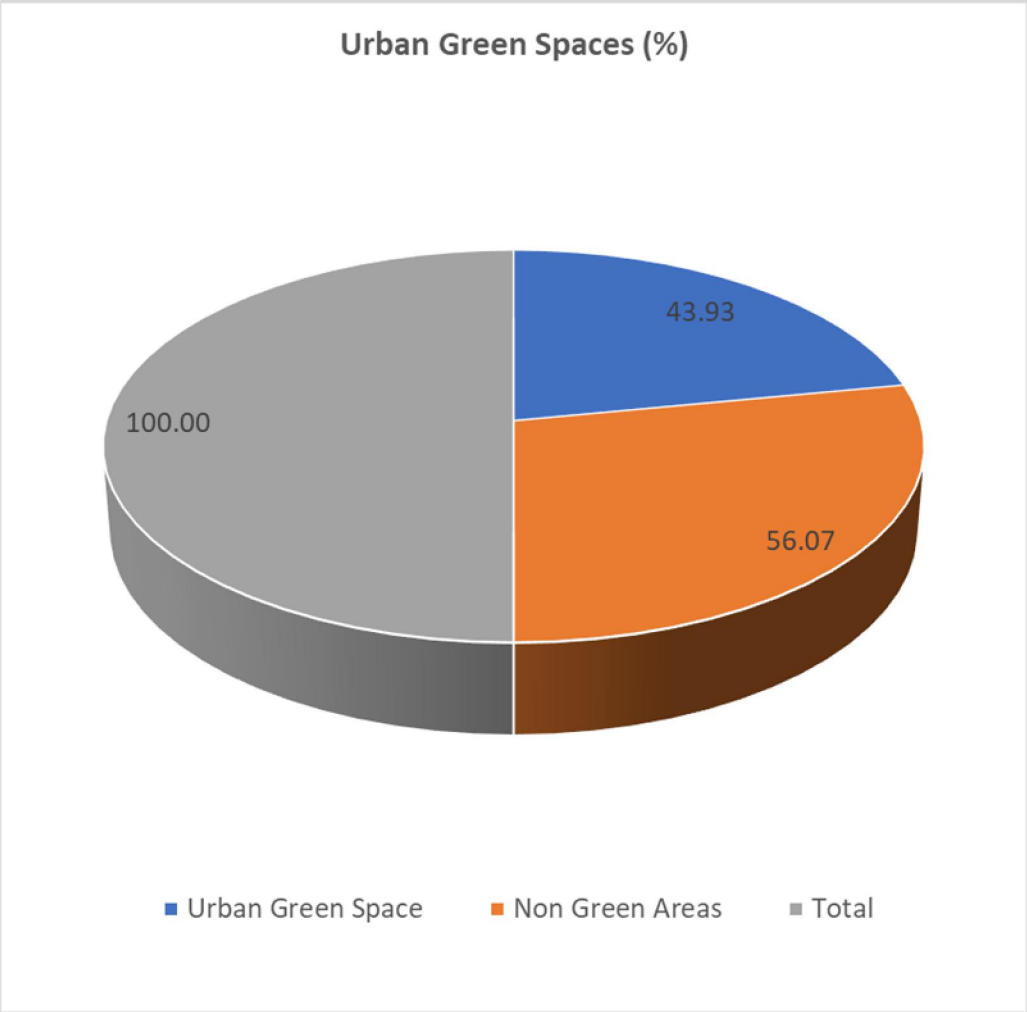

Fig 9: Urban Green Space Percentage in the study area

4.3 Urban Green Space

Non-green areas were merged and the total area was found to be 9305.02 ha (56.07%), while as the green space area included (agriculture, closed forest, forest scrub, grassland, horticulture, open forest, TOF and wetland) was found to be 7291.10 ha (43.93%) of the total study area as tabulated in Table 4 (Fig. 8 and Fig. 9)

4.4 Accuracy assessment

4.4.1 Accuracy assessment for validation of LULC map

Accuracy assessment was carried out using ground truth points. A total of 96 ground truth points were taken across the study area for validation of LULC and FCD map. The producer's accuracy as well as user's accuracy was calculated for each LULC class as shown in Table 5 and 6. The overall classification accuracy of LULC map was estimated as 91 per cent.

Table 5: Confusion matrix for LULC and FCD mapping (2021) of Urban Forest Division Srinagar

CLASS	Agriculture	Horticulture	Habitation	Wasteland	Wetland	Waterbody	Grassland	Forests (Open)	Urban utilities	TOF	Forest Scrub	Forest (Closed)	Row Total
Agriculture	**7**	0	0	0	0	0	1	0	0	0	0	0	**8**
Horticulture	0	**7**	0	0	0	0	0	0	0	1	0	0	**8**
Habitation	0	0	**8**	0	0	0	0	0	0	0	0	0	**8**
Wasteland	0	0	0	**7**	0	0	0	0	0	0	1	0	**8**
Wetland	0	0	0	0	**8**	0	0	0	0	0	0	0	**8**
Waterbody	0	0	0	0	0	**8**	0	0	0	0	0	0	**8**
Grassland	1	0	0	0	0	0	**7**	0	0	0	0	0	**8**
Forests (Open)	0	0	0	0	0	0	0	**7**	0	0	1	0	**8**
Urban utilities	0	0	0	1	0	0	0	0	**7**	0	0	0	**8**
TOF	0	1	0	0	0	0	0	0	0	**7**	0	0	**8**
Forest Scrub	0	0	0	0	0	0	0	1	0	0	**7**	0	**8**
Forest (Closed)	0	0	0	0	0	0	0	0	0	0	0	**8**	**8**
Column total	**8**	**8**	**8**	**8**	**8**	**8**	**8**	**8**	**7**	**8**	**9**	**8**	**96**

Overall, Kappa Accuracy: 91%

Table 6: Accuracy assessment for validation of LULC map (2021) of Urban Forest Division Srinagar

Class	Producers Accuracy	Users Accuracy
Agriculture	87.50	87.50
Horticulture	87.50	87.50
Habitation	100.00	100.00
Wasteland	87.50	87.50
Wetland	100.00	100.00
Waterbody	100.00	100.00
Grassland	87.50	87.50
Forests (Open)	87.50	87.50
Urban utilities	100.00	87.50
TOF	87.50	87.50
Forest Scrub	77.78	87.50
Forest (Closed)	100.00	100.00

The conditional kappa for accuracy assessment of LULC map was calculated using kappa coefficient formula. Using the formula, the overall accuracy for the LULC map of Urban Forest Division Srinagar (2021) was found to be 91 per cent. The producers and users' accuracy were estimated for different LULC classes. Producers' accuracy and user's accuracy for agriculture was found to be 87.50% and 87.50%. For Horticulture 87.50% and 87.50. For Habitation 100% and 100%. For Wasteland 87.50% and 87.50%. For Wetland 100% and 100%. For Waterbody 100% and 100%. For Grassland 87.50% and 87.50%. For Forests (Open) 87.50% and 87.50%. For Urban utilities 100% and 87.50%. For TOF 87.50% and 87.50%. For Forest Scrub 77.78% and 87.50%. For Forest (Closed) 100% and 100% respectively.

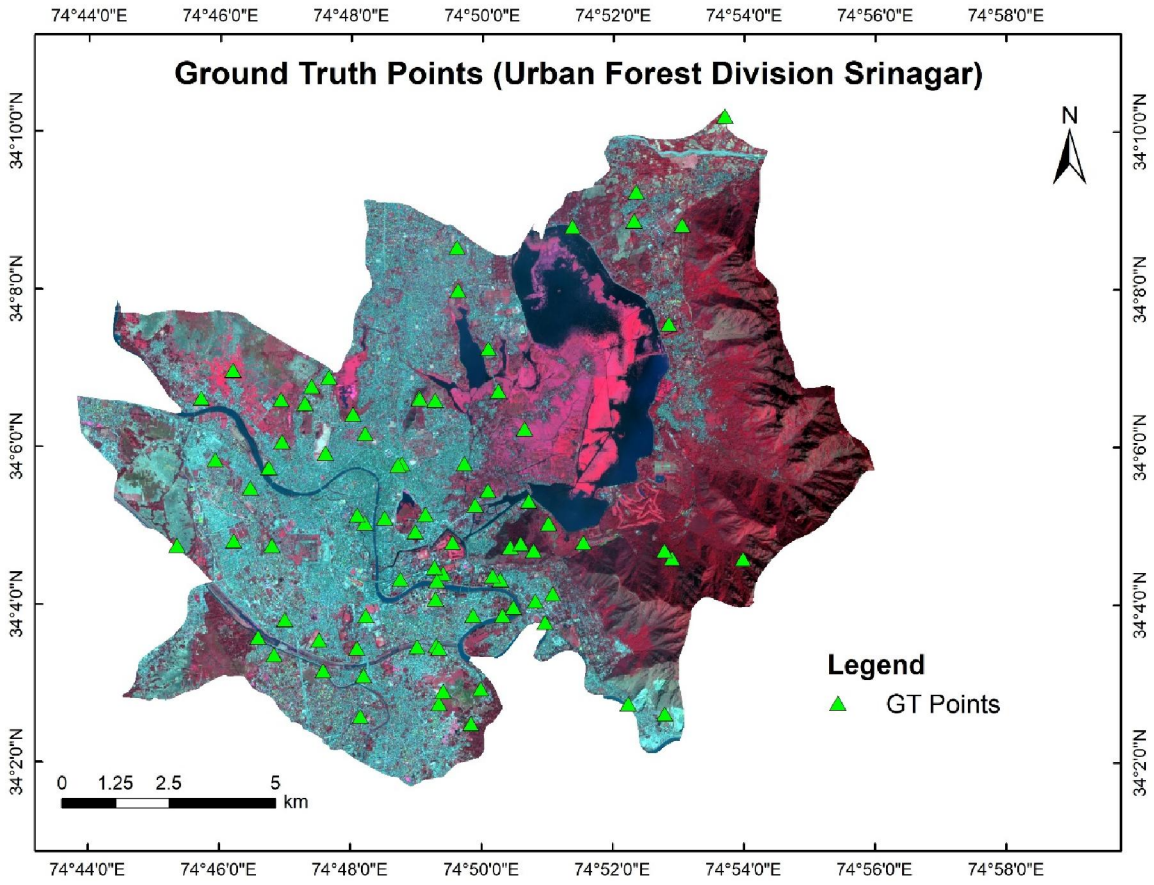

Fig 10: Ground truthing map for LULC mapping of Urban Forest Division Srinagar

4.5 Variability assessment of PAR

4.5.1 Variability of Canopy Density with biophysical factors

The strength of the association between the dependent variable canopy density and the independent variables species strata, tree density, aspect, elevation, and average tree diameter was examined using regression modelling. Only three of the five expected variables including elevation, aspect, and slope showed a substantial impact on the variation in canopy density (Fig. 11). According to the computed Coefficient of Determination R^2 (0.41) at the 5% significance level. In order to determine the impact of various variables on the variability of canopy density, an analysis of variance was conducted. The test statistics values (t value) revealed that the parameter estimates for elevation and slope had a negative relationship with the variability of canopy density, meaning that as these parameters were increased, the canopy density decreased (Table 7, 8, 9 and 10) (Fig. 12, 13, 14 and 15). The highest canopy density was observed in the south-west aspect, and it also increased from the northern to the southern aspect and further increased to the western aspects (Fig. 14). The values of aspect to canopy density that are coded according to their significance are listed below.

Aspect is coded as follows

1	2	3	4	5	6	7
N	S	W	NE	NW	SE	SW

Regression equation model:

stepwise regression modelling was used to create a model for predicting the canopy density at any site.

General model: $\mathbf{Y = \beta_\circ + B_1 x_1 + B_2 x_2 + B_3 x_3}$

model built: $\mathbf{Y=3450.159-1.55\ x_1 - 13.852\ x_2 + 78.045\ x_3}$

Where:

Y = Canopy density $\beta_\circ$ = Intercept X_1 = elevation X_2 = slope X_3 = aspect

Table 7: Model Summary for Variability of Canopy Density

R	0.642	RMSE	185.273
R-Squared	0.412	Coef. Var	20.152
Adj. R-Squared	0.392	MSE	34326.044
Pred R-Squared	0.285	MAE	128.849

RMSE: Root Mean Square Error
MSE: Mean Square Error
MAE: Mean Absolute Error

Table 8: ANOVA for Variability of Canopy Density

	Sum of Squares	DF	Mean Square	F	Sig.
Regression	2208424.581	3	736141.527	21.446	0.0000
Residual	3157996.064	92	34326.044		
Total	5366420.645	95			

Table 9: Parameter Estimates for Variability of Canopy Density

model	Beta	Std. Error	Std. Beta	t	Sig	lower	Upper
(Intercept)	3450.159	620.357		5.562	0.000	2218.077	4682.241
Elevation	-1.551	0.387	-0.467	-4.012	0.000	-2.318	-0.783
Slope	-13.852	3.464	-0.558	-3.998	0.000	-20.732	-6.971
Aspect	78.042	21.385	0.482	3.649	0.000	35.569	120.514

Table 10: Stepwise Selection Summary for Variability of Canopy Density

Step	Variable	Added/ Removed	R-Square	Adj. R-Square	C(p)	AIC	RMSE
1	Elevation	Addition	0.293	0.285	18.5370	1294.5641	200.9105
2	Slope	Addition	0.326	0.312	15.3180	1291.9204	197.1611
3	Aspect	Addition	0.412	0.392	4.0000	1280.9418	185.2729

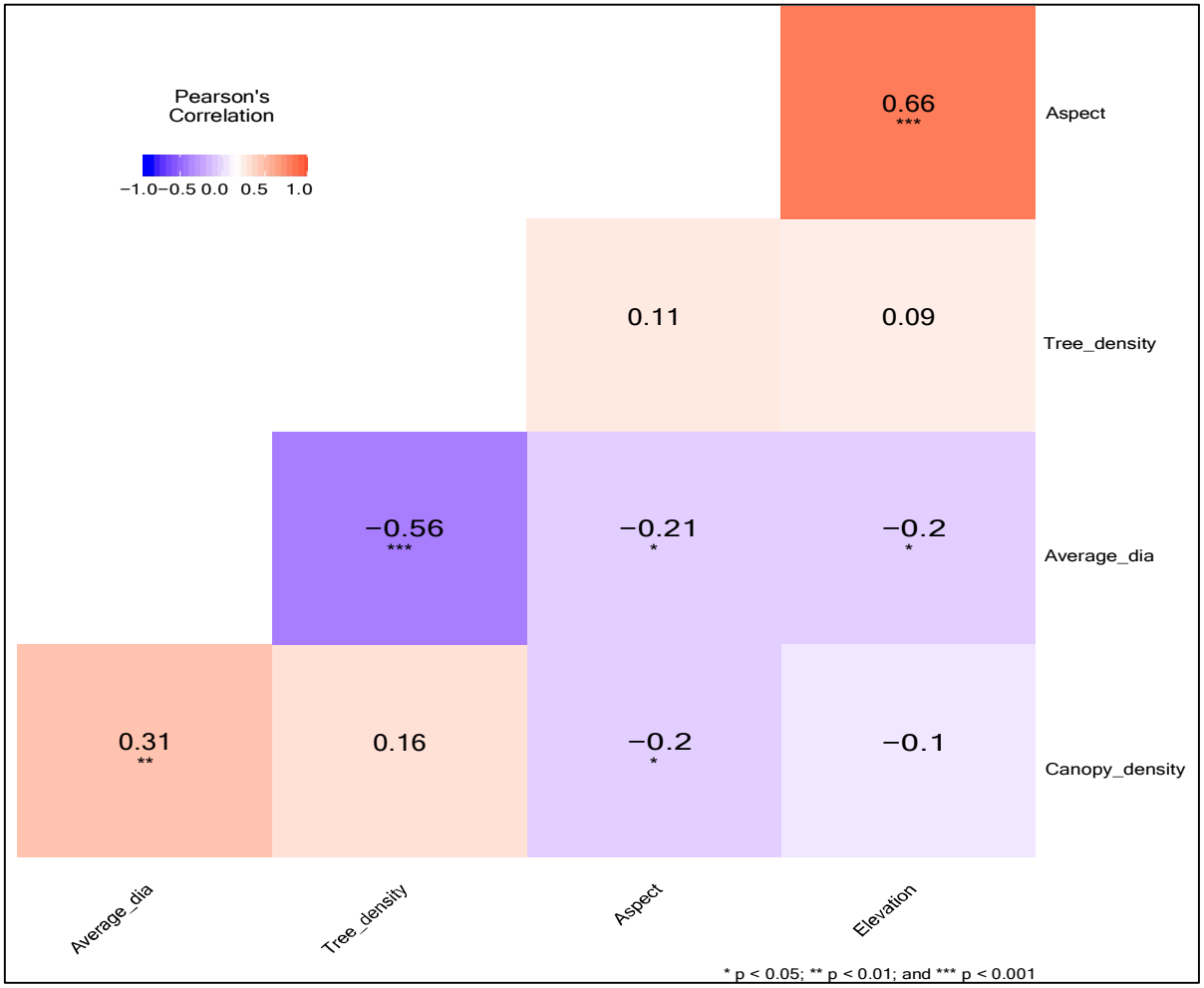

Fig 11: Pearson's correlation map for variability of canopy

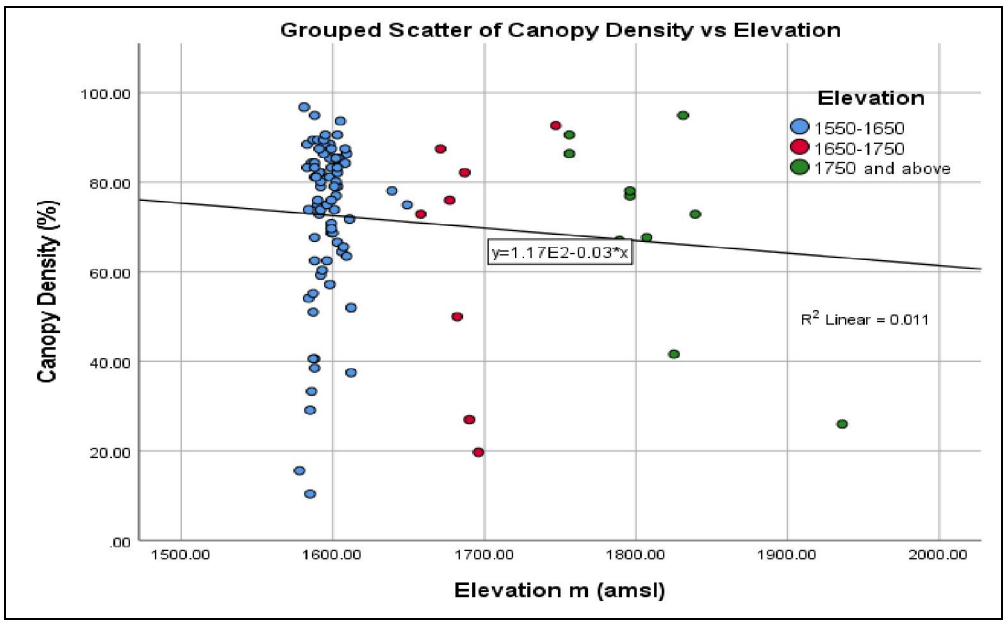

Fig 12: Grouped scatter plot between Canopy Density and Elevation

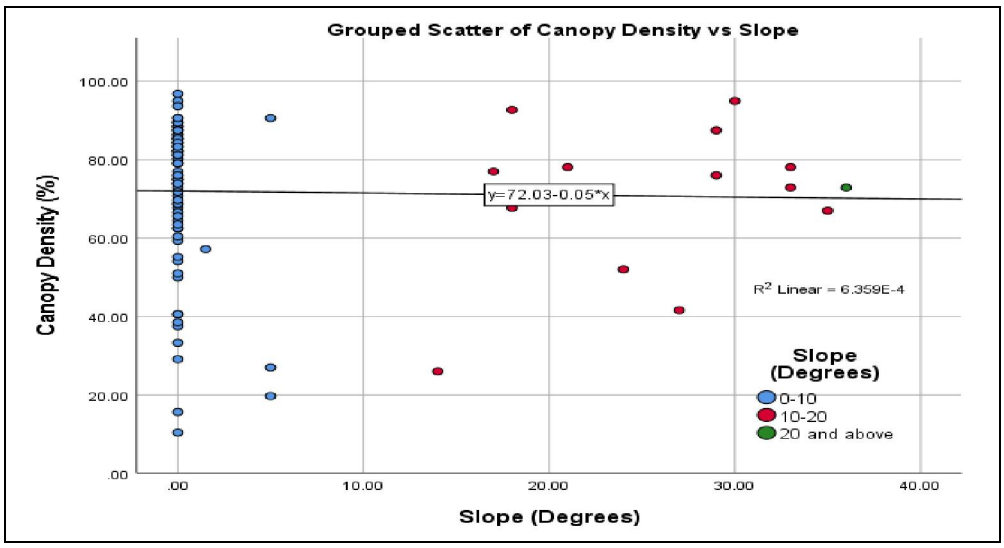

Fig 13: Grouped scatter plot between Canopy Density and Ground Slope

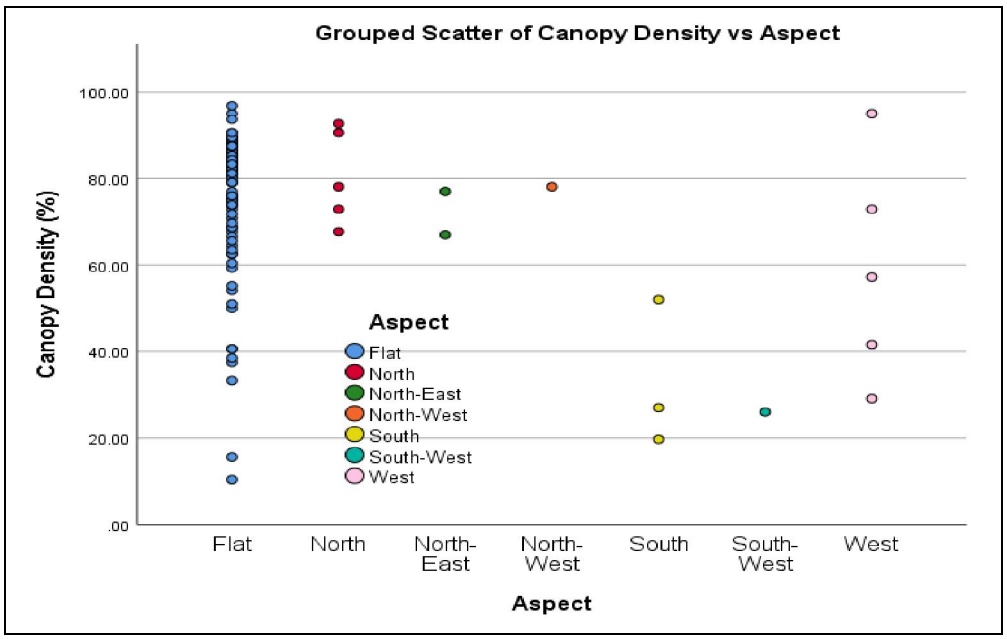

Fig 14: Grouped scatter plot between Canopy Density and Aspect

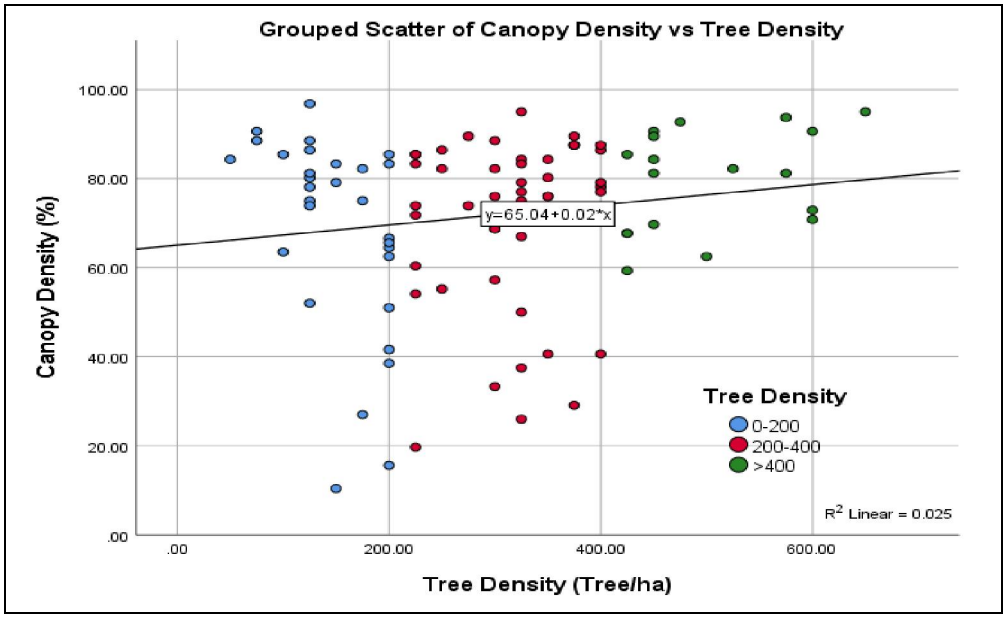

Fig 15: Grouped scatter plot between Canopy Density and Tree Density

4.5.2 Variability of PAR with biophysical factors under open conditions

The variability of PAR was assessed in relation to three biophysical parameters viz., elevation, aspect, and ground slope, under open conditions (sites devoid of any overhead vegetation). Only the slope and aspect of the three factors had a significant influence on the variability of the PAR (Fig. 16). The analysis of variance estimates showed that these two variables did not show any strong effect on the variance of total PAR at the ground, as indicated by the R^2 value of 0.064 at the 5% level (Table 11, 12, 13 and 14).

Although both of these parameters did not show any strong correlation with total PAR. PAR in open conditions exhibited positive relation with the slope (Fig. 17, 18 and 19). However, the relationship was not found to be very strong (R^2 =0.028). The regression modelling of the variables was done by following the stepwise regression modelling approach. The regression model generated that describes the relation of PAR in open conditions with significant values is given below:

$$\mathbf{Y = 83.746 + 20.664x_1 - 2.381x_2}$$

Where:

Y = PAR

$\beta_\circ$ = Intercept

X_1 = Aspect

X_2 = slope

Table 11: Model Summary for Variability of PAR in open conditions

R	0.253	RMSE	73.381
R-Squared	0.064	Coef. Var	84.618
Adj. R-Squared	0.044	MSE	5384.742
Pred R-Squared	-0.071	MAE	45.998

RMSE: Root Mean Square Error
MSE: Mean Square Error
MAE: Mean Absolute Error

Table 12: ANOVA for Variability of PAR in open condition

	Sum of Squares	DF	Mean Square	F		Sig.
Regression	34306.314	2	17153.157	3.186		0.0459
Residual	500780.977	93	5384.742			
Total	535087.291	95				

Table 13: Parameter Estimates for Variability of PAR in open conditions

model	Beta	Std. Error	Std. Beta	t	Sig	lower	upper
(Intercept)	83.746	8.187	-	10.230	0.000	67.489	100.003
Aspect	20.664	8.196	0.404	2.521	0.013	4.389	36.939
Slope	-2.381	1.257	-0.304	-1.894	0.041	-4.877	0.115

Table 14: Stepwise Selection Summary for Variability of PAR in open conditions

Step	Variable	Added/ Removed	R-Square	Adj. R-Square	C(p)	AIC	RMSE
1	Aspect	addition	0.028	0.018	-76.8480	1103.7898	74.3842
2	Slope	addition	0.064	0.044	-75.4110	1102.1555	73.3808

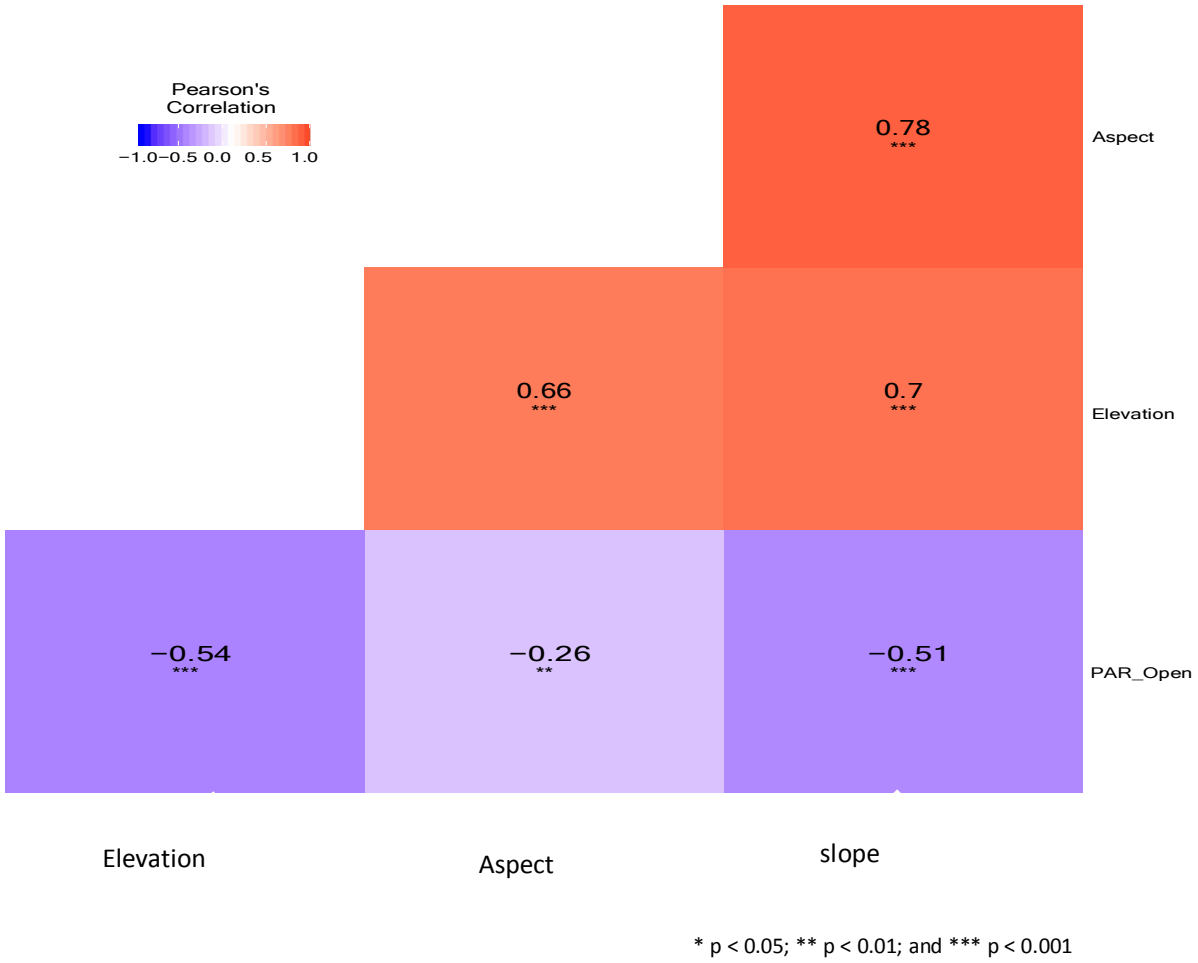

Fig 16: Pearson's correlation map for variability of PAR in open conditions

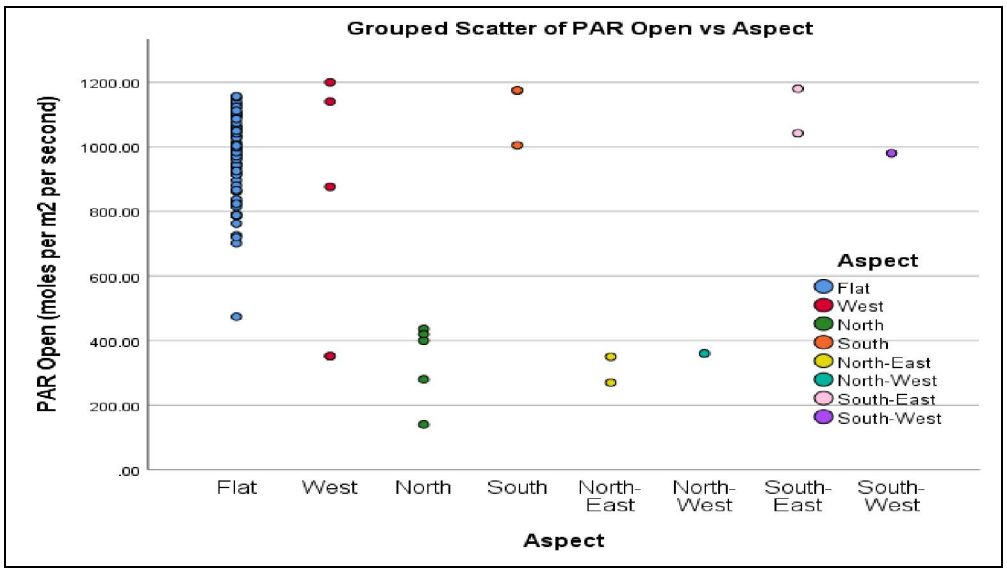

Fig 17: Grouped scatter plot between PAR in Open and Aspect

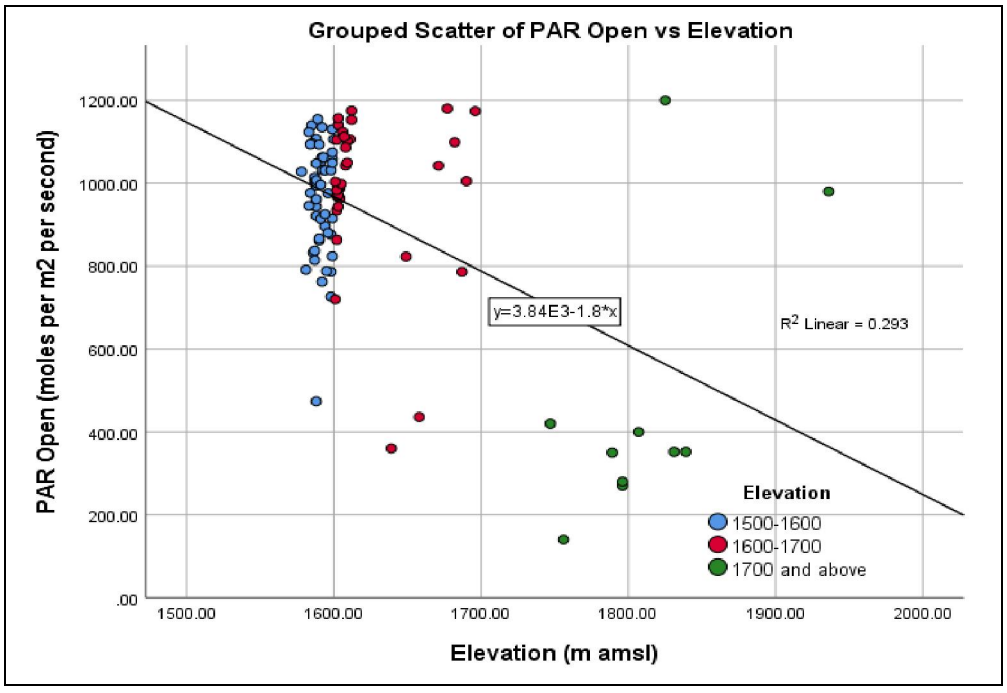

Fig 18: Grouped scatter plot between PAR in Open and Elevation

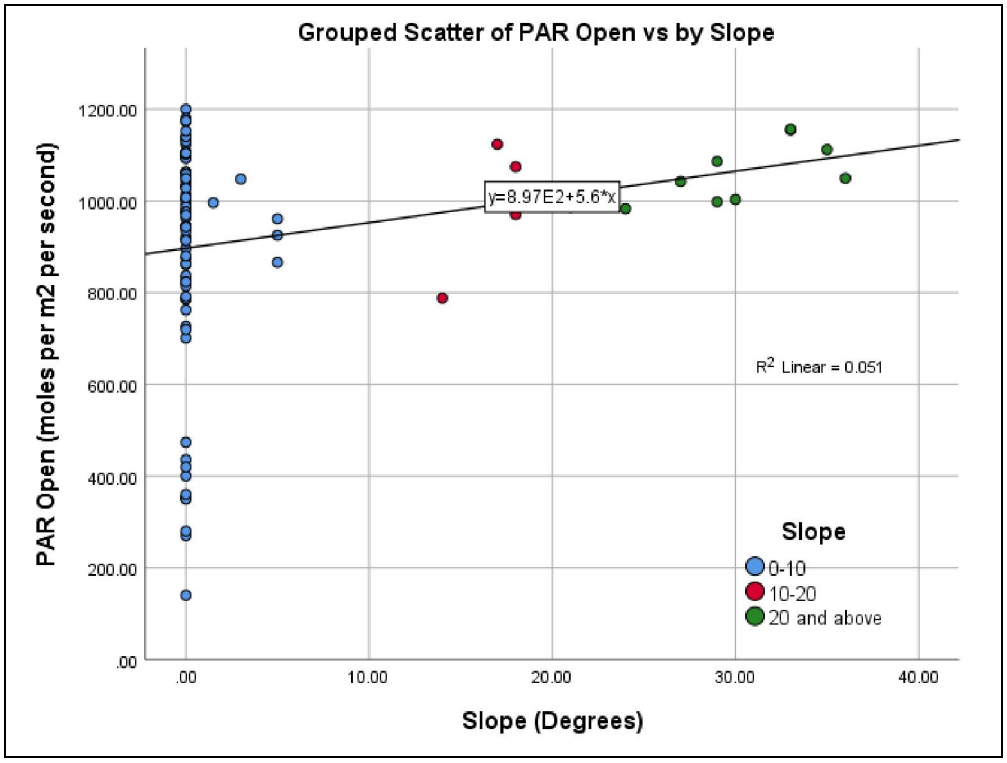

Fig 19: Grouped scatter plot between PAR in Open and Ground Slope

4.5.3 Variability of PAR with biophysical factors Under Canopy

Aspect, Elevation, Slope, Tree Density, Tree Diameter, Canopy Density, and Age of the Trees were employed to analyse the PAR Variability under the Canopy (Fig. 20). Only canopy density and tree density out of all the aforementioned biophysical characteristics demonstrated a substantial impact on PAR variability when using the regression analysis method with calculated Coefficient of Determination (R^2 =0.35) at the 5% level (Table 15).

The tree density, with an R^2 value of 0.351, had the significant impact on the PAR under canopy, followed by the canopy density, with an R^2 value of 0.314 (Table 16, 17 and 18). The PAR under the canopy was found to be negatively correlated with both the canopy density and tree density factors, meaning that when these parameters increased in value, the PAR under the canopy decreased and vice versa (Fig 21, 22, 23, 24, 25 and 26).

The regression model built by following stepwise regression modelling approach is given as follows:

$$\mathbf{Y = 266.972 - 2.057x_1 - 0.108x_2}$$

Where:

Y = PAR

$\beta_\circ$ = Intercept

X_1 = Canopy density

X_2 = Tree density

Table 15: Model Summary for Variability of PAR Under Canopy

R	0.593	RMSE	61.087
R-Squared	0.351	Coef. Var	70.442
Adj. R-Squared	0.337	MSE	3731.602
Pred R-Squared	0.290	MAE	41.842

RMSE: Root Mean Square Error
MSE: Mean Square Error
MAE: Mean Absolute Error

Table 16: ANOVA for Variability of PAR Under Canopy

	Sum of Squares	DF	Mean Square	F	Sig.
Regression	188048.313	2	94024.157	25.197	0.0000
Residual	347038.977	93	3731.602		
Total	535087.291	95			

Table 17: Parameter Estimates for Variability of PAR Under Canopy

model	Beta	Std. Error	Std. Beta	t	Sig	lower	upper
(Intercept)	266.972	26.231	-	10.178	0.000	214.882	319.063
Canopy density	-2.057	0.329	-0.529	-6.257	0.000	-2.710	-1.404
Tree density	-0.108	0.047	-0.196	-2.315	0.023	-0.201	-0.015

Table 18: stepwise selection summary of variability of PAR under canopy

Step	Variable	Added/ Removed	R-Square	Adj. R-Square	C(p)	AIC	RMSE
1	Canopy density	addition	0.314	0.307	4.4870	1070.3272	62.4870
2	Tree density	addition	0.351	0.337	1.2300	1066.9492	61.0868

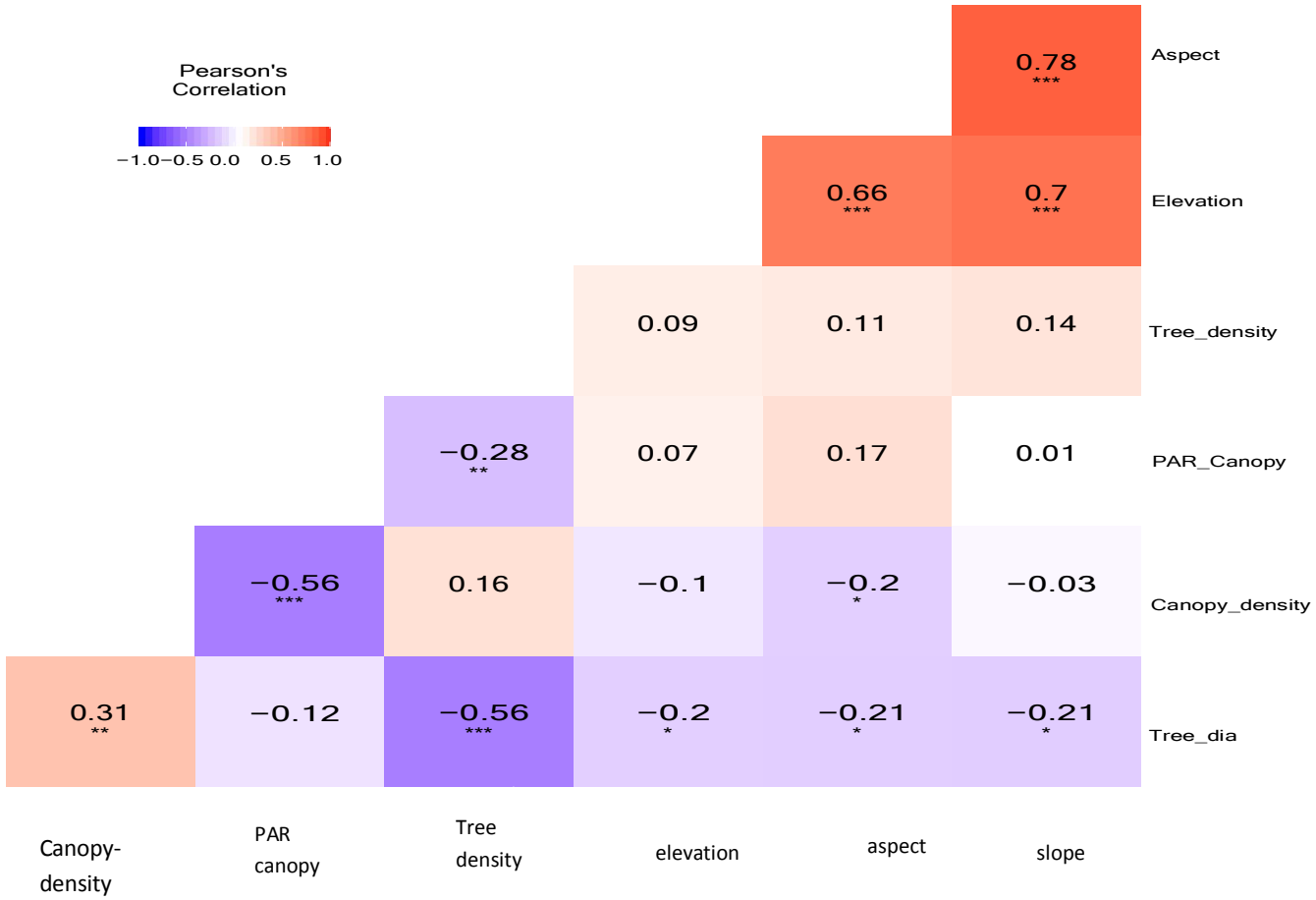

Fig 20: Pearson's correlation map for variability of PAR under canopy

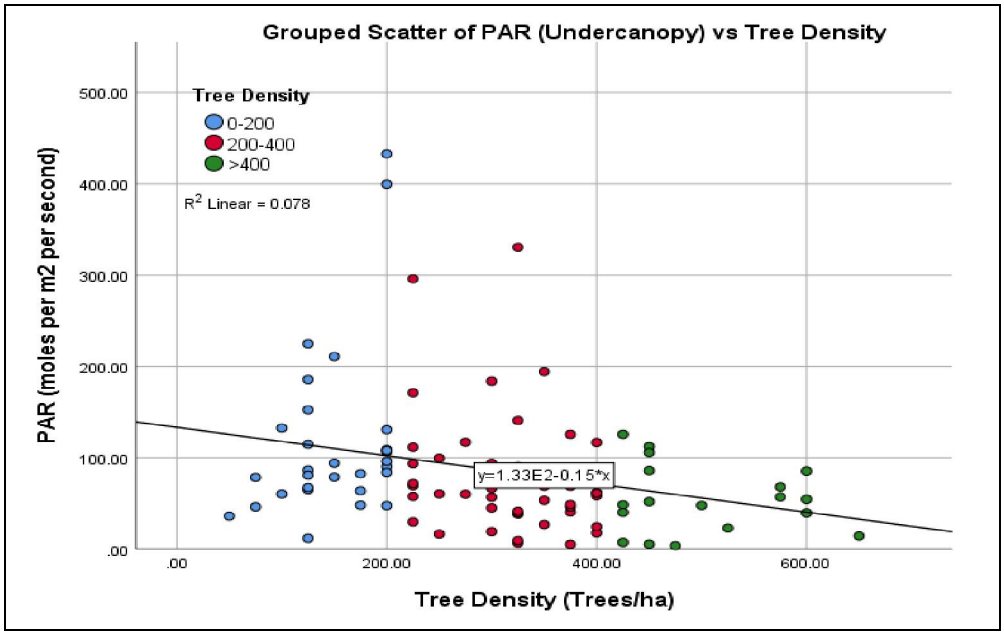

Fig 21: Grouped scatter plot between PAR under canopy and Tree Density

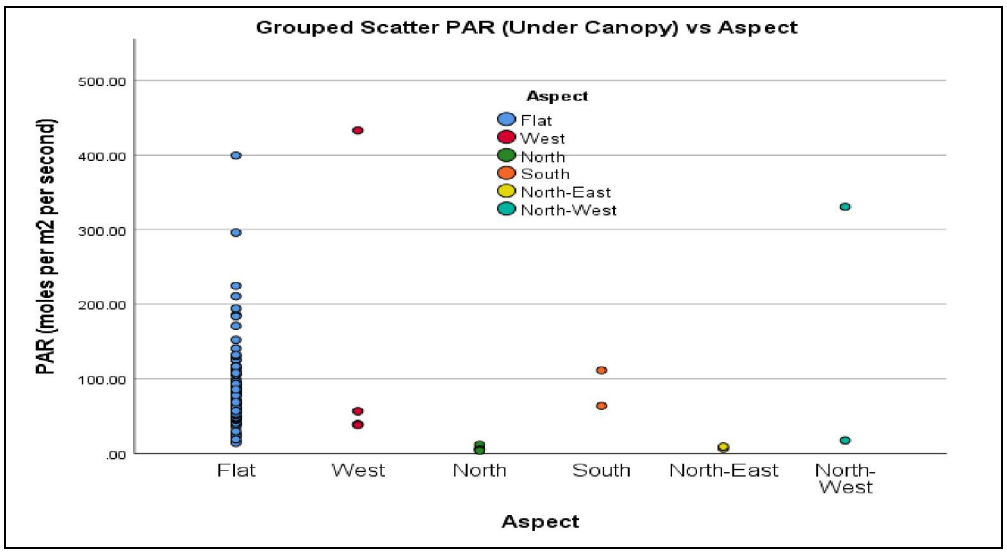

Fig 22: Grouped scatter plot between PAR under canopy and Aspect

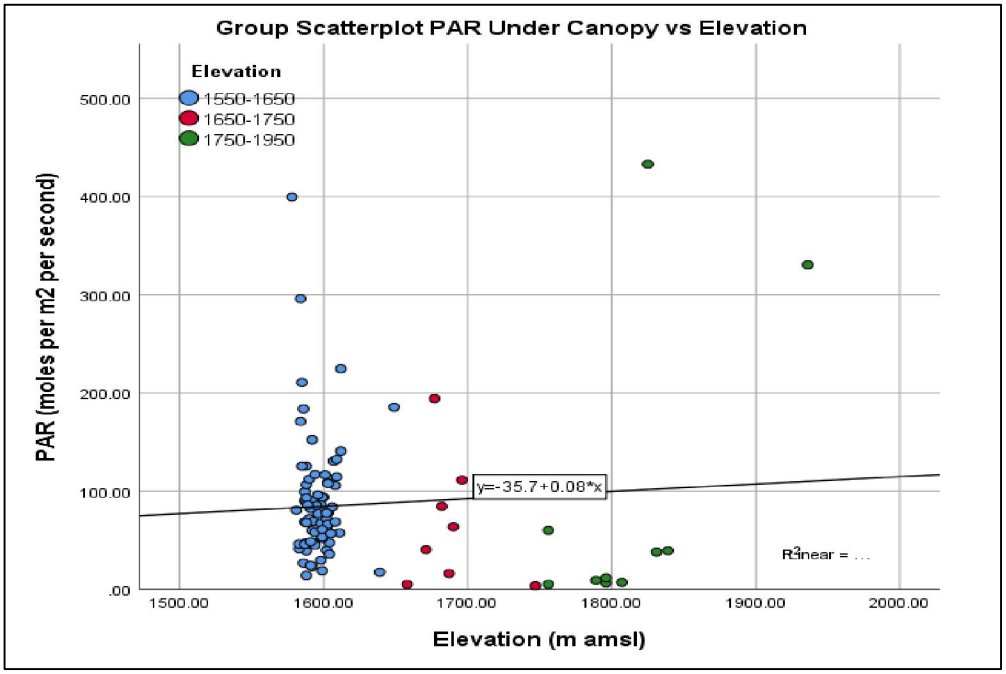

Fig 23: Grouped scatter plot between PAR under canopy and Elevation

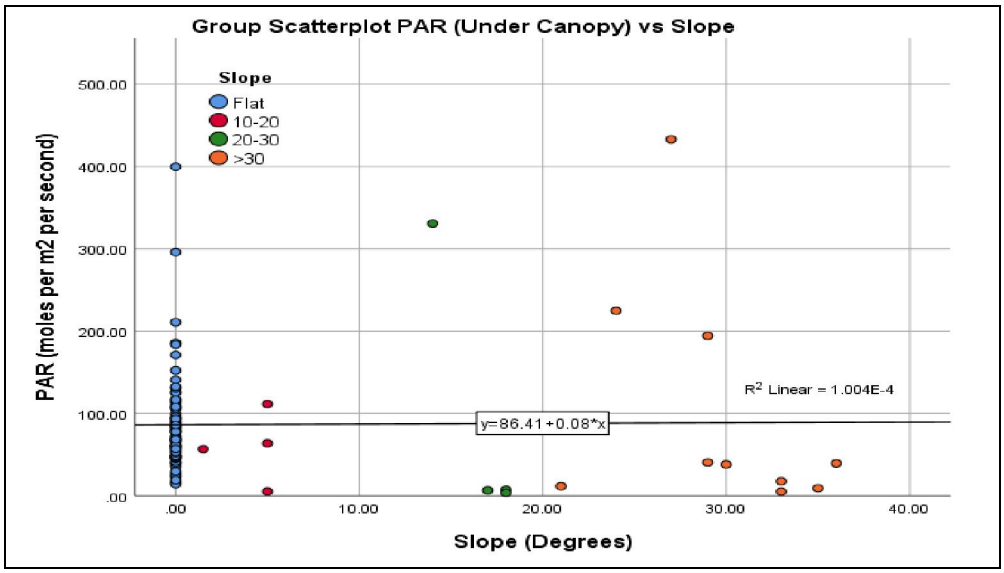

Fig 24: Grouped scatter plot between PAR under canopy and Ground Slope

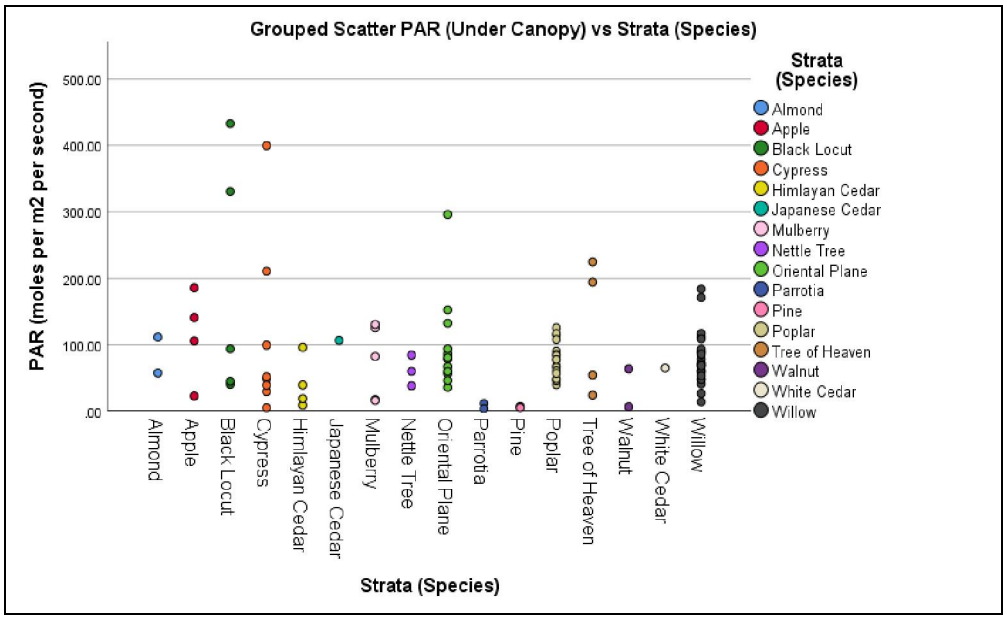

Fig 25: Grouped scatter plot between PAR under canopy and species strata

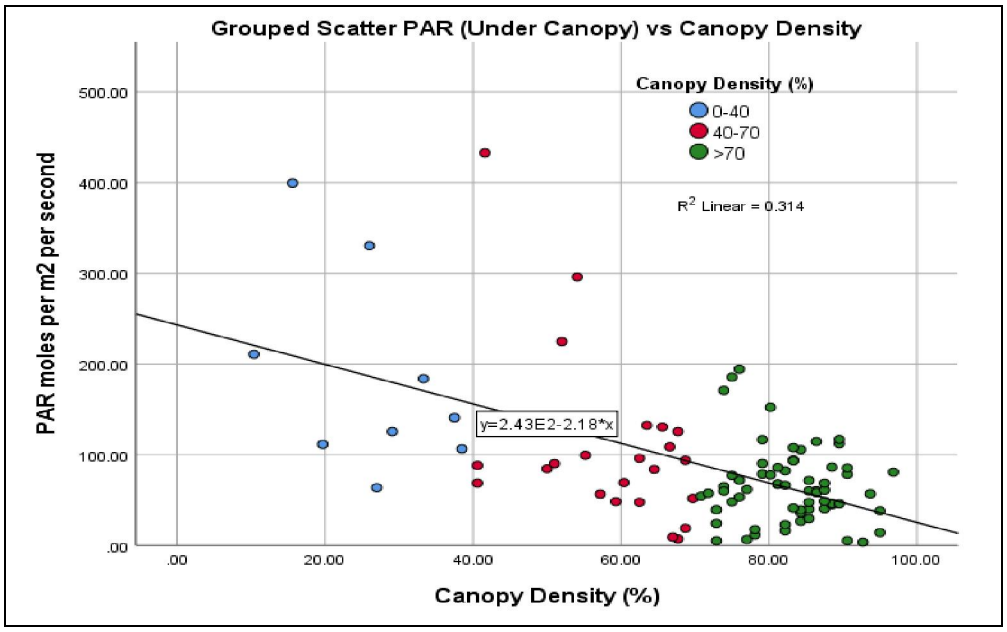

Fig 26: Grouped scatter plot between PAR under canopy and Canopy Density

4.5.4 Variability of Surface temperature

Different biophysical factors, such as aspect, elevation, tree density, tree diameter, species strata, and tree age, were taken into account to analyse the variability of soil surface temperature (Fig.27, 28, 29, 30 and 31). To examine the effect of these variables on the variability of surface temperature, several statistical calculations were carried out. Only three of these variables including canopy density, aspect, and elevation showed a significant impact on the variability of surface temperature with a coefficient of determination (R^2) value of 0.233 (Table 19).

Out of the three significant covariates, elevation had the most impact on variability, with an R^2 value of 0.233. This was followed by aspect, which had an R^2 value of 0.203, and canopy density, which had an R^2 value of 0.167 (Table 20, 21 and 22).

The soil surface temperature regression equation model is shown below, taking into account the elevation and canopy density aspects of that particular area.

$$\mathbf{Y=45.026 - 0.077\ x_1 + 0.972\ x_2 - 0.013\ x_3}$$

Where:

Y = soil surface temperature

$\beta_\circ$ = Intercept

X_1 = Canopy density

X_2 = Aspect

X_3 = elevation

Table 19: Model Summary for Variability of Surface temperature

R	0.482	RMSE	3.663
R-Squared	0.233	Coef. Var	19.921
Adj. R-Squared	0.208	MSE	13.419
Pred R-Squared	0.104	MAE	2.563

RMSE: Root Mean Square Error
MSE: Mean Square Error
MAE: Mean Absolute Error

Table 20: ANOVA for Variability of Surface temperature

	Sum of Squares	DF	Mean Square	F	Sig.
Regression	374.502	3	124.834	9.303	0.0000
Residual	1234.555	92	13.419		
Total	1609.057	95			

Table 21: Parameter Estimates for Variability of Surface temperature

model	Beta	Std. Error	Std. Beta	T	Sig	lower	upper
(Intercept)	45.026	11.302	-	3.984	0.000	22.580	67.473
Canopy density	-0.077	0.020	-0.362	-3.880	0.000	-0.117	-0.038
Aspect	0.972	0.347	0.347	2.799	0.006	0.282	1.661
Elevation	-0.013	0.007	-0.232	-1.902	0.060	-0.027	0.001

Table 22: Stepwise Selection Summary for Variability of Surface temperature

Step	Variable	Added/ Removed	R-Square	Adj. R-Square	C(p)	AIC	RMSE
1	Canopy density	addition	0.167	0.158	5.7540	531.4832	3.7753
2	Aspect	addition	0.203	0.185	3.6180	529.3329	3.7144
3	Elevation	addition	0.233	0.208	2.0770	527.6315	3.6632

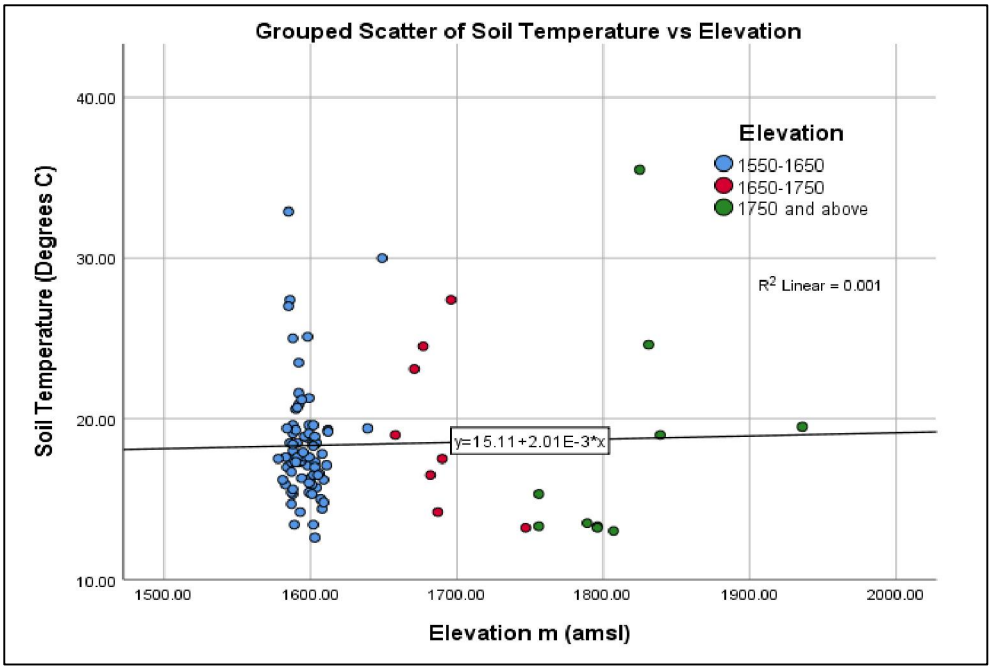

Fig 27: Grouped scatter plot between Soil Temperature and Elevation

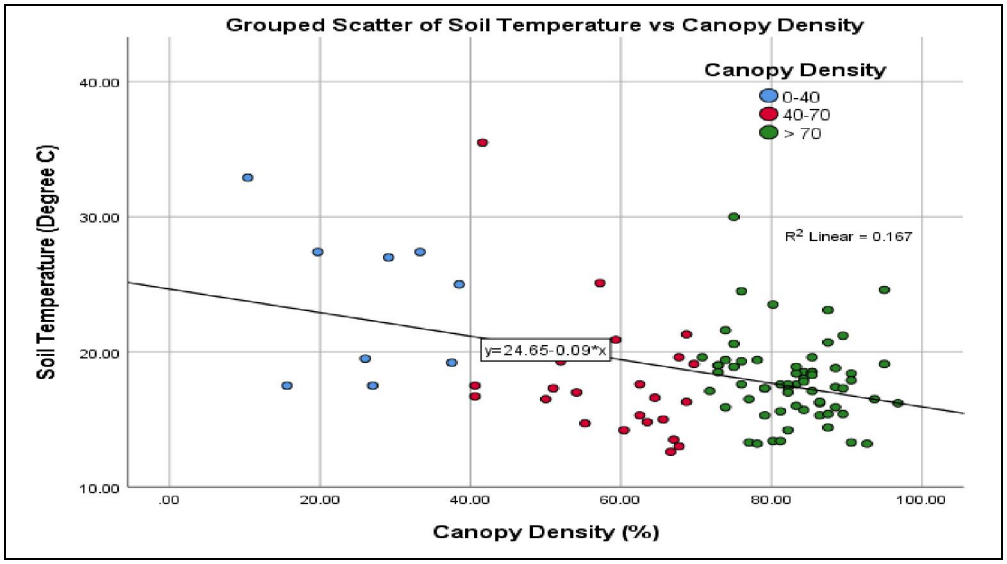

Fig 28: Grouped scatter plot between Soil Temperature and Canopy Density

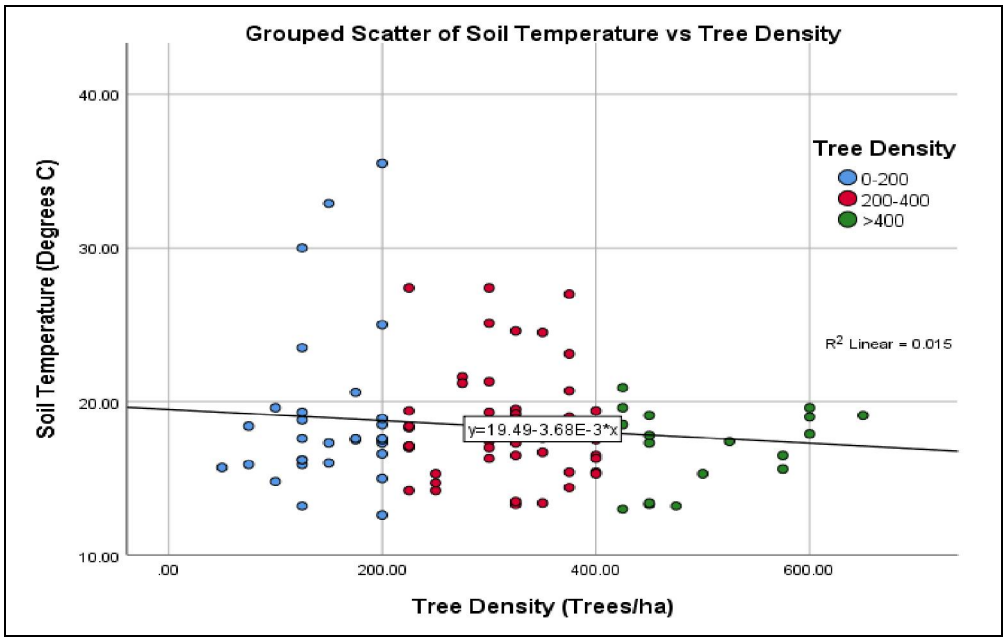

Fig 29: Grouped scatter plot between Soil Temperature and Tree Density

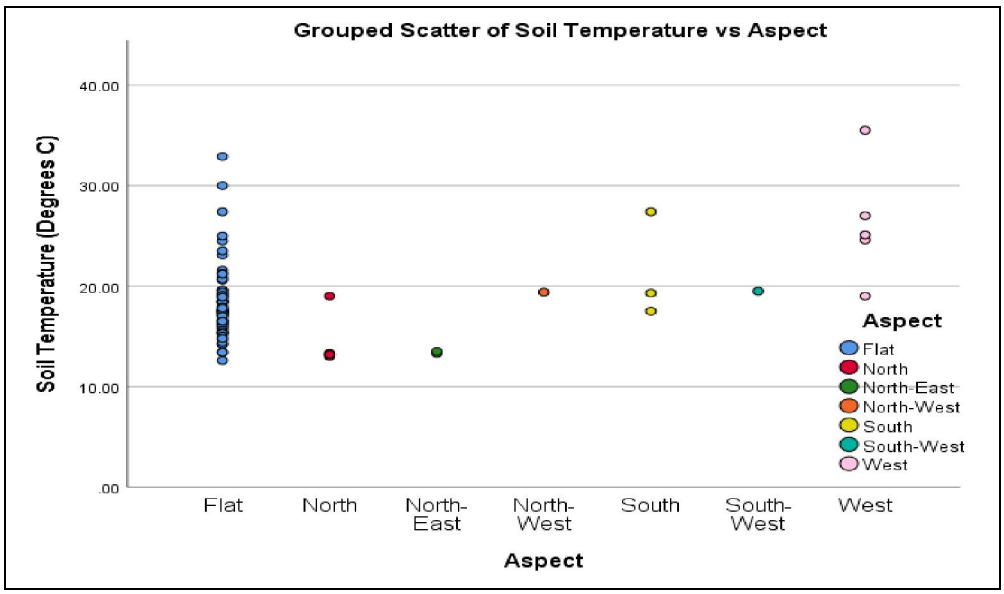

Fig 30: Grouped scatter plot between Soil Temperature and Aspect

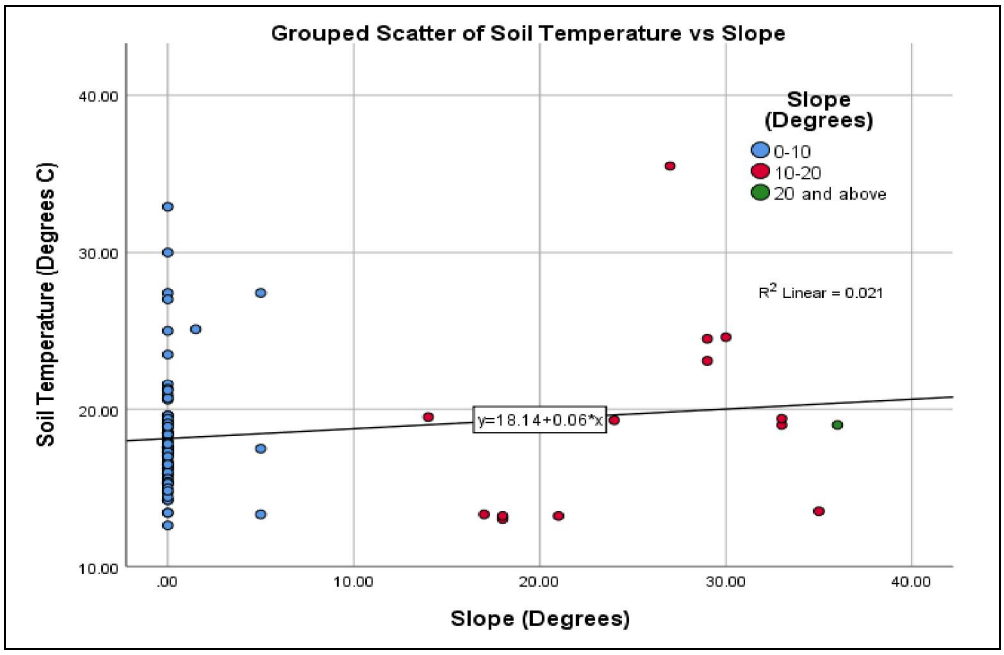

Fig 31: Grouped scatter plot between Soil Temperature and Ground Slope

4.6 Individual relations of different biophysical variables with photosynthetically active radiation (PAR)

Under the natural conditions of Srinagar's urban forest division, the relationship between PAR and other biophysical factors was evaluated. Following is a brief summary of the outcomes.

A comparison of the relationship between PAR and various classifications of forest density was made. The open forest, which had an average PAR of 135.448 $\mu molm^{-2}s^{-1}$, and the closed forest, which had an average PAR of 76.4207 $\mu molm^{-2}s^{-1}$, were shown to have the greatest variability effects. The forest scrub, which had vegetation less than 10%, had the least effect on the variability of total PAR with average PAR value of 305.15($\mu molm^{-2}s^{-1}$) (Table 23).

The variability of PAR with respect to tree density indicated that the areas with tree densities up to 200 trees/ha had the least impact on the total PAR, with an average PAR received of 117.4043 $\mu molm^{-2}s^{-1}$, followed by tree density of 200-400/ha. The highest impact on the total PAR was detected in areas with tree densities of 400 trees/ha with average PAR of 56.0568 $\mu molm^{-2}s^{-1}$recorded under the canopy, thus the increasing tree density showed a negative corelation to the amount of PAR transmitting through the tree canopies (Table 23).

When the variability of PAR was evaluated in relation to tree age, the findings revealed that the young aged trees with higher tree density had the most effect on PAR variability, followed by middle aged trees and old aged tree class (with lower tree density) having the least impact, thus showing a negative relation of tree age with the total PAR. The average PAR under old-aged trees was found to be 120.1 $\mu molm^{-2}s^{-1}$, with middle-aged trees coming in second with 83.902 $\mu molm^{-2}s^{-1}$and young-aged trees coming in third with 90.1507 $\mu molm^{-2}s^{-1}$ (Table 23).

According to the variability of PAR with regard to the Aspect, the South-East Aspect had the highest average values of PAR (111.15 $\mu molm^{-2}s^{-1}$) and the North-East Aspect had the lowest average value of (310 $\mu molm^{-2}s^{-1}$) (Table 24).

The relationship between elevation and PAR variability showed that the PAR decreased as elevation increased. Average PAR values were found to be 977 $\mu molm^{-2}s^{-1}$ for the elevation range of 1550–1650(mamsl), 885.0556 $\mu molm^{-2}s^{-1}$ for the elevation range of 1650–1750(mamsl), and 502.57 $\mu molm^{-2}s^{-1}$ for the elevation range of 1750–1950(mamsl), which recorded the lowest amount of PAR values (Table 25).

The study of the correlation between PAR and the degree of ground slope revealed, the intensity of total PAR dropped as ground slope increased. The maximum average PAR value, 977.7795 $\mu molm^{-2}s^{-1}$, was observed on flat terrain. This was followed by a reduction, 658.225 $\mu molm^{-2}s^{-1}$, at slopes between 10° and 20°, and the lowest values, 370 $\mu molm^{-2}s^{-1}$, at slopes over 30° (Table 25).

The classified PAR values exhibited a variability with the average soil temperature. The soil temperature increased as total PAR received increased and vice-versa, employing a direct correlation between the amount of PAR received and the surface temperature. The following data was gathered regarding the average soil temperature and total PAR (Table 26).

- In open conditions
  - 100-300 $\mu molm^{-2}s^{-1}$= 13.2°C, 300-600 $\mu molm^{-2}s^{-1}$=20.8°C, 900 $\mu molm^{-2}s^{-1}$ and above=27.4°C.
- In closed conditions
  - 0-100 $\mu molm^{-2}s^{-1}$= 11.56°C, 100-200 $\mu molm^{-2}s^{-1}$=13.7°C, 200-300 $\mu molm^{-2}s^{-1}$=15.3°C, 300 $\mu molm^{-2}s^{-1}$ and above= 16.11°C.

While comparing the PAR values that were recorded under the canopy of various tree layers. The trees that transmitted the most PAR through their canopies were as *Robinia pseudoacacia* (188.552 $\mu molm^{-2}s^{-1}$) followed by the *Malus domestica* (113.7575 $\mu molm^{-2}s^{-1}$) and *Cryptomeria japonica* (106.5 $\mu molm^{-2}s^{-1}$). the tree species with lowest PAR values under canopy were *Aesculus indica* (6.55 $\mu molm^{-2}s^{-1}$) and *Pinus wallichiana* (6.205 $\mu molm^{-2}s^{-1}$). However, conifers exhibited higher average PAR values than broadleaved species under canopy (Table 27).

Table 23: Average PAR against Forest Density, Tree Density and Tree Age

PAR in relation to forest density	Forest density class	closed forest 40% and above	open forest 10%-40%	forest scrub less than 10%	**Mean (S. E)**
	Average PAR ($\mu mol\ m^{-2}\ s^{-1}$)	**76.42**	**135.44**	**305.15**	**172.3 (7.65)**
PAR in relation to tree density	Tree density class	0-200	200-400	400 and above	
	Average PAR ($\mu mol\ m^{-2}\ s^{-1}$)	**117.40**	**82.91**	**56.05**	**85.4 (7.65)**
PAR in relation to tree age	Tree age class	young	middle	Old	
	Average PAR ($\mu mol\ m^{-2}\ s^{-1}$)	**90.15**	**83.90**	**120.1**	**98.05 (8.61)**

Table 24: Average PAR in relation to Aspect

PAR in relation to Aspect	Aspect	flat	west	north	south	north-east	north-west	south-west	south-east	Mean (S. E)
	Average PAR ($\mu mol\ m^{-2}\ s^{-1}$)	971.28	784.08	335.24	1082.4	310	360	980.2	1111.15	**741.7 (24.2)**

Table 25: Average PAR in relation to Elevation and Slope

PAR in relation to elevation	elevation range	1550-1650	1650-1750	1750-1950		**Mean (S. E)**
	Average PAR ($\mu mol\ m^{-2}\ s^{-1}$)	**977.51**	**885.05**	**502.57**		**788.3 (24.25)**
PAR in relation to degree of slope	Slope range	Flat	10-20	20-30	30 and above	
	Average PAR ($\mu mol\ m^{-2}\ s^{-1}$)	**977.77**	**658.22**	**975.46**	**370**	**754.3 (24.25)**

Table 26: Average soil surface Temperature in relation to PAR

PAR in relation to soil surface Temperature (In open conditions)	PAR Range **(µmol m^{-2} s^{-1})**	100-300	300-600	600-900	900 above	**Mean (S. E)**
	Average soil surface Temperature (**°C**)	**13.26**	**20.86**	**24.63**	**27.46**	**21.5 (0.42)**
PAR in relation to soil surface Temperature (Under canopy)	PAR Range **(µmol m^{-2} s^{-1})**	0-100	100-200	200-300	300-above	
	Average soil surface Temperature (**°C**)	**11.56338**	**13.75789**	**15.37778**	**16.11111**	**14.2 (0.)**

Table 27: Average PAR under plant canopy of different species strata

Species strata	**Average PAR ($\mu mol\ m^{-2}\ s^{-1}$)**
Robinia pseudoacacia	188.552
Cedrus deodara	40.8875
Celtis australis	60.93
Cupressus sp.	66.57
Pinus wallichiana	6.205
Aesculus indica	6.55
Parotia jacquemontiana	7.62
Malus domestica	113.7575
Morus sp.	74.412
Prunus armeniaca	111.41
Juglans regia	63.67
Platinus orientalis	125.42
Alainthus altissima	124.4
Populus sp.	83.624
Salix sp.	53.45
Prunus dulcis	57.5
Thuja orientalis	64.9
Cryptomeria japonica	106.5
Mean	**75.35**
S. D	**47.379**
S. E	**11.16**

Chapter-5

DISCUSSION

This chapter includes discussion of the results from the experiments carried out to study the "Vegetation mapping and variability assessment of photosynthetically active radiation (PAR) in urban forest division of Srinagar". The findings from the current study are discussed under the following topics in light of the literature that is currently available from various sources:

5.1 Landuse/Landcover (LULC)/Urban vegetation mapping using Sentinel-2A data

Using Sentinel-2A data from 2021, a Landuse/Landcover map of Srinagar's Urban Forest Division was produced for the current study. 12 LULC groups were created for this investigation utilising a visual image interpretation technique (Table 2) viz. Agriculture, Closed Forest, Forest Scrub, Grassland, Horticulture, Habitation, Open Forest, trees outside forest (TOF), Urban green Utilities, Wasteland, Waterbody and Wetland respectively. It was observed that the highest coverage was under habitation (37.22%) > waterbodies (11.19%) > trees outside forest (10.47%) > closed forest (8.77%) > agriculture (6.95%) > open forest (5.10%) > wetland (5.03%) > grassland (4.67) > urban green utilities (3.87%) > wasteland (3.78%) > forest scrub (1.83%) > horticulture (1.10%). Landuse/Landcover map of study area has been shown in Fig. 5. The mapping was carried out using mapping software ArcGIS at 1:20000 mapping scale. Several researchers have carried out studies on LULC assessment utilising different types of satellite data such as work conducted by Mohammadpour *et al.* (2022), Gebreslasie *et al.* (2020), Nguyen *et al.* (2020) and Qiu *et al.* (2020). Several researchers in the past have also used Sentinel-2A imageries to generate LULC maps, like the study conducted by Randazzo *et al.* (2021) where Sentinel-2A data was used while carrying out investigations for LULC mapping of the Pocket beaches (PBs) located in the province of Messina, Italy.

5.2 Forest cover density map

Area under forest in Urban Forest Division of Srinagar was assessed using Sentinel-2A data with mapping carried out at 1:20000 mapping scale. The forest of study area was classified into closed forest, open forest and forest scrub as per the scheme of density wise classification of forests in india (FSI, 2001). Forest cover density map of Urban Forest Division of Srinagar (2021) has been shown in Fig. 7. Exposition of data presented in Table. 4 revealed that the highest coverage in the study area was under closed forest (8.77%) > open forest (5.10%) > forest scrub (1.83%). The delineated forest density classes in Urban Forest Division of Srinagar were based on tone and texture of the image complemented by ground truth points. Several studies have categorised forest cover density classes using the similar classification scheme (Wani *et al.,* 2019 and Wani *et al.,* 2014)

Alam *et al.* (2014) while assessing the forest canopy density of a tropical protected area in Gir National Park and Sanctuary using geospatial techniques, it was discovered that about 63.5 percent of the forest area was covered with a density of less than 10 to 40 percent, and that 35.89 percent of the forest area fell into the density class of 40 to more than 70 percent. Similarly, Wani *et al.* (2016) While assessing deforestation and forest degradation in the context of the REDD+ policy using multi-temporal (1980-2030) forest cover dynamics in the Kashmir Himalayan region, it was discovered that closed forest area remained dominant in the region across all time periods with 24.81 percent in 2009 and open forest formed the dominant forest strata with 11.27 percent, while the lowest area was registered for grasslands with 2.5 percent.

The accuracy assessment and map validation of LULC maps of study area was calculated from ground truth points (reference points) collected by using stratified random sampling (Fig. 10.). With a kappa statistic of 0.909, the LULC map's overall classification accuracy was determined to be 91.67 percent (Table 5 and 6).

5.3 Variability of Photosynthetically Active Radiation (PAR)

Terrestrial ecosystems' organic and biological cycles depend critically on the spectral range of photosynthetically active radiation (PAR) (Mayer *et al.,* 2002; Sudharsan *et al.,* 2013), which determine the rate of vegetation's photosynthetic activity, influencing the productivity of natural and agricultural ecosystems (Akitsu *et al.,* 2015). A plant canopy is a complex structure made primarily of stems, branches, and leaves that are arranged in a specific volume. Despite the fact that sun-oriented radiation's quantity and quality are constantly fluctuating, the majority of it is devoured by overhanging leaves and little of it is reflected (Campbell and Norman 1998). As a result, the PAR absorption of a canopy roughly corresponds to the ratio of the incident PAR above the canopy (PARi) to the transmitted PAR below the canopy (PARt).

The variability of Photosynthetically Active Radiation (PAR) was assessed in respect to different biophysical parameters viz. canopy density, tree density, tree age, elevation, degree of slope, aspect and soil temperature in the study area. canopy density and tree density had an inverse relation with the PAR under canopy (R^2 0.35). The results showed that when the PAR passed through the canopy cover the lowest amount of PAR amount was transmitted by the closed forest canopy with an average of 76.4207($\mu molm^{-2}s^{-}$) while, as the forest scrubs has shown the highest values for PAR (305.15 $\mu molm^{-2}s^{-}$). PAR with respect to tree density further revealed that the lowest amount of PAR was transmitted with tree density of 400 trees/ha while as, tree densities upto 200/ha showed least values for the PAR. When the variability of PAR was evaluated in relation to tree age, the findings revealed that the young aged trees with high tree density had high PAR transmission, followed by middle aged trees and old aged tree class with reducing number of stems (Table 23) illustrating that with the increase in canopy density and tree density the impact on the variability of PAR also increased. These findings closely resemble those of Rosati *et al*. (2021), who

discovered that crops grown in super high density (SHD) olive systems had significantly more spatial variation in transmitted PAR (0.21 mol m^{-2} under tree row, upto 0.59 mol m^{-2} in the Alley center). Low PAR values are more frequently received in shaded positions, which causes the daily PAR frequency distribution to fluctuate more. Many other works are also in confirmation with the present study (Ningyi *et al.,* 2020 and Tian *et al.,* 2021)

According to the variation in PAR with respect to aspect, the north-east aspect had the lowest values of PAR and the south-east aspect had the highest values. Comparing it to the degree of slope further revealed that as the slope of the ground increased, the amount of PAR likewise reduced, with the majority of the PAR amount being received on flat ground. These findings are supported by research conducted by Tian *et al*. (2001), who found that the actual amount of solar radiation that a surface receives depends greatly on its geometry (slope and aspect). Additionally, as the angle between the solar beam and the normal of the horizontal surface is at its lowest in the summer, an increase in slope causes a decrease in solar radiation. He further said that the solar radiations are lower on the northern aspect at a given latitude and slope (south in southern aspect).

When the soil surface temperature was correlated with the amount of PAR, it was observed that the temperature increased under both open and closed circumstances when the amount of PAR increased. PAR and elevation showed a direct correlation, the intensity of PAR showed a declining trend as elevation increased and vice versa. These observations are very much similar to the study conducted by Hu *et al.* (2007) on spatiotemporal characteristics of photosynthetically active radiation in China. In their study it was revealed that with high altitudes there is lower amount of short-wave radiation and high fractions of PAR, which may be due to thinner atmosphere that reduces Rayleigh Scattering of short-wave radiations. Other studies (Nikolas *et al.,* 2019 and Guangren *et al.,* 2007) showed a similar relation.

Further it was observed that coniferous tree layers transmit more PAR toward the ground than deciduous tree layers, according to an assessment of the change in the PAR with respect to various tree strata. This statement is supported by Gendron *et al.* (2006) while carrying their study on the angular distribution of diffused PAR within deciduous and conifer forest stand of British Columbia, Canada. They conclude that at the higher altitudes conical crown of conifers transmit greater amount of light at higher elevation angles pertaining to their tall, narrow crowns with majority of their shoots oriented close to the horizontal position. Some other studies also reflected a similar trend (Kume *et al.,* 2011 and Leuchner *et al.,* 2011).

Stepwise regression modelling approach was carried out for model building of variability assessment of PAR with different parameters. The regression model for variability of PAR under canopy was $Y= 266.972 - 2.057x_1 - 0.108x_2$. the regression model for variability of PAR under open conditions was $Y= 83.746 + 20.664x_1 - 2.381x_2$. regression model for variability of PAR with respect to soil surface temperature was $Y=45.026 – 0.077\ x_1 + 0.972\ x_2 – 0.013\ x_3$ and the regression model for checking the variability of canopy density was $Y=3450.159-1.55\ x_1- 13.852\ x_2+ 78.045\ x_3$. These models are quite helpful in deriving the results with greater accuracy. Many researchers have been using this method for deriving relation of biophysical factors in the forest ecosystem (Naesset *et al.,* 2004; Merian *et al., 2011* and Paruelo *et al.,* 1997).

5.4 Variability of canopy density

In the study region, the variation in canopy density in connection to biophysical variables was evaluated. When relating the canopy density to biophysical characteristics, factors such as species strata, tree density, aspect, elevation, and average tree diameter were taken into account. The elevation, aspect, and slope demonstrated their significant effect on the canopy density (R2 0.41).

According to the test results, aspect, slope, and elevation all had a negative association with canopy density, indicating that when these variables were raised, the percentage of canopy density fell. The northern aspect had the lowest canopy density, whereas the southern aspect had an increasing trend. South-western aspects had the highest percentage values of canopy density. The ground slope trend followed a similar pattern; as the degree of ground slope increased, the proportion of canopy density decreased. Additionally, as elevation increased, the percentage of the canopy density exhibited a decreasing trend. These observations are similar to the study conducted by Pinag *et al.* (2007) who studied the Relationships among slope, canopy height and vegetation greenness over coastal wet tropical forests in Australia and Brazil. In their study they found that Brazilian site showed significant differences in canopy greenness associated to different slope ranges. Some other studies also reflected a similar trend (Menak Panta 2003 and Gao *et al.,* 2000).

Chapter 6

SUMMARY AND CONCLUSION

The salient findings during the course of investigation entitled, "Vegetation mapping and variability assessment of photosynthetically active radiation (PAR) in urban forest division of Srinagar" are summarized as below:

- The study area was delineated via visual image interpretation technique into 12 Landuse/Landcover (LULC) classes viz, Agriculture, Closed Forest, Forest Scrub, Grassland, Horticulture, Habitation, Open Forest, trees outside forest (TOF), Urban green Utilities, Wasteland, Waterbody and Wetland.

- LULC map (2021) revealed that among all the LULC classes, habitation occupied maximum area of the map i.e., 37.22 per cent while as horticulture with an area of 1.10 per cent occupied minimum portion of the map.

- The overall classification accuracy of LULC map came out to be 91.67 per cent with kappa coefficient of 0.909.

- FCD map of study area was classified into closed forest, open forest and forest scrub as per the scheme of crown density wise classification of forests in india (FSI, 2021)

- Density wise forest cover (2021) of study area reveals that closed forest occupied maximum portion (8.77%) of the total area (16596.12 ha) while as forest scrub occupied minimum portion (1.83%) of the total area of division.

- Regression modelling was done to check the variability pattern of canopy density, variability of PAR under canopy, variability of PAR in open

conditions and variability of PAR with soil temperature using stepwise regression modelling method.

- With increase in canopy density total PAR transmitted showed a decreasing trend with open forest showing highest amount of PAR of 135.448 $\mu molm^{-2}s^{-1}$ and the lowest in closed forest with average PAR transmitted as 76.4207 $\mu molm^{-2}s^{-1}$.

- With increase in tree density the average PAR transmitted decreased with highest average PAR recorded at 200 trees/ ha and the lowest at tree density of 400 trees/ha and above.

- Young aged trees with high tree density showed the lower transmission of total PAR towards ground and highest values of PAR were recorded in old aged tree stands with reduced number of stems.

- With increase in elevation the total PAR showed a decreasing trend and vice-versa.

- The increase in ground slope resulted in the decrease in total PAR with highest PAR recorded at flat grounds.

- Highest amount of PAR was seen in South-East aspect and lowest levels were recorded at North-East aspects.

- Conifer tree strata recorded the highest level of average PAR transmission towards ground in comparison to other deciduous tree layers.

- The change in the soil surface temperature was seen directly proportional to the amount of PAR received in both open and closed conditions

Conclusion

The conclusion of whole study is as under

- Forest and urban vegetation form a significant portion of Land use/Land cover of Urban Forest division Srinagar signifying its importance and need to conserve it.
- There is a significant correlation between different biophysical parameters and PAR in the study area, exhibiting a wide range of variability.
- Management of urban vegetation and its structure is extremely important for measuring and utilizing PAR as per the requirement of different tiers of vegetation.

LITERATURE CITED

Adrian, V.R., Rose, A., Syndonia, M. Bret-Harte, Eugenie, S. E., Salmon, V. and Gaius, S. 2021. Solar position confounds the relationship between ecosystem function and vegetation indices derived from solar and photosynthetically active radiation fluxes. *Agricultural and Forest Meteorology* **10**(1) 298-299.

Ahmadizadeh, S., Yousef, M. and Saghafi, M. 2014. Land use change detection using remote sensing and artificial neural network: Application to Birjand, Iran. *Computational Ecology and Software* **4**(4): 276-288.

Ahmed B., Khellouk, R., Aafaf, E. J., Fatima, T. and Samir N. 2018. Monitoring of forest cover dynamics in eastern area of Beni-Mellal Province using ASTER and Sentinel-2AA multispectral data. *Geology, Ecology, and Landscapes* **2**(3):203-215.

Akitsu, T., Kume, A., Hirose, Y., Ijima, O. and Nasahara, K. N. 2015. On the stability of radiometric ratios of photosynthetically active radiation to global solar radiation in Tsukuba, Japan. *Agricultural and Forest Meteorology* **2**(1):59–68.

Alam, M. S., Khan, J. A., Pathak, B. J., and Kumar, S. 2014. Assessment of forest density using geospatial techniques of a tropical protected area. *International Journal of Scientific and Research Publications* **4**(3): 1-6.

Ankana. 2016. Land and forest management by land use/ land cover analysis and change detection using remote sensing and GIS. *Journal of Landscape Ecology* **9**(1): 63-77.

Baird. Alec, S., Leander, D.L., Anderegg, Melissa, E., Lacey, Janneke, H. and Elizabeth, V. V. 2017. Comparative leaf growth strategies in response to

low-water and low-light availability: variation in leaf physiology underlies variation in leaf mass per area in Populus tremuloides. *Tree Physiology* **37**(9):1140-1150.

Basavarajappa, T. H., Pushpavathi, N. K. and Manjunatha, C. M. 2017. Land use land cover classification analysis in Chamarajanagara taluk, southern tip of Karnataka state, India using geo-informatics. *Journal of Environmental Science, Computer Science and Engineering & Technology* **6**(3): 209-224.

Breidenbach, J., Waser, L. T., Debella-Gilo, M., Schumacher, J., Rahlf, J., Hauglin, M., Puliti, S., and Astrup, R. 2021. National mapping and estimation of forest area by dominant tree species using Sentinel-2 data. *Canadian Journal of Forest Research*, **51**(3): 365-379.

Campbell, G. S. and Norman, J. M. 1998. An introduction to environmental biophysics, *2nd edn. Springer-verlag,* New York. Pp.167-183

Cavur, M., Duzgun, H. S., Kemec, S., and Demirkan, D. C. 2019. Land use and land cover classification of Sentinel 2-A: St Petersburg case study. *The International Archives of Photogrammetry, Remote Sensing and Spatial Information Sciences*, **42**(1): 13-16.

Choosri, P., Janjai, S., Nunez, M., Buntoung, S., Charuchittipan, D. 2017. Mapping diffuses photosynthetically active radiation from satellite data in Thailand. *Advances in Space Research* **17**(8): 1177-30634.

Crowther, T. W., Glick, H. B. and Bradford, M. A. 2015. Mapping tree density at a global scale. *Nature* **525**(1): 201–205.

Doke, B. A. 2017. Land Use/Cover Mapping of Konkan Region, Maharashtra. *International Journal of Current Research* **9**(10):1-6.

Dong, T., Wu, B., Meng, J., Du, X., and Shang, J. 2016. Sensitivity analysis of retrieving fraction of absorbed photosynthetically active radiation (FPAR) using remote sensing data. *Acta Ecologica Sinica*, **36**(1): 1-7.

Dostalova, D., Wagner, W., Milenkovic, M. and Hollaus, M. 2018. Annual seasonality in Sentinel-1 signals for forest mapping and forest type classification. *International Journal of Remote Sensing* **39**(21):1-23.

Drusch, M., Del Bello, U., Carlier, S., Colin, O., Fernandez, V., Gascon, F. and Bargellini, P. 2012. Sentinel-2: ESA's optical high-resolution mission for GMES operational services. *Remote sensing of Environment* **120**(1): 25-36.

FAO. 2000 Food and Agriculture Organization: on definitions of forest and forest change. Working paper 33, Forest Resource Assessment, Rome, pp. 14-15.

FAO. 2001 Food and Agriculture Organization. Global Forest Resources Assessment 2000 Main Report. FAO Forestry Paper 140. FAO, Rome, Italy. pp. 112-114.

FAO. 2010 Food and Agriculture Organization. Global Forest Resources Assessment Main Report. FAO Forestry Paper163, Rome. pp. 21-24.

Francis, R., Pruthviraj, U. and Shetty, A. 2017. Temporal forest cover analysis of Udupi district in Karnataka using remote sensing and GIS. *International Journal of Engineering Research in Electronics and Communication Engineering* **4**(5): 59-64.

FSI. 2021. State of Forest Report, Forest survey of India, Ministry of Environment, Forests and Climate change, Dehradun, India. pp. 21-22.

Gao, X., Huete, A. R., Ni, W., and Miura, T. 2000. Optical–biophysical relationships of vegetation spectra without background contamination. *Remote sensing of environment*, **74**(3): 609-620.

Gebreslasie, M., Gyamfi, A., Enoch, M. P. and Alma 2020. Mapping natural forest cover using satellite imagery of Nkandla Forest reserve, KwaZulu-Natal, South Africa. *Remote Sensing Applications: Society and Environment* **18**(1):10-13.

Gendron, F., Messier, C., Lo, E., and Comeau, P. G. 2006. The angular distribution of diffuse photosynthetically active radiation under different sky conditions in the open and within deciduous and conifer forest stands of Quebec and British Columbia, Canada. *Annals of Forest Science* **63**(1): 43-53.

Grabska, E., Szwagrzyk, P, H., Dirk, P. and Katarzyna, O. 2019. Forest Stand Species Mapping Using the Sentinel-2 Time Series. *MDPI Remote Sensing* **11**(10):1197-1198.

Guangren, BO, H., Wong, Y. and, L. 2007. Ultraviolet radiation spatio-temporal characteristics derived from the ground-based measurements taken in China. *Atmospheric Environment* **41**(27): 5707-5718.

Hoscilo, Agata, Lewandowska and Aneta 2019. Mapping Forest Type and Tree Species on a Regional Scale Using Multi-Temporal Sentinel-2 Data. *Remote Sensing,* **11**(8): 929-930.

Hu, B., Wang, Y., and Liu, G. 2007. Spatiotemporal characteristics of photosynthetically active radiation in China. *Journal of Geophysical Research: Atmospheres* **112**(1): D14.

Kara, F. 2017. Spatio-temporal analysis of land cover changes of Izmir province of Turkey using Landsat TM and OLI imagery. *International Journal of Geography, Environment and Earth Science* **10**(4): 1-14.

Kayet, N., Khanindra, P., Abhisek, C. and Satiprasad, S. 2016. Spatial impact of land use/land cover change on surface temperature distribution in Saranda Forest, Jharkhand. *Springer* **2**(3): 1-10.

Kiran, V. S. S. 2013. Change detection inland use/land cover using remote sensing & GIS techniques: a case study of Mahananda catchment, West Bengal. *International Journal of Research in Management Studies* **2**(2): 68-72.

Koch, B., Dees, M., van Brusselen, J., Eriksson, L., Fransson, J., Gallaun, H., Leblon, B., McRoberts, R. E., Nilsson, M., Schardt, M., Seitz, R. and Waser, L.T. 2008. Forestry applications. **In**: *Advances in photogrammetry, remote sensing and spatial Information—ISPRS 2008 Congress Book*. Taylor & Francis Group, London, pp. 439–468.

Kume, A., Nasahara, K. N., Nagai, S., and Muraoka, H. 2011. The ratio of transmitted near-infrared radiation to photosynthetically active radiation (PAR) increases in proportion to the adsorbed PAR in the canopy. *Journal of plant research*, **124**(1): 99-106.

Leuchner, M., Hertel, C., and Menzel, A. 2011. Spatial variability of photosynthetically active radiation in European beech and Norway spruce. *Agricultural and Forest Meteorology*, **151**(9): 1226-1232.

Leuchner, M., A. Menzel and H. Werner. 2007. Quantifying the Relationship between Light Quality and Light Availability at Different Phenological Stages within a Mature Mixed Forest. *Agricultural and Forest Meteorology* **142**(1): 35–44.

Liakatas, A., Proutsos, N. and Alexandris, S. 2002. Optical properties affecting the radiant energy of an oak forest. *Meteorological Applications* **9**(1):433–436.

Ma, L., Zheng, G., Ying, Q., Hancock, S., Ju, W., and Yu, D. 2021. Characterizing the three-dimensional spatiotemporal variation of forest photosynthetically active radiation using terrestrial laser scanning data. *Agricultural and Forest Meteorology* **301**(1): 108-346.

Mayer, H., Holst, T. and Schindler, D. 2002. Microclimate within beech stands—part I: photosynthetically active radiation. *Forstwiss Centralbl* **121**(1): 301–321.

McCree, K. J. 1972. Test of current definitions of photosynthetically active radiation against leaf photosynthesis data. *Agricultural Meteorol* **10**(1): 443– 453.

Merian, P. and Lebourgeois, F. 2011. Size-mediated climate-growth relationships in temperate forests: A multi-species analysis. *Forest Ecology and Management*, **261**(8):1382-1391.

Mohammadpour, P., Viegas, D. X., and Viegas, C. 2022. Vegetation Mapping with Random Forest Using Sentinel 2 and GLCM Texture Feature—A Case Study for Lousa Region, Portugal. *Remote Sensing*, **14**(18): 4585-4586.

Mohan, S., Mehta, N. S. and Patel, P. 1990. Radar remote sensing for land applications - A review, *Scientific Report* pp. 36-91.

Monsi, M. and Saeki, T. 1953. On the Factor Light in Plant Communities and its Importance for Matter Production**.** *Japanese Journal of Botany* **14**(1): 22–52.

Moskal, L. M., Styers, D. M., and Halabisky, M. 2011. Monitoring urban tree cover using object-based image analysis and public domain remotely sensed data. *Remote Sensing*, **3**(10):2243-2262.

Mottus, M., Sulev, M., Baret, F., Lopez-Lozano, R., and Reinart, A. 2013. Photosynthetically active radiation: measurement and modeling. In *Solar energy*. Springer, New York, NY. pp 140-169.

Naesset, E., Gobakken, T., Holmgren, J., Hyyppä, H., Hyyppä, J., Maltamo, M. and Soderman, U. (2004). Laser scanning of forest resources: the Nordic experience. *Scandinavian Journal of Forest Research*, **19**(6):482-499.

Navalgund, R. R., Jayaraman, V. and Roy, P.S. 2007. Remote sensing applications: an overview. *Current Science* **93**(12): 1747-1766.

Nguyen, H. T. T., Doan, T. M., Tomppo, E., and McRoberts, R. E. 2020. Land Use/land cover mapping using multitemporal Sentinel-2 imagery and four classification methods—A case study from Dak Nong, Vietnam. *Remote Sensing*, **12**(9): 1367.

Ningyi, Z., Arian, W., Niels, P.R., Anten, Jochem, B., Evers and Leo, F.M. Marcelis. 2020. Disentangling the effects of photosynthetically active radiation and red to far-red ratio on plant photosynthesis under canopy shading: a simulation study using a functional tructural plant model. *Annals of Botany* **126**(1):635–646.

Nowarji, K, D. 2019. The effect of production tank dimensions through the use of NET-POT non-circulating hydroponic method for the production of (REX) lettuce. Masters' thesis, Faculty of California state polytechnic university, USA, pp. 63-64.

Panta, M. 2003. Analysis of forest canopy density and factors affecting it using RS and GIS technology [Master's thesis, International Institute for Geo-information science and earth observation]. Enschede, Netherland.

Paruelo, J., and Tomasel, F. 1997. Prediction of functional characteristics of ecosystems: a comparison of artificial neural networks and regression models. *Ecological Modelling*, **98**(2-3):173-186.

Phiri, D., Simwanda, M., Salekin, S., Nyirenda, V. R., Murayama, Y., and Ranagalage, M. 2020. Sentinel-2 data for land cover/use mapping: a review. *Remote Sensing* **12** (14): 2291-2292.

Pimple, U., Sitthi, S., Simonetti, D., Pungkul, S., Leadprathom, K. and Chidthaisong, A. 2017. Topographic correction of Landsat TM-5 and Landsat OLI-8 imagery to improve the performance of forest classification in the mountainous terrain of northeast Thailand. *Sustainability* **9**(258): 1-26.

Pinag, R. E., Xie, Z., Scaranello, M., Ma, X., Longo, M.,Santos, M. N. and Huete A. 2007. *Relationships among slope, canopy height and vegetation greenness over coastal wet tropical forests in Australia and Brazil*. climate Change Cluster (C3) University of Technology Sydney Ultimo, Sydney NSW 2007: Australia

Proutsos, N., Aristotle, L. and Alexandris, S. 2019. Ratio of photosynthetically active to total incoming radiation above a Mediterranean deciduous oak forest. *Theoretical and Applied Climatology* **137**(1):2927–2939.

Proutsos, N. D., Liakatas, A., Alexandris, S. G., Tsiros, I. X., Tigkas, D., and Halivopoulos, G. 2022. Atmospheric Factors Affecting Global Solar and Photosynthetically Active Radiation Relationship in a Mediterranean Forest Site. *Atmosphere*, **13**(8): 1207.

Proutsos, N., Liakatas, A., Alexandris, S. and Tsiros, I. 2017. Carbon fluxes above a deciduous forest in Greece. *Atmosfera* **30**(4):311–322.

Qiu, C., Lichao, M., Michael, S. and Xiao, X, Z. (2020). Fusing Multiseasonal Sentinel-2 Imagery for Urban Land Cover Classification with Multibranch Residual Convolutional Neural Networks. *IEEE Geoscience and Remote Sensing Letters* **17**(10):1787-1791.

Rabinowitch, E. E.1951. Photosynthesis and related processes. **In**: *Spectroscopy and fluorescence of photosynthetic pigments: Kinetics of photosynthesis*. Interscience, New York, pp. 837-844.

Randazzo, G., Cascio, M., Fontana, M., Gregorio, F., Lanza, S., and Muzirafuti, A. 2021. Mapping of Sicilian Pocket Beaches Land Use/Land Cover with Sentinel-2 Imagery: A Case Study of Messina Province. *Land*, **10**(7): 678-679.

Rosati, A., Marchionni, D., Mantovani, D., Luigi, P. and Franco, F. 2021. Intercepted Photosynthetically Active Radiation (PAR) and Spatial and Temporal Distribution of Transmitted PAR under High-Density and Super High-Density Olive Orchards. *MDPI journal of agriculture **11***(4): 351-352.

Rwanga, S. S. and Ndambuki, J. M. 2017. Accuracy assessment of land use/land cover classification using remote sensing and GIS. *International Journal of Geosciences* **8**(1): 611-622.

Sajjad, A., Hussain, A., Wahab, U., Adnan, S., Ali, S., Ahmad, Z. and Ali, A. 2015. Application of remote sensing and GIS in forest cover change in tehsil Barawal, district Dir, Pakistan. *American Journal of Plant Sciences*, **6**(1):1501-1508.

Sanchez-Espinosa, A., and Schroder, C. 2019. Land use and land cover mapping in wetlands one step closer to the ground: Sentinel-2 versus landsat 8. *Journal of Environmental Management*, **247**(1): 484-498.

Spurr, S. H. 1960. Photogrammetry and photo-interpretation, 2nd edn. Ronald Press, New York Stibig HJ, Achard F, Fritz S 2004. A new forest cover map of continental southeast Asia derived from spot-vegetation satellite imagery. *Applied Vegetation Science* **7**(2):153–162.

Sreenivasulu, G., Nadimikeri, J. and Lakshmi, P. T. 2014. Landuse and Landcover analysis using Remote Sensing and GIS: A case study in and around Rajampet, Kadapa District, Andhra Pradesh, India. *International Journal of Multidisciplinary Research and Development* **2**(1): 186-191.

Sudharsan, D., Adinarayana, J., Reddy, DR., Sreenivas, G., Ninomiya, S. and Hirafuji, M. 2013. Evaluation of weather-based rice yield models in India. *International Journal of Biometeorol* **57**(1):107–123.

Taiz, L., and E. Zeiger. 2010. Plant physiology, 3rd edition. *Annals of botany* **91**(6): 750–751.

Tavares, P. A., Beltrao, N. E. S., Guimaraes, U. S., and Teodoro, A. C. 2019. Integration of sentinel-1 and sentinel-2 for classification and LULC mapping in the urban area of Belem, eastern Brazilian Amazon. *Sensors* **19**(5): 1140.

Tian, S., Zheng, G., Eitel, J.U., Zhang, Q. 2021. A Lidar-Based 3-D Photosynthetically Active Radiation Model Reveals the Spatiotemporal Variations of Forest Sunlit and Shaded Leaves. Remote Sens 13(1):1002.

Tian, Y. Q., Davies-Colley, R. J., Gong, P., and Thorrold, B. W. 2001. Estimating solar radiation on slopes of arbitrary aspect. *Agricultural and Forest Meteorology* **109**(1): 67-74.

Tigges, J., and Lakes, T. 2017. High resolution remote sensing for reducing uncertainties in urban forest carbon offset life cycle assessments. *Carbon balance and management* **12**(1), 1-18.

Timo, P., Timo, K. and Pauline, S. 2008. Below□Canopy distribution of photosynthetically active radiation and its relation to seedling growth in a boreal *Pinus sylvestris* stand. *Scandinavian Journal of Forest Research* **8**(3): 313-325.

Wang, L., Gong, W., Ma, Y., Hu, B., and Zhang, M. 2014. Photosynthetically active radiation and its relationship with global solar radiation in Central China. *International Journal of Biometeorology*, **58**(6):1265-1277.

Wang, L., Gong, W., Hu, B., Lin, A., Li, H., and Zou, L. 2015. Modeling and analysis of the spatiotemporal variations of photosynthetically active radiation in China during 1961–2012. *Renewable and sustainable energy reviews* **49** (1): 1019-1032.

Wani, A. A., Bhat, A. F., Gatoo, A. A., Zahoor, S., Mehraj, B., Mir, N. A., Wani, N., Qasba, S. S., Islam, M. A and Masoodi, T. H. 2019. Relationship of forest biomass carbon with biophysical parameters in north Kashmir region of Himalayas. *Environmental monitoring and assessment*, **191**(9): 1-13.

Wani, A. A., Joshi, P. K., Singh, O. and Bhat, J. A. 2014. Estimating soil carbon storage and mitigation under temperate coniferous forests in the southern region of Kashmir Himalayas. *Mitigation and Adaptation Strategies for Global Change* **19**(8): 1179-1194.

Wani, A. A., Joshi, P. K., Singh, O. and Shafi, S. 2016. Multi-temporal (1980-2030) forest cover dynamics in Kashmir Himalayan region for assessing deforestation and forest degradation in the context of REDD+ policy. *Journal of Mountain Science* **13**(8): 1431-1441.

Waser, L. T., Boesch, R., Wang, Z., & Ginzler, C. 2017.Towards automated forest mapping. **In**: *Mapping Forest Landscape Patterns*. Springer, New York, pp. 263-304.

Wolf, K. L., Lam, S. T., McKeen, J. K., Richardson, G. R., van den Bosch, M., & Bardekjian, A. C. 2020. Urban trees and human health: A scoping review. *International journal of environmental research and public health* **17**(12): 1712-4371.

APPENDIX

Table 28: sampling unit sites

Site No.	Location	Latitude	Longitude	Elevation	Species strata
1	Shankar Acharaya	34° 4' 44"N	74° 50' 26"E	1825	*Robinia* Mix
2	Shankar Acharaya	34° 4' 46.5"N	74° 50' 35.7"E	1839	*Deodar* Mix
3	Shankar Acharaya	34° 4' 41.2"N	74° 50' 47.5"E	1831	*Celtis* Mix
4	Shankar Acharaya	34° 5' 74"N	74° 50' 39"E	1658	*Cupressus* Mix
5	Pari Mahal Juliet	34° 4' 35.2"N	74° 53' 59"E	1807	*Pinus* Mix
6	Pari Mahal Juliet	34° 4' 35.6"N	74° 52' 54"E	1796	*Aesculus* Mix
7	Pari Mahal Juliet	34° 4' 41.4"N	74° 52' 47.1"E	1789	*Deodar* Mix
8	Pari Mahal Juliet	34° 4' 35.1"N	74° 2' 57.6"E	1796	*Parotia jacquemontiana*
9	Royal Spring Golf Couse	34° 50' 17.9"N	74° 52' 17.2"E	1649	*Malus domestica*
10	Skuast Shalimar	34° 8' 49.2"N	74° 53' 3.1"E	1639	*Morus* Mix
11	Sadipora Harwan	34° 10' 36.5"N	74° 53' 16.6"E	1696	*Prunus* Mix
12	Fakir Gujri Harvan Dara	34° 10' 12"N	74° 53' 42"E	1936	*Robinia* Mix
13	Harvan	34° 9' 47.3"N	74° 54' 33.6"E	1690	*Juglans* Mix
14	Dachigam	34° 9' 39"N	74° 54' 28"E	1682	*Celtis* Mix
15	Shalimar Garden	34° 8' 52.4"N	74° 52' 19.1"E	1598	*Platinus* Mix
16	Nishat Garden	34° 7' 33.9"N	74° 52' 51"E	1598	*Platinus* Mix
17	Dachigam National Park	34° 8' 46.2"N	74° 55' 7.7"E	1756	*Pinus* Mix
18	Dachigam National Park	34° 8' 59.9"N	74° 54' 58.9"E	1756	*Celtis* Mix
19	Dachigam National Park	34° 9' 12.2"N	74° 54' 38"E	1747	*Parotia* mix
20	Dachigam National Park Lower	34° 9' 26.7"N	74° 54' 43.1"E	1687	*Morus* Mix
21	Pazwalpora	34° 9' 14.4"N	74° 52' 21"E	1599	*Alainthus* Mix
22	Batpora Tailbal	34° 9' 44.5"N	74° 51' 19.4"E	1588	*Populus patch*
23	Duck Pond Road	34° 8' 53.1"N	74° 50' 39.7"E	1585	*Cupressus*
24	Fore Shore Road	34° 8' 47.8"N	74° 51' 22.5"E	1584	*Platinus* Mix
25	Nigeen Club	34° 7' 15"N	74° 50' 5.6"E	1592	*Cupressus*
26	Kojarbal Nigeen	34° 6' 42.5"N	74° 50' 14.9"E	1588	*Salix* Mix
27	Nand Pora	34° 5' 2.2"N	74° 48' 13"E	1586	*Salix* Mix
28	Battbagh Hazratbal	34° 7' 59"N	74° 49' 38"E	1590	*Salix* Mix
29	Lal Bazar	34° 8' 32"N	74° 49' 37"E	1592	*Malus domestica* Mix
30	Karapora Payeen	34° 5' 16"N	74° 49' 54"E	1587	*Salix* Mix
31	Dal West	34° 5' 26.8"N	74° 50' 5.5"E	1602	*Populus* Mix
32	Dalgate	34° 4' 55.4"N	74° 48' 59"E	1604	*Platinus orientalis*
33	Rainawari	34° 5' 47.5"N	74° 49' 43.9"E	1591	*Alainthus* Mix
34	Badamwari	34° 6' 35.6"N	74° 49' 17.1"E	1611	*Prunus dulcis* Mix
35	Hari Parbat	34° 6' 37.5"N	74° 49' 2.3"E	1677	*Alainthus* Mix
36	Hari Parbat	34° 6' 36.6"N	74° 49' 3.1"E	1671	*Robinia* Mix
37	Khaniyar	34° 5' 47.2"N	74° 48' 46.8"E	1601	*Thuja* Mix
38	Gojwara	34° 5' 46"N	74° 48' 43"E	1598	*Cupressus* Mix

39	Ganga Bag Hyderpora	34° 3' 35"N	74° 46' 35.6"E	1588	*Salix* Mix
40	Tengpora	34° 3' 21.8"N	74° 46' 50.1"E	1588	*Populus* Mix
41	Bulbul Bagh	34° 3' 9.6"N	74° 47' 35.1"E	1587	*Salix* Mix
42	Tengpora Bypass	34° 3' 48.6"N	74° 46' 59.9"E	1586	*Salix*
43	Housing Colony Bemina	34° 4' 48.2"N	74° 46' 13"E	1585	*Morus*
44	SDA Colony Bemina	34° 5' 28.5"N	74° 46' 28.1"E	1588	*Cupressus* Mix
45	JVC Bemina	34° 4' 44.9"N	74° 45' 21.1"E	1590	*Salix* Mix
46	Degree College Bemina	34° 4' 45"N	74° 46' 48"E	1583	*Salix* Mix
47	Parimpora Bemina	34° 5' 50"N	74° 45' 56"E	1592	*Populus* Mix
48	Athwajan	34° 2' 37.2"N	74° 52' 47.6"E	1612	*Alainthus* Mix
49	Amusement Park Athwajan	34° 2' 44.8"N	74° 52' 14.3"E	1592	*Salix* Mix
50	Badamibagh	34° 3' 46.8"N	74° 50' 58"E	1592	*Platanus* Mix
51	Indra Nagar Bb Kant	34° 4' 8.6"N	74° 51' 5"E	1594	*Robinia* Mix
52	Sonwar	34° 4' 19.2"N	74° 50' 16.8"E	1583	*Platanus orientalis*
53	Gupkar Road	34° 4' 47.6"N	74° 51' 32.9"E	1599	*Deodar* Mix
54	Chinar Park Gupkar	34° 4' 22"N	74° 50' 10"E	1603	*Platanus orientalis*
55	Sonwar Park	34° 4' 3"N	74° 50' 49"E	1609	*Populus* Mix
56	Gagribal	34° 5' 2"N	74° 51' 1"E	1612	*Malus domestica* Mix
57	Dal View Point	34° 5' 19"N	74° 50' 43"E	1600	*Robinia* Mix
58	Sazgari Pora Eid Gah	34° 6' 25"N	74° 48' 2"E	1602	*Salix* Mix
59	Eid-Gah	34° 5' 55.1"N	74° 47' 37"E	1587	*Cupressus* Mix
60	Dangerpora	34° 6' 10"N	74° 48' 13"E	1603	*Salix* Mix
61	Munawar Abad	34° 5' 8.7"N	74° 49' 8.2"E	1587	*Populus* Mix
62	Fateh Kadal	34° 5' 6"N	74° 48' 31"E	1593	*Salix* Mix
63	Karan Nagar	34° 5' 8"N	74° 48' 6"E	1598	*Platanus* Mix
64	Batamaloo	34° 3' 51"N	74° 3' 51"E	1602	*Platanus orientalis*
65	Noorbagh	34° 5' 44"N	74° 46' 45"E	1604	*Salix* Mix
66	Shooglipora Noorbagh	34° 6' 4"N	74° 46' 57"E	1596	*Populus* Mix
67	Anchar	34° 7' 26"N	74° 47' 23"E	1594	*Salix* Mix
68	Sher-I-Kashmir Park Sgr.	34° 4' 23.8"N	74° 49' 24.6"E	1581	*Platanus* Mix
69	Golf Course TRC	34° 4' 47.2"N	74° 49' 33.3"E	1584	*Salix* Mix
70	M A Road	34° 4' 28.5"N	74° 49' 16.7"E	1578	*Cupressus* Mix
71	Pratap Park	34° 4' 19.5"N	74° 48' 45.4"E	1588	*Cryptomeria* Mix
72	Jehlum Bund GPO	34° 4' 18.3"N	74° 49' 18.9"E	1599	*Platanus* Mix
73	Aram Wari Rajbagh	34° 3' 51.9"N	74° 50' 19.2"E	1591	*Populus* Mix
74	Hazuri Bagh Rajbagh	34° 4' 4.3"N	74° 49' 17.6"E	1596	*Deodar* Mix
75	Iqbal Park	34° 3' 51"N	74° 48' 14.2"E	1599	*Cupressus* Mix
76	Aloochi Bagh	34° 3' 27"N	74° 48' 6"E	1602	*Salix* Mix
77	Khadi Mil Aloochi Bagh	34° 3' 33"N	74° 47' 31"E	1599	*Salix*
78	Rambagh	34° 3' 6"N	74° 48' 12"E	1591	*Morus* Mix
79	Parraypora	34° 2' 35"N	74° 48' 9"E	1588	*Salix* Mix
80	Harinambal Budhshah Nagar	34° 2' 44.9"N	74° 49' 21.1"E	1588	*Populus*
81	Harinambal Budhshah Nagar	34° 2' 54.3"N	74° 49' 24.8"E	1590	*Salix*
82	Bonpora Nowgam	34° 2' 29.5"N	74° 49' 50.3"E	1594	*Salix* Mix

83	Naik Pora Nowgam	34° 2' 56"N	74° 49' 59.3"E	1595	*Populus* Mix
84	Rambagh	34° 3' 29"N	74° 49' 18.3"E	1606	*Populus* Mix
85	Jawahar Nagar	34° 3' 28"N	74° 49' 1"E	1603	*Populus* Mix
86	Warpora Jawahar Nagar	34° 3' 27"N	74° 49' 21"E	1599	*Populus* Mix
87	Kursoo Rajbagh	34° 3' 52"N	74° 49' 52"E	1603	*Salix*
88	Kursoo Rajbagh	34° 3' 58"N	74° 50' 29"E	1602	*Populus* Mix
89	Gori-Pora Maloora Sgr	34° 6' 37"N	74° 45' 43"E	1608	*Salix* Mix
90	Gori-Pora Maloora Sgr	34° 6' 58"N	74° 46' 12"E	1605	*Populus*
91	Bagwan Pora Noorbagh	34° 6' 36"N	74° 46' 56"E	1608	*Malus domestica* Mix
92	Sangam	34° 7' 43"N	74° 46' 44"E	1601	*Populus* Mix
93	Sangam	34° 7' 26"N	74° 46' 55"E	1589	*Salix*
94	Chindhari- Demari Nowhatta	34° 6' 33"N	74° 47' 18"E	1603	*Populus* Mix
95	Saidpora Srinagar	34° 6' 46"N	74° 47' 24"E	1607	*Morus* Mix
96	Eid-Gah Saidpora	34° 6' 53"N	74° 47' 40"E	1609	*Platanus* Mix

Sher-e-Kashmir
University of Agricultural Sciences & Technology of Kashmir
Faculty of Forestry, Division of Natural Resources and Management, Benhama, Ganderbal

Certificate

Certified that all the corrections/amendments as suggested by external Examiner **Dr. Majid Farooq,** Scientist Remote Sensing, Directorate of Ecology, Environment and remote Sensing, Bemina Srinagar (JK) during Viva-Voice examination held on 16-03-2023 have been incorporated in the manuscript entitled, **"Vegetation mapping and variability assessment of Photosynthetically Active Radiation (PAR) in Urban Forest Division of Srinagar"** submitted by Mr. **Jamsheed Bin Jabar (Regd. No. MSF-2020-121)**.

Prof. Akhlaq Amin Wani
Chairman
Advisory Committee